Journal of
Materials Chemistry A

Materials for energy and sustainability

Accepted Manuscript

ROYAL SOCIETY OF CHEMISTRY

rsc.li/materials-a

J. Mater. Chem. A.

ARTICLE

Carbon fibre surface chemistry and its role in fibre-to-matrix adhesion.

Received 00th January 20xx,
Accepted 00th January 20xx

DOI: 10.1039/x0xx00000x

www.rsc.org/

Daniel J. Eyckens,[1,2] Filip Stojceveski,[1] Andreas Hendlmeier,[1] James D. Randall,[1] David J. Hayne,[1] Melissa K. Stanfield,[1] Ben Newman,[1] Filip Vukovic,[1] Tiffany R. Walsh,[1] Luke C. Henderson.[1*]

A key factor determining the performance of carbon fibre reinforced polymer (CFRP) composites is their fibre-to-matrix interactions, the interface and interphase, as these allow for the efficient transfer of stress from the relatively weak and ductile resin to the strong reinforcing fibres. The manipulation of the interface via modulation of surface chemistry has been been an active area of research with many apporaches being taken. In this work we cover efforts in this area from traditional manufacturing condition optimisations, plasma, wet chemical, and electrochemical approaches to induce favourable properties in composites. The design of molecular interactions at the interface are exceedingly difficult to determine and design, and thus, we finish this review with a section on the use of molecular dynamics to design complementary interfaces for the next generation of composites.

1.0 Introduction

The desire to make materials lighter and/or stronger has been persistent for millennia, causing the transition from bronze tools and weapons to those made from iron and steel over 2000 years ago. In modern times, the need for weight reduction is typically linked to increased fuel efficiency for mass transport, and to this end, composite materials have featured heavily. The correlation between removing a vehicle's mass and better design was noted as early as 1923 by Henry Ford, who stated, "*Saving even a few pounds of a vehicle's weight... could mean that they would also go faster and consume less fuel. Reducing weight means involves reducing materials, which, in turn, means reducing cost as well*", but there is a limit to this approach. Effecting weight reductions by simply removing a material can compromise aspects of safety or performance, thus lighter composite materials are employed as replacements. These composites are commonly composed of glass and/or carbon fibre reinforced plastics, referred to as the fibre and matrix, respectively. The latter of these two reinforcing agents (carbon) will be the focus of this review.

The use of carbon fibre composites in modern structures is a significant means to reduce weight in mass transport to increase fuel efficiency and decrease CO_2 emissions. As society transitions to alternative energy sources, such as electric and hydrogen powered vehicles, wind energy, *etc.*, significant removal of weight will be required to increase range and allow for the installation of batteries and/or hydrogen storage modules. As such, the requirement to make better performing composites is more important than ever. The understanding of the fibre-matrix interface and interphase, and how to tailor these is critical to realising the potential of carbon fibre composites for these applications.

As a composite consists of two dissimilar materials, the interface (the physical contact) of each material and interphase (the localised area surrounding the physical contact) plays a critical role in the overall performance of the composite part. The interface and interphase are intimately linked as the molecular interactions at the interface typically define the interphase. It is somewhat counterintuitive to consider that this very small physical region, typically at the nanometre scale, has a significant impact on the macroscopic properties of a material. The role of the interface and interphase is to mediate the transfer of stress and other forces experienced by the weak supporting polymer to the strong reinforcing material.[1-3] Therefore, a physical or chemical disconnect between the two constituents is detrimental to the overall performance of a composite and ultimately leads to premature catastrophic failure.

It is important to note that there have been several reviews written on this topic in the past,[1, 3, 4] with a focus on how surface treatments affect adhesion. This unique area requires an understanding of organic chemistry, molecular interactions, and the relative strength or complementarity of these in complex systems, which is what we hope to contribute in this review.

A major hurdle in the development of 'next generation' carbon fibres is the strict proprietary control over their manufacture and processing. The most pertinent manufacturing processes to the interfacial adhesion are the final two processing steps – fibre surface treatment and sizing.

[1.] *Deakin University, Institute for Frontier Materials, Waurn Ponds, Victoria 3216, Australia.*
[2.] *Commonwealth Scientific and Industrial Research Organisation (CSIRO), Clayton, Victoria 3081, Australia.*
* Corresponding Authors: luke.henderson@deakin.edu.au;

The conditions of surface treatment (e.g., electrolyte identity and/or concentration, current and/or potential applied, duration, etc.) are not typically divulged to the end-user. Similarly, the sizing agent, a proprietary cocktail of ingredients, is applied to the fibre in the final step to protect it from post-processing, make the fibre tractable, and enhance interfacial adhesion. However, this last point has a large degree of conjecture in the literature, with frequently conflicting results being reported over the past 4 decades.

The ambiguity of these processes results in 'systematic' evaluation of commercially available fibres being highly inconsistent as there are dozens of variables which could be changed between samples, unknown to the researcher. Of these, each may have a slight effect on interfacial adhesion. Therefore, many attempts to replicate published work have been problematic; thus, a prominent 'black box' surrounding the nature and impact of carbon fibre surface treatment and sizing remains.

1.1 Carbon Fibre Manufacture

Carbon fibres have been manufactured from a myriad of materials, indeed the search for alternative precursors is a major research area targeting a step-change in carbon fibre cost.[5-7] Presently, the vast majority of carbon fibres manufactured are derived from Polyacrylonitrile (PAN) (with various copolymers), with a small remainder of commercial fibres (<10%) originating from Pitch or Rayon precursors. The following discussion of manufacture is with respect to PAN-derived carbon fibres. This area has been reviewed previously, and the reader is referred to these excellent accounts; therefore this process will be only briefly covered herein.[8]

First, PAN fibres are passed through an oxidation process, usually heating the fibres (250-300 °C) in an air atmosphere, to stabilise the fibres and prevent their melting or burning when exposed to much higher temperatures. Then, heating the oxidised PAN in a low-temperature furnace (~600-900 °C) in a nitrogen atmosphere initiates the formation of a ladder polymer structure, and subsequent heating at high temperatures (>1000 °C) extrudes a large volume of non-carbonaceous species and sets the crystalline structure of the fibres. In some instances, a third furnace (ultra-high temperature) is used to generated carbon fibres with extremely high Young's Modulus, resulting from an increase in the graphitisation percentage of the underlying chemical structure.

At this point, after HT furnace treatment, the surface chemistry is quite heterogeneous, with loosely bound amorphous carbon being present and residual nitrogen and oxygen species from the parent PAN polymer. This hydrophobic and rather unreactive surface is then passed through an electrochemical oxidation bath to remove any lubricious carbon species, and to install oxygenated functional groups. Finally, the surface treated carbon fibres are passed through a sizing bath which adheres a coating to the exterior of the fibres making them tractable and processable for weaving into usable fabrics.

It is important to note that these processes are heavily guarded industry secrets and so there is much conjecture in the literature regarding the exact effect of surface treatments and sizings.

1.2 Role of the Interface and Interphase

The interface and interphase are dictated by the surface chemistry of the carbon fibres, which is very challenging to characterise. Carbon fibres are distinct entities from carbon nanotubes, graphite, graphene, carbon nanofibres, etc. The characterisation of even the graphitic nature of the surface has been reported recently using surface profiling Raman spectroscopy showing a high degree of heterogeneity (Figure 1).[9] It is interesting that the PAN derived carbon fibres have a more consistent D/G ratio (Figure 1, top) than the ones derived from mesophase pitch (Figure 1, bottom).

Considering that the chemistry which is attached to this graphitic heterogeneity is also difficult to characterise there is a tendency for surface treatment and effects on properties to be referred to in terms of trends rather than quantifiable contributions from functional groups.

This surface heterogeneity will be reflected in the homogeneity of the treated surface of the fibre, as they are directly and intimately linked. Though it is important to consider the consistency of surface treatments along a fibre length is relative to the scale of analysis. For example, at a micron scale, two sections of the fibre may be significantly different with respect to the atomic constituents, hybridisation of carbons, and oxidation states of those very species. Whereas, at a meter scale, two sections of fibre may seem similar as the subtle chemical changes and speciation has averaged out over these larger areas. Similarly, when the fibres are sized and woven into a fabric, often incorporating up to kilometres of fibres, the average surface chemistry will likely be consistent over the whole fabric.

Regardless, the translation of various forces across the interphase and interface of a composite is critical to the performance. It is also difficult for some to connect the molecular and macroscopic scale, in that the interactions present at the molecular scale can dictate the performance of a material composed of kilometres of fibre. Nevertheless, the connection between micro-, meso-, and macroscale testing has had some preliminary connections made in recent years.[10-13]

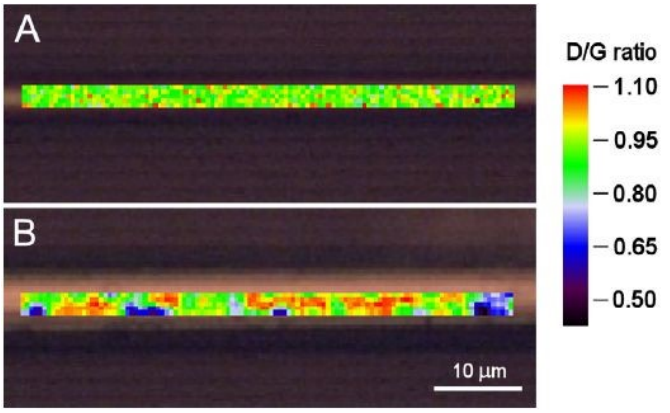

Figure 1 Surface profiling of (A) PAN based and (B) Pitch based carbon fibres. Reproduced with permission.[9] Copyright 2014, Elsevier Inc.

There is a myriad of testing mechanisms available to researchers in the composites field to determine interfacial adhesion. These have been reviewed and are examined in the literature,[2, 14, 15] and the interested reader is referred to those works.

1.3 Considerations regarding process scale up and industrial translation

The ability to scale up and translate a carbon fibre (or any) surface treatment process is an important consideration for industrial or broad end user translation. There are obvious implications in an OH&S context, where strong acids or oxidant etches are routinely used, high electrical currents and potentials, and the incorporation of inert or reactive atmospheres. Most of these considerations are already used in industrial or large-scale plants and so are not insurmountable by any means.

Significantly more challenging for scale up are processes which are limited by the fibre bundle geometry, speed of treatment, and the potential for deleterious effects. For example, the use of plasma oxidation is widely used, and discussed below, but suffers from only treating the periphery of a fibre bundle or tow. Thus, the use of tow spreading for consistent surface treatment is a significant challenge faced by many industries and has high potential for fibre twisting and damage *via* excessive handling.

Again, these challenges are not insurmountable but any perceived barrier of entry to incorporate such processes on large scale will be a deterrent. Such a process would have to induce a significant step change in terms of performance or quality to be truly considered as an alternative to existing methodologies.

Nevertheless, the high performance and largely niche application of carbon fibre means that there is still significant value in surface treatments that are not able to be scaled up. As low volumes of carbon fibres with well-defined surface structure and chemistry may shed light on long standing questions in the field regarding interface/interphase interactions, mechanisms by which novel functionality can be installed, and how to maximise macroscopic performance.

1.4 Scope of this review

The volume of work published on carbon fibre and composite interfaces since the development of this material is far too large to be captured in this review. Here, we intend to examine cases where surface treatments can be tracked back to the chemistry of the surface and how these treatments have affected the adhesion to the supporting polymer. While this may sound like a straightforward process, the surface of the starting fibres is very heterogenous and poorly characterised, thus complicating matters. Every effort has been made to cover relevant work, though some omissions are inevitable, with respect to this we apologise to any authors who were overlooked.

2.0 Manufacturing processes

The manufacturing process of carbon fibres has largely remained constant since their commercialization. This section will focus on the surface treatment aspect of their manufacture, and thus only a brief mention of the manufacturing processes prior to this will be mentioned. For the interested reader, this topic was covered in excellent detail, including precursors and other manufacturing parameters, by Buchmeiser *et al*.[8], and we refer the reader to that work.

It should be mentioned that when using PAN as the precursor fibre, the physical morphology of the fibre will also influence the interfacial adhesion in the final composite. Carbon fibres are often depicted as cylindrical, though it is well known that other radial geometries are known (*e.g.,* kidney-bean shaped). This variation in fibre geometry is even more pronounced and exotic when textile-grade PAN is employed to reduce the cost of raw materials for low-cost carbon fibres. A very recent example was reported by Lee *et al.*[16] showing that textile grade PAN could achieve similar interfacial adhesion values as T700 fibres by surface morphology alone. Unfortunately, the geometry of the fibres used in many studies is not routinely reported, and thus is difficult to consider in these discussions.

2.1 Variations on the in-line manufacturing process

With all oxidations and surface treatments for carbon fibre it is important to note that the correlation between surface treatment and interfacial shear strength (IFSS) of the final composite may not be linear, but instead periodic. To illustrate the cyclic nature of this relationship, hypothetical periodic oxidation vs. IFSS curves have been constructed (Figure 2a) using three different applied potentials (1, 5, and 10 V). It is possible, in this hypothetical scenario, to conduct experiments examining oxidation potential and time to optimize IFSS. In this instance, at t_1 for example, it would seem as though 5 V oxidation is optimal, while poor IFSS is observed at 1 V and 10 V. Similarly, at t_2, one would assume that both 5 V and 10 V are optimized for IFSS. While, finally at t_3, an optimized surface treatment would appear to be present for all three potentials.

Nevertheless, without thinking of this process periodically, that data would appear to have no correlation or would be difficult to justify. The shape, period, stability, and consistency of these curves may also vary depending on the fibre origin (PAN vs. Pitch vs. Rayon), manufacturing of the precursor materials (air gap vs. wet spinning), stabilization and oxidation conditions, and electrolyte used in the bath (e.g. Figure 2b).

Therefore, given the number of variables, the authors recommend that each optimised surface treatment reported in the literature be considered, largely, in isolation. This is further complicated by additional treatments used in each study, such as alternative desizing processes (thermal vs. solvent). To be clear, we are not doubting the data and outcomes of these reports, but merely suggesting that they be used to guide researchers in their studies rather than be considered as unambiguous physical truths.

An electrochemical oxidation process follows immediately after PAN fibres have passed through the carbonisation furnaces. This step is essential for improving their adhesive properties as,

directly after carbonisation, the carbon fibres are highly chemically inert[17] with weakly bound graphitic layers exposed on the outside of the fibres.[18] The electrochemical oxidation process addresses both these flaws by exfoliating the fibres[19] and increasing their chemical reactivity *via* the installation of oxygenated species such as phenols, carboxylic acids, and undefined carbonyl derived species (aldehyde, ketone, quinone, *etc*.).[20, 21]

Electrochemical oxidation involves applying an electrical potential to the carbon fibres, whilst they are submerged in an aqueous bath. A contact point to the fibres is required (typically in the form of a graphitic roller) which acts as the anode, while graphitic plates submerged in the electrolyte solution act as the cathode.[22] Once a potential is applied through this circuit, electron exchange occurs between the fibres and the electrolyte solution. This process subsequently alters fibre topography, mechanical properties and surface chemistry.[23-25] While this method is currently the most used protocol for surface modification, there remains several input variables which can be altered to improve adhesion. These are: *electrolyte selection* (thought this is typically ammonium bicarbonate)*, bath conductivity, amperage applied, voltage applied* and *treatment time*. Some of these variables are not independent, for example amperage and voltage, which are applied either galvanostatically (controlled current density) or potentiostatically (controlled voltage). As such, to maintain a consistent amperage, the applied voltage may change significantly, depending on the resistivity of the submerged fibres. Given the complexities of combining the aforementioned variables, a complete understanding of how each affects one another, and subsequent fibre properties is incomplete. Ideally, a multivariate analysis looking into all parameters would exist.

Gulyás *et al.*[21] examined a range of electrolytes, with varied concentrations (2-20 wt%) and voltages (0.5-5 V) for the electrochemical oxidation of PAN-based fibres. This work is one of the earliest analyses of input parameters relative to interfacial adhesion and selected entries are presented in Table **1**, below. This investigation was conducted in a continuous process at two rates 20 and 30 cm min^{-1}, and the effect on performance in an epoxy composite was evaluated using the single fibre fragmentation test (SFFT) originally reported by Kelly and Tyson.[26] Results of which are reported as the interfacial shear strength (IFSS).

Table 1 Effect of electrolytes at 20 wt% on the IFSS of carbon fibre when oxidised at 0.5 V. Adapted from Gulyás *et al.*[21]

Electrolyte	IFSS (MPa)
Neat	17.3±2.8
$(NH_4)_2CO_3$	18.8±2.5
NH_4HCO_3	17.1±2.1
HNO_3	36.0±14.2
NaOH	37.7±8.6
	27.5±5.9*
H_2SO_4	20.6±7.6
	36.0±9.6*

*IFSS was determined for fibres treated with a 5 V potential.

The electrolyte, concentration, and voltage (or amperage) used for fibre surface treatment all contribute to the performance of the carbon fibre composite. This is particularly apparent for the electrolytes NaOH and H_2SO_4 in Table 1, with them exhibiting an inverse relationship to each other when comparing the effect, the applied potential has on IFSS. At higher voltages, oxidation in the acidic medium results in greater IFSS than at lower potentials. The reverse is true for the basic environment, with greater IFSS achieved using a lower voltage.

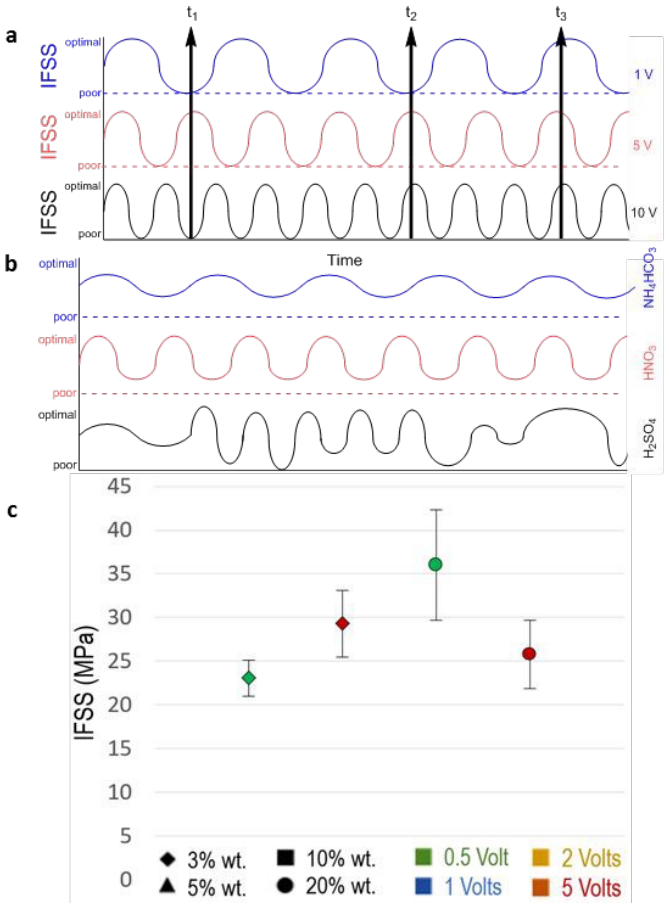

Figure 2 a) Hypothetical IFSS-Potential correlation at various surface treatment applied potentials and time points (t_{1-3}). **b)** Hypothetical IFSS-Electrolyte correlations over time. **c)** Relationship of HNO_3 electrolyte concentration and oxidation potential.

The anodic oxidation of PAN carbon fibre in either H_2SO_4 or NaOH (2-20 wt%) at a range of potentials (0.5- 5.0 V) and in a continuous process was also explored by Százdi *et al.*[27] The use of NaOH (20 wt%) at 5.0 V resulted in an increase in IFSS (determined by SFFT in epoxy) to 27.5 MPa (compared to 17.3 MPa, control), identical to the finding by Gulyás *et al.*[21] In terms of surface chemistry, oxidation in H_2SO_4 increased the presence of surface bound sulfur-containing and quinodal groups. Conversely, NaOH lead to an increased proportion of carboxylic acid groups, and the occurrence of NaOH adsorbed to the surface. Interestingly, the IFSS of the sample oxidised in NaOH (20 wt%, 5.0 V) could be drastically improved through the removal of excess NaOH from the fibre bundle. Soaking the treated fibres in water for 20 hours resulted in a pH increase to

~10 and the resulting fibres exhibited a further improvement in IFSS to 44.8 MPa (compared to unsoaked (27.5 MPa) and control 17.3 MPa). This was suggested to be the due to adsorbed NaOH hindering the coupling of surface functional groups to the matrix.

These data reveal that altering voltage or electrolyte concentration alone is not necessarily a singularly viable strategy to optimise IFSS. Instead, the outcome is highly subjective and dependent on numerous input parameters, which the intended application of the composite may further confound.

The implications of how process variability in surface treatments C results in seemingly unpredictable effects on IFSS is perhaps best highlighted when HNO_3 was examined as an electrolyte (Figure 2c).[20] Maintaining concentration at 3 wt%, IFSS increased from 23.1 MPa to 29.3 MPa as the applied potential was increased from 0.5 V to 5 V, respectively. Conversely, when the electrolyte concentration was maintained at 20 wt%, IFSS decreased from 36.0 MPa to 25.8 MPa as the applied voltage was increased from 0.5 V to 5 V.

A complete listing of IFSS values found by Gulyas *et al.* is available in the accompanying reference[21] and associated ESI. Interested readers are encouraged to examine this study. To date, it contains the most comprehensive multivariable analyses of electrochemical oxidation input parameters (voltage, concentration, and electrolyte). It highlights the problematic nature of predicting the effect when altering treatment variables for improved interfacial adhesion. With this said, valuable information can still be extracted by isolating individual treatment variables in their own right.

2.2 Electrolyte selection

During the infancy of the carbon fibre industry, the primary electrolyte of choice was nitric acid.[28] For the benefit of workers, and with improvements in electrolyte understanding, less hazardous chemicals are now commonplace for the oxidative surface treatment of fibres. Common electrolytes investigated within literature include potassium nitrate,[19, 29] nitric acid,[21, 30] ammonium bicarbonate,[21, 31-33] aqueous ammonia,[34] sulfuric acid,[21, 27, 35, 36] sodium hydroxide,[21, 27] ammonium oxalate,[37] and phosphoric acid.[38]

One of the most common electrolytes used in commercial treatment of fibres is ammonium bicarbonate. Accordingly, a large body of literature exists regarding this electrolyte's effect on carbon fibre surface chemistry. Various studies show that passing the fibres through an electrochemical bath with ammonium bicarbonate as the electrolyte increases the surface content of oxygen-containing functional groups. Qian *et al*.[31] examined the resulting surface chemistry of CF treated using an ammonium bicarbonate electrolyte and applied current of 20 A/m^2. Overall oxygen content on the fibre surface increased after treatment, which corresponded to increases of 5.6% and 5.0% in –C=O and –COOH moieties, respectively. Conversely, a study conducted by Fukenaga *et al*.[33] showed a decrease of 3.31% in C-OH content on the fibre surface occurs after undergoing electrochemical treatment in ammonium bicarbonate. The O1s/C1s ratio on the fibre surface however was found to increase by 5.0% but further deconvolution of this data was not carried out. Results by Jiang *et al.* reinforce this finding,[32] as an 8.5% increase in O_{1s}/C_{1s} ratio was observed with relative increases to C-O and O=C-O of 15.2% and 42.8% following oxidation, and a simultaneous 5.6% reduction occurring in C=O.

While most work has considered only aqueous ammonium with a bicarbonate anion, ammonium oxalate monohydrate as a mixture with ammonium bicarbonate has also been explored. Using ratios of 1:2, 1:1 and 2:1 (NH_4HCO_3:$(NH_4)_2C_2O_4 \cdot H_2O$), some control over the presence of C-OH, C=O and COOH groups was documented.[39] While the overall oxygen content on the fibres remained generally constant throughout all 3 doping ratios, within a standard deviation of 2.7%, a 2:1 ratio of ammonium bicarbonate to ammonium oxalate monohydrate provided the greatest content of C=O and COOH. Conversely, a 1:2 ratio (bicarbonate:oxalate) resulted in less of these functional groups. A trend was observed demonstrating that as C=O and COOH content decreased, C-OH content increased, maintaining the overall oxygen content on the fibre surface at 4.4%. The mechanism for the interchange of these oxygenated functional group is not known, but in this way the desired surface chemistry could possibly be fine-tuned, depending on the intended composite application. This trend of increasing C=O and COOH content with decreasing C-OH surface concentration was also observed by Qian *et al.* when considering ammonium bicarbonate electrolytes.[31]

Mildly acidic and basic electrolytes (phosphoric acid and ammonium bicarbonate) were compared in parallel by Nakao *et al.*[38] For both electrolytes, increases in the O_{1s}/C_{1s} ratio was documented. Untreated fibres with an O_{1s}/C_{1s} ratio of 0.075 increased to 0.155 and 0.195 after being subjected to electrolysis in phosphoric acid and ammonium bicarbonate solutions, respectively. In both cases oxidation was found to alter fibre surface roughness, though with different outcomes. Phosphoric acid smoothed the fibre surface by 0.01 m^2/g while ammonium bicarbonate roughened the fibre surface by 0.04 m^2/g. This would suggest that electrochemical oxidation is not only a chemical modification process, but also elicits a morphological change. Interfacial analysis showed negligible changes in IFSS between the two electrolyte types, suggesting that the physical interactions (keying and interlocking) were not the major contributors to adhesion in this instance.

While ammonium bicarbonate has been the most investigated electrolyte, insight can be gained from treating the fibres in alternative solutions or solvents. Kim *et al.*[35] showed the use of a sulfuric acid electrolyte can attach $–SO_3H$ and $–SO_4$ functional groups to the fibre surface, both of which possess strong acidity. These authors proposed this to be an influential factor for improving PAN fibre-to-matrix adhesion, however no interfacial assessment was conducted. Kainourigios *et al.*[36] similarly observed sulfuric acid to introduce SO_3H and SO_4H functional groups to carbon fibres. However, that study concluded that although tensile strength and modulus increase, the concentration of oxygen groups on the surface was too small to induce any significant change to interfacial adhesion.

Thus far, the impact of electrolyte selection and its effect on surface chemistry has been considered. While this undoubtedly plays a role to modify surface chemistry, many processing variables must also be considered which will affect the final fibre's performance. These variables include solution conductivity, applied current, applied voltage, and treatment time. Each of these variables have been investigated at different times (*vide infra*) within the confines of limited electrolyte selection and fibre type. Therefore, only a limited understanding for the scope of the oxidation treatment when considering interfacial adhesion is available.

2.3 Amperage

Over the years emphasis has also been placed on the effects of current density (galvanostatic treatment) applied to the fibres in the electrolyte bath to alter fibre topography and chemistry. Qian *et al.*[31] used an ammonium bicarbonate bath and altered bath amperage between 0 A, 1 A, 5 A, 12 A, and 20 A. Overall, oxygen containing functional groups on the fibre surface increased from 28.7% at 0 Amps to 34-35% between 1 A/m^2, 5 A/m^2 and 12 A/m^2 and any subsequent increase to current density saw decreases in oxygen containing groups. This suggests that the impact of amperage on the total surface oxidation is highly sensitive and indeed shows a plateauing effect (between 1 A/m^2 and 12 A/m^2) before significant drop off may occur.

Interestingly, the ratios of carbonyl, carboxylic acid and alcohol groups was highly variable between the 1 A/m^2, 5 A/m^2 and 12 A/m^2 conditions. The degree of detected carboxylic acids increased with larger current densities, while carbonyl species decreased. However, when amperage was further increased to 20 A/m^2, a notable increase of hydroxyl (C-OH) groups was observed, in addition to an overall increase in oxygen content. This suggests that oxygen group tailoring is possible over a certain range before severe exfoliation and chemical change occurs at extreme amperages. This exfoliation can lead to significant deterioration of the intrinsic fibre properties, due to the development of surface defects.

A similar study conducted by Yue *et al*.[19] using potassium nitrate showed the similar trend of oxygen group tailoring. While unsized fibres were found to have the highest content of C-OH and COOH groups on the surface. Any form of alternative oxidation was seen to reduce the presence of these groups and introduce simple carbonyl groups. The overall oxygen content however remained unchanged. With careful application of amperages between 0.05 A, 0.1 A, 0.3 A, 0.5 A, 0.6 A, and 1 A, slightly varied oxygen content was observed, again, with a clear interplay between carbonyl and alcohol/carboxylic acid groups occurring. Again, this supports the theory of amperage being a method of tailoring functional groups while keeping overall oxygen content consistent.

A proposed mechanism for the oxidation of the carbon fibre surface, resulting in changes in C-O functional groups, is outlined above (Figure 3). This sequential oxidation highlights the evolution and potentially cyclic type of surface changes occurring over oxidative treatments. The generation of such functional groups, and subsequent etching that would result, would also account for the exfoliation of quantum dots from carbon fibres, reported in 2021.[40] This exfoliation process would also cumulatively lead to the generation of pits and defects on the fibre surface, deteriorating the final properties of the carbon fibres.

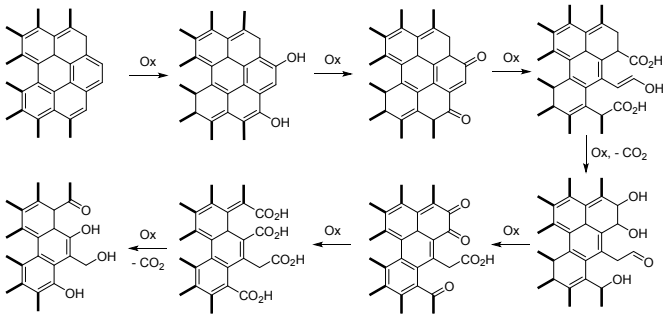

Figure 3 Possible oxidation scheme to show how the graphitic surface can be eroded, and potentially exfoliated from the carbon fibre surface.

While these studies are of value, it is also worth highlighting that the deconvolution of amperage and voltage within an electrochemical oxidation process is near impossible. When one variable changes, so does the other which is further influenced by electrolyte conductivity and the resistivity of the carbon fibres themselves.

In a study conducted by Szazdi *et al.*[27] the role of voltage and current density for NaOH and H_2SO_4 were investigated. For NaOH, as voltage rose from 1 V to 5 V, the peak current increased from ~5 mA to ~6.5 mA, respectively. However, under the same conditions in a H_2SO_4 electrolyte, peak current increased exponentially from ~5 mA to ~14 mA. The study also found surface roughness of fibres to increase by ~60% with greater electrolyte concentration and current density. These factors suggest that an erosion process or exfoliation is at play. Interestingly, with increasing potential applied in the cell, the content of carboxyl groups doubled for H_2SO_4 and increased four-fold for NaOH electrolytes.

Work conducted by Stojcevski *et al.*[24] found increases in amperage from 0 A, 2 A and 3.4 A resulted in increases to IFSS for unsized, lightly sized, moderately sized, and heavily sized carbon fibres by up to 59.7%, 26.3%, 39.5% and 35.1%, respectively, when tested in epoxy resin. Fibre manufacturing was conducted on a pilot scale carbon fibre line and used an ammonium bicarbonate electrolyte in the oxidation bath, which had a measured conductivity 20.4 µS/cm during oxidation. Increases in amperage were also observed to increase oxygenated functional groups on the carbon surface while reducing its roughness. The trends observed at a single fibre scale[25] were also shown in subsequent work to be translatable to both mesoscale and macroscale testing of composite laminates.[41]

In similar research conducted by Hendlmeier *et al*.[41], a comparison of electrolyte (NH_4HCO_3) conductivity (8, 16 and 24 µS/cm), current density (0.5, 1 and 1.5 A/m^2) and sizing (epoxy, polyamide, polyurethane compatible) across 27 fibre types was conducted. A comparison of IFSS in thermoset epoxy and polymethyl methacrylate (PMMA) thermoplastic resin were

conducted and compared. For epoxy sized fibres, amperage was found to have an 'optimal' region for improvements to IFSS, however this optimal condition changed depending on the electrolyte concentration. For polyamide sized fibres, increased current density showed improvements in IFSS for low and moderate electrolyte conductivities however by applying both high current density within a highly conductive oxidation bath, IFSS results rapidly decline. For polyurethane, trends were highly variable across all conditions with no clear trends being determined. The true unique point of this research was the creation of a second order polynomial equation that attempts to provide a mathematic model to predict IFSS as a function of the three input variables. Within this relationship, current density is shown to have a positive impact on improved IFSS.[42]

2.4 Sizing

In the manufacturing process, subsequent to electrochemical oxidation, fibres go through a washing process to remove all excess electrolyte before entering a sizing bath. This is usually the last step within the carbon fibre production line. Sizings used to coat carbon fibres are typically proprietary blends of polymer, emulsifiers, anti-static agents, and stabilisers amongst a cocktail of other additives. The identity of these chemicals is withheld from the end user and are kept in strict confidence. The sizing layer is typically between 100 – 500 nm, depending on the dilution of the parent emulsion, though some studies suggest it is only 30 to 50 nm thick.[43-45]

Irrespective of thickness, it is typically between 0.5 – 1%, by weight, of the fibre, and the vast majority (80-90%) is comprised of film formers. The sizing assists in the processing of fibres into woven materials by protecting the fibre surface from abrasion, preventing the fibre from breaking at contact points, and keeping chopped fibre bundles together to make them easy to handle.[46] Also, according to a sizing manufacturer, it has benefits for material processing, by such mechanisms as protecting a chopper's blade life and reducing bundle fuzz generation. Sizing is usually selected by its 'compatibility' with the intended matrix. However, the compatibility term is not (or is poorly) defined, leading to sizing optimisations for a given resin being conducted empirically. Broadly, the resins for which sizings can be purchased are epoxy, vinyl ester, polyamide, polyurethane, polypropylene, polycarbonate, and polyphenylenesulfide, and thus a very large potion of the commonly used resins are encompassed within this list. Usually, a main constituent of the sizing, as indicated by the manufacturer, is a polymer (or oligomer) of the same type as the intended supporting matrix. For example, a sizing which is targeted towards a final application in polypropylene, will likely contain a portion of polypropylene including a maleated co-monomer to enhance compatibility and adhesion at the interface. Similar, scenarios are true for polyamides, polyurethanes, and thermosets. Also present, to ensure emulsion formation, are a range of surfactants that can be either anionic, cationic, or neutral in structure, and combinations of these (e.g. anionic/neutral) are often used in the same sizing formulation. These ionic or amphiphilic constituents are commonly not considered when investigating the effect of sizing on fibre-matrix adhesion. Therefore, while a sizing may be classed as compatible overall for a given resin, not all the constituents of that material may be optimal for that resin. Moreover, the fate of these surfactants, film formers, buffers, etc. is not clear as they may be removed from the fibre surface during deposition of the sizing. This further complicates the picture of the fibre-matrix interface and the effects of surface chemistry and physical mechanics.

The remaining 10 – 20% of sizing components are the lubricants, anti-static agents, wetting agents, colour modifiers, etc. Sizing can have several effects on the fibre such as discoloration, resin wetting, ease of chopping, reduction of static, fuzz, and bundle integrity. These can also effect the properties of the final composite part, including thermal stability, surface finish, water resistance, colour, and adhesion.[46] Sizing forms part of the region where the fibre and the matrix meet, known as the 'fibre-matrix-interface'. The interface displays a unique set of mechanical properties that differs from those of the individual constituents. An illustration of the carbon fibre matrix interface (Figure 4) and interphase, which is a key focus in the following sections, is provided below.

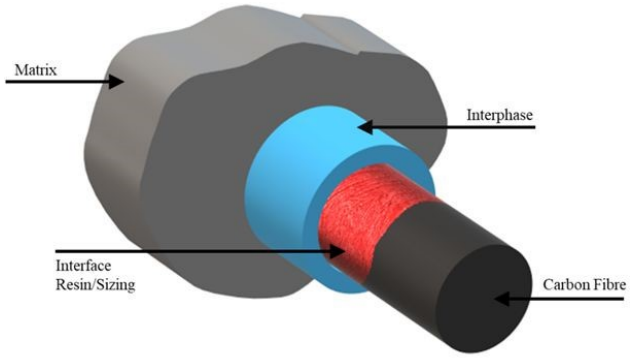

Figure 4 Illustration of interface and interphase within a CFRP composite.

The effect of sizing is not restricted to only having a positive impact on fibre and composite performance. Dilsiz *et al.*[47] reported that the sizing process itself caused fibre damage and decreased the tensile strength from 3.2 GPa of an unsized fibre to 2.5 GPa of a sized fibre. Interestingly, Bascom *et al.*[48] states that sizing agents in commercial use are only tailored for processing purposes and not to improve fibre-matrix adhesion. When looking at the effect of sizing on fibre surface roughness, the literature provides contradicting findings that suggest the application of sizing increases roughness and other studies report sizing decreases fibre roughness. These inconsistencies are commonplace throughout the carbon fibre literature as, again, this stems from the many unknown variables of manufacture, precursor type, and surface treatment conditions. Luo *et al.*[49] reports that sizing a CCF300 fibre, smooths its surface. In that case, two different sizings were used, one provided by Toho (J4 sizing) and one developed by Fudan University (A436). The roughness, as determined by AFM and reported as R_a, of unsized fibre (R_a = 88.5 nm), J4 sized (R_a = 71.7 nm), and A436 (58.9 nm) were described. The sized fibres were

~19% and 33% smoother for the J4 and A436 sizings, respectively. The same effect was found by Yuan *et al*.[50] where the roughness of unsized to sized fibres changed from 52.3 nm to 40.7 nm, respectively.

Alternatively, Yang *et al.* found that almost no difference (<2 nm) between unsized (~16.3 nm) and sized (~14.6 nm).[51] When examining the effect of sizing on roughness, the amount of sizing applied and subsequent effect on R_a was reported by both Zhang *et al*. and Stojcevski *et al* [52, 53]. The former found that a higher concentration of sizing resulted in a smoother fibre. While the latter, examined three dilutions of sizing with no meaningful difference in overall roughness of the sized fibres. Though it is important to note, in that instance, the sized fibres were ~40% smoother than the unsized samples.

Fernández *et al.* reported a slight increase in surface roughness (37.0 nm to 40.5 nm) after removing the sizing of commercially obtained carbon fibre fabrics (Hexcel).[54] These desized fibres were then resized with an in-house developed sizing or a commercially available material. Fibres treated to give a 0.7 wt% sizing of the diglycidyl ether of bisphenol a (DGEBA) (Figure 5) diosplayed a roughness of 33.9 nm. While a sizing of 0.7 wt% *N,N,N',N'*-tetraglycidyl-4,4'-diaminodiphenylmethane (TGDDM) resulted in fibres of 34.3 nm roughness.

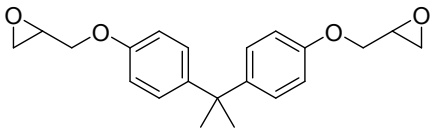

Figure 5 Chemical structure of DGEBA.

Similar results are reported by Kafi *et al.*[55] where unoxidized Panex 35 PAN-based automotive grade fibres had a surface roughness of 37(±17) nm and the sized fibres 33(±13) nm. Whereas the oxidized fibres revealed the highest roughness with 50(±10) nm.

In general, the removal of surface features from the fibre periphery is considered detrimental to adhesion, based on reduced mechanical interlocking. A possible mechanism by which the sizing reduces the roughness of the underlying fibre is outlined below (Figure 6). Here, depending on the level or sizing deposition, the longitudinal striations and corrugations are either exposed for light sizing, contoured, or entirely masked by the sizing material.

In contrast to the reports above, Dilsiz *et al.*[56] found that sizing would increase the roughness. In that study, Hercules AS-4 fibres were sized in polyetherimide (Ultem®), developed by General Electric, and poly(thioarylene phosphine oxide) (PTPO). The roughness of the unsized fibre was 7.5 nm, marginally increasing to 9 nm with the Ultem sizing, while a larger increase (to 15 nm) was found using the PTPO sizing.[57] The same effect was found by Hendlmeier *et al.* when investigating the surface roughness of unsized/untreated fibres versus sized fibres.[42] The unsized/untreated DowAksa fibres had an R_a value for roughness of 22 nm. Different sizings (epoxy, polyurethane, and polyamide) were used in this study and all fibres were rougher than the untreated/unsized fibres, ranging from an R_a of 22 – 38 nm after surface treatment.

The conflicting reports of the effect of sizing on surface roughness reinforces the observation that the influence of sizing on surface topography is mixed, with some studies suggesting it increases roughness while others say it smooths roughness.[58]

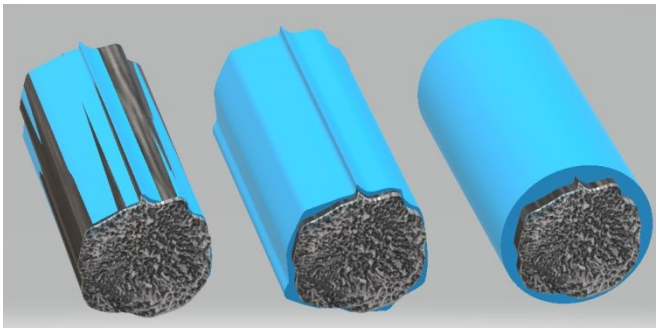

Figure 6 A schematic of potential sizing depositions on the surface of carbon fibres either sporadically coated (left), contoured (middle), or masking (right) the surface chemistry and topology of the underlying fibre.

2.5 Contradicting roles of sizing on adhesion

While sizing is an undoubtedly necessary feature to protect the fibres during the processing stages, it also influences the interfacial adhesion of fibres to the surrounding resin. Whether this is beneficial or not remains a point of conjecture within the literature. The following sections contain examples that have been grouped according to whether they find that sizing reduces, improves, or has no effect on the fibre-to-matrix adhesion.

2.6 Sizing as a detrimental influence on fibre-matrix adhesion.

A study conducted by Dai *et al.*[59] determined the IFSS of sized T300 and T700 fibres in an epoxy resin using the microdroplet test (sizing/resin compatibility was not divulged). The sized T300 sample was found to have an IFSS of 63.7 MPa, while desized fibres were significantly higher at 87.8 MPa, an improvement of 38%. An improvement for desized fibres, though much smaller in magnitude, of 9% was also observed for the T700 fibre sample (89.4 MPa compared to the sized 81.4 MPa). This would suggest that the inherent surface chemistry present between aerospace and automotive grade carbon fibres is fundamentally different.

The negative influences of sizing on IFSS was also found by Dilsiz and Wightman.[47] In that study, the IFSS in epoxy (DGEBA) for unsized Zoltek® fibres was compared to the same fibres sized with either Ultem® or polyurethane (PU) compatible sizing. Using SFFT, the unsized fibre had an IFSS of 28 MPa, which decreased by 31% when sized with Ultem® (19.4 MPa). This decrease in IFSS was larger for the PU sized fibres (13.5 MPa), exhibiting a 52% drop.

Cheng *et al.* investigated a comparison of sizing agents in two different epoxy resins, and the effect on IFSS.[60] Both epoxies had Epikote 828, a flexibilized diglycidyl ether of bishenol A, as a base material. However, the mixing ratios were different. Epoxy 1 had 57 wt% of the Epikote compared to 72 wt% of epoxy 2, and therefore, the amount of hardener was different

as well as the corresponding physical properties. As a hardener, Araldite GY298 and Nadic Methyl Anhydride (NMA) was used. The fibres for this study were composed of unsized fibre or those treated with wither an epoxy compatible sizing or an antistatic sizing. For both epoxy matrices the unsized fibres showed the highest IFSS, with IFSS values of 51.9 MPa and 66.0 MPa for epoxy 1 and epoxy 2, respectively. Almost no change was observed for the epoxy compatible sized fibres, with IFSS found to be 50.7 MPa and 64.3 MPa, respectively. Conversely, the presence of the antistatic sizing was clearly detrimental to interfacial adhesion, giving 43.4 MPa and 58 MPa, respectively.
An extensive investigation by Gnädinger *et al.* used a cross-section of sizings with various compatibilities (epoxy, polyurethane, polyamide, and commercially obtained polyurethane), determining IFSS in a polyurethane matrix.[61] In that instance, unsized fibres resulted in an IFSS of 84 MPa, a significant improvement compared to all of the sized fibre samples. Interestingly, the in-house developed PU sizing and the epoxy sizing were the best performing of the sized fibres, giving an IFSS of 71 MPa and 69 MPa, respectively. The commercially obtained PU compatible sizing resulted in a marked decrease in IFSS (61 MPa), with the polyamide compatible sizing being the poorest performing sample (53 MPa). This work emphasises why sizing optimisation has been (and still is) carried out empirically by most researchers and industries, despite the significant time and cost investment. This is especially true considering that an 'off the shelf' compatible sizing agent was one of the least suitable for its 'compatible' resin.

2.7 Sizing enhancing interfacial adhesion

In contrast to the reports above, the following studies have found that sizing is advantageous to interfacial adhesion and acts as an intermediate bonding layer between the fibres and the matrix.
In 1993, a study conducted by Drzal and Madhukar examined unsized fibre which had not undergone surface treatment (untreated/unsized), then sized these fibres with epoxy sizing, and surface treated unsized fibres.[44] Using the SFFT in epoxy, it was found that the epoxy sizing dramatically improves the fibre-matrix adhesion. A 119% increase (37.2 MPa to 81.4 MPa) was found for the epoxy-sized fibres relative to the surface treated/unsized. By evaluating the untreated/unsized fibres they found an IFSS of 68.3 MPa. Therefore, in a simplified view, the sizing component alone accounts for at least 13 MPa of this increase.
When a solvent-free polyamic acid (PAA) sizing was applied by Yuan *et al.* on unsized polyacrylonitrile-based fibres, a significant increase in IFSS was observed for adhesion in polyether sulfone (PES; 33.6 MPa to 49.7 MPa, being a 48% increase).[62] In that instance, IFSS improvement was attributed to a higher surface energy of the fibres provided by the very polar sizing agent, leading to better wetting. However, as the IFSS was determined by single fibre pull-out (SFPO), the test samples were heated up to 300 °C before testing which might have implications on converting the sizing, partially or completely, onto a polyimide (PI) type backbone.
As reported by Yuan *et al.*, an unsized, commercially sized (Takemoto S64-size), and a laboratory sized fibre was used to determine the interlaminar shear strength (ILSS) *via* short beam shear test in an epoxy matrix.[50] The laboratory sizing was an emulsion of maleic anhydride and glycidyl methacrylate, that were polymerised in the emulsion to generate a polymeric sizing. For unsized fibres an ILSS of 81.2 MPa was found, and the commercially sized fibres resulted in an increase of 6.8% to 86.7 MPa. While a 14.2% increase of the laboratory sized fibres was found (92.7 MPa) compared to the unsized fibres. It was stated that this is due to a better compatibility of the laboratory made sizing and resin, compared to the commercial sizing.
In the same study mentioned earlier by Gnädinger *et al.* it was found that within an epoxy matrix, the epoxy sized fibres perform better (64 MPa), though only marginally, than surface treated/unsized fibres (60 MPa).[61]
In work by Yumitori *et al.*, unoxidised and unsized fibres from Akzo and oxidised and sized fibres from Toho Rayon were examined.[63] A comparison of the IFSS (using SFFT) between un treated unsized (UTUS), surface treated unsized (TUS), surface treated (brominated epoxy) sized (TBrES), and surface treated PES sized (TPESS) fibres was undertaken in an epoxy and PES resin. An increase in IFSS was observed for both sizing types in both resin systems, where a 100% increase was observed from 20 MPa (UTUS in PES resin) to 40 MPa (TBrES) and a 75% increase to 35 MPa (TPESS). The enhancement in IFSS was assumed to come from the penetration of the sizing into the matrix. A different trend was observed for adhesion in an epoxy matrix. Although the IFSS of TBrES (25 MPa) and TPESS (~24 MPa) fibres was higher than the UTUS (~20 MPa), it was still lower than the TUS (~33 MPa) fibres. The low IFSS of the TPESS may be due to the brittle interface with a chemisorbed and physisorbed layer.
Paipetis *et al.*[64] also found that sizing is advantageous to interfacial adhesion, where unsized and sized fibres (sizing being EP-PH-BMI compatible) supplied by Soficar, were examined. The epoxy, provided by Ciba-Geigy, gave an IFSS increase of 20% for sized fibres (35 MPa to 42 MPa).
A 15.5% increase in IFSS was found by Liu *et al.* for sized vs. desized fibre in a poly(phthalazinone ether ketone) resin and Toray T700 fibres.[65] The sizing was removed by refluxing in boiling acetone, then resized via dip tank with a poly (phthalazinone ether ketone) (PPEK) sizing agent containing a phthalazinone-containing diamine (DHPZDA) moiety. The desized fibres posessed an IFSS of 64.5 MPa, with the resized fibres increasing to 74.5 MPa, showing a clear benefit of the sizing agent on adhesion.

2.8 Sizing is Impartial

Lou *et al.* stated that sizing only fulfils the purpose of a lubricant since decreasing the roughness is a negative effect on the interfacial adhesion and therefore the right choice of sizing is only determined by being compatible with the matrix.[49] Similarly, Gnädinger *et al.* highlights the requirement of

matching sizings for the desired resin to facilitate both fibre-matrix adhesion and protect the fibre during processing.[61] In a study conducted by Wu *et al.* the IFSS was determined using a microbond test with different high strength carbon fibres from different manufactures in both an epoxy and a bismaleimide (BMI) resin.[66] A comparison of the results was drawn between commercially sized and desized fibres highlighting that a definite conclusion from that work cannot be made since each fibre sample (sized and desized) and resin combination provides unique properties. It is stated that roughness and oxygen content are less effective at influencing IFSS than wetting (contact angle) and reactions of sizing and resin. This seems conflicting as the wettability and reactions of the sizing would be influenced by the oxygenous species on the fibre surface.

2.9 Concurrent Effects

The variables associated with electrochemical oxidation and sizing have thus far been considered independently. There remains a question regarding how these surface treatments may influence one another concurrently to impact final fibre properties.

Stojcevski *et al.* provided a comprehensive study into the effects of altered sizing content and electrochemical oxidative current density across 15 fibre types.[53] By quantifying relative improvements to IFSS attributed to oxidation and sizing separately, comparisons between 'true' IFSS, and 'predicted' IFSS may be made. For epoxy system RIM935/937 the difference between true and predicted value was below 14.8%. For epoxy system DGEBA/DDM, this difference was below 30.8%. This suggests that there may be some masking in IFSS performance occurring between the two treatment mechanisms. It is possible that the two variables work independently to improve fibre-to-matrix adhesion, however the degree to which this occurs may also depend on the resin system being analysed. Further research into such concurrent effects is required.

Hendlmeier *et al.* similarly investigated the effects of electrolytic conductivity (8, 16, 24 µS/cm), current density (0.5, 1.0, 1.5 A/m^2) and sizing variation (epoxy, polyamide, polyurethane) for both epoxy and thermoplastic resin.[24, 42] When comparing the results of both studies, the underlaying chemical structure of the surface treatment seemed to play a major role on the effect of interfacial adhesion. Different treated fibres performed better in different resins.

2.10 Summary of Traditional Surface Treatments and Sizings

Conflicts within the literature are likely derived from studies investigating fibres with different specifications and from different manufactures. The next unknown factor comes with commercially available sizing. Most suppliers label their sizing as 'compatible' with a given resin; however, the reasons for this compatibility are unclear. To combat this, several studies reported the effects of prepared sizings, investigated on a laboratory scale. The next variable is the resin matrix. Even though most of the research is done with epoxy resin, it is rarely provided from the same supplier between studies. Therefore, subtle changes in chemical compositions, curing regimes *etc.* can be expected and lead to different interactions at the fibre surface. Additionally, looking at a large body of research in which different resin systems were used, other than epoxy, makes it difficult to compare results between studies. Another pertinent factor is studies in which fibres are desized and subsequently resized. It remains unclear what effect desizing has on the fibre surface morphology, chemical composition, and if residual sizing is present. Given these variables, it is difficult to compare the interfacial adhesion of a desized fibre to a commercially sized fibre or even an unsized fibre.

The extent of this variation between techniques and samples precludes the outright identification of sizing's distinct effect on interfacial adhesion. This discrepancy exists through difficulty in aligning factors completely enough to be able to draw scientifically fair comparisons, and this issue may not be rectified in future investigations.

3.0 Plasma Treatments and Modification

Chemical bonding and physical interlocking serve as crucial requirements for improving interfacial adhesion between carbon fibres and the supporting resin. A powerful method towards achieving both properties is via plasma treatments.

In most systems, plasmas form by the ionization of a gas or vapor by thermal excitement and/or by applying strong magnetic fields. In such highly energetic systems, plasmas comprise of molecules or atoms that exist as positively charged ions (usually by the abstraction of an electron) and are countered by negatively charged free electrons, making the entire system (approximately) electrically neutral.[67]

Upon exposing a material or substrate to a plasma source, chemical functional groups can be imparted from the plasma onto the surface of a material. Furthermore, by altering the exposure limits of the substrate, the degree of surface chemistry imparted can be adjusted. Often these exposure limits are varied via modulation of magnetic fields, temperature, substrate distance from source, or the plasma source itself.

Plasmas can operate under a wide set of parameters, and because of this, a single variable adjustment (*i.e.* flow rate, time, substrate distance, power and frequency) can lead to dramatic effects on the physical and chemical properties of the surface.[68] For the case of carbon fibres, most modifications focus on their direct exposure to a plasma source. In some instances, a chemical vapor with a relatively low ionization energy is also injected into the system - depositing a film onto the substrate surface. A monomeric vapor can also be injected, reacting with highly energetic free-electrons and initiating free-radical polymerisation within the vapor phase. In both cases, thick (100 nm - 1 mm) films can be deposited or grown on the carbon fibre surface. In this section plasma treatments that evidently lead to monolayer-grafted chemistries are grouped into non-polymer forming plasmas, whereas those that form thin films are considered as polymer-forming plasmas.

3.1 Non-polymer forming plasmas

These plasmas are usually sourced from a combination of elemental gases (such as Helium, Argon, Nitrogen, Oxygen, etc), however some exceptions include ammonia and some fluorocarbon sourced plasmas.[69, 70]

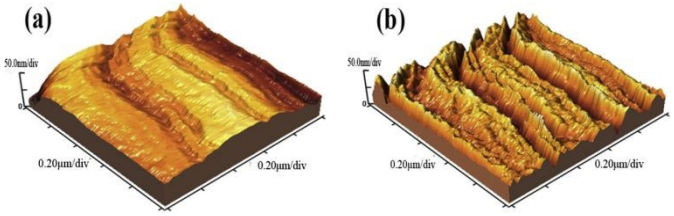

Figure 7 (left) AFM surface profile of untreated carbon fibre, (right) carbon fibre exposed to 125 W atmospheric plasma (1 min). Reproduced with permission.[71] Copyright, 2016, Elsevier Inc.

In many cases these plasmas are used as a tool to remove organic contaminants on the surface of carbon fibres and facilitating the removal of weak boundary layers. At higher energies, ablation of the surface can mill into the fibre, increasing fibre surface area, and enabling greater fibre wettability with increased adhesion (Figure 7). Though, of course, excessive ablation can lead to deterioration of the physical properties of the fibres.Depending on the plasma source and energy levels used, proton-abstracted sites can react further either within or outside the plasma to typically install a broad range of desirable functional groups; such as carbonyl, carboxylic and hydroxyl groups.[72]

Elemental plasmas

Over the last decade, a number of studies have investigated the effect of elemental plasmas on the interfacial adhesion of carbon fibres. In many instances, these studies perform plasma treatments at atmospheric pressures, circumventing the requirement of a pressure chamber. Accordingly, these conditions should be favoured under the context of scale-up as atmospheric plasma apparatus are the most ideal for retrofitting onto existing industrial carbon fibre production lines. As such, treatments that use atmospheric conditions are clearly stated.

In 2011, Zhao and co-workers used helium/oxygen gas blends at atmospheric pressures to install polar chemistries over a range of short treatment times (1-5 minutes).[73] After 1 minute, very little improvement in the adhesion was obtained (6.9%), however after 5 minutes adhesion rose significantly, 61.2%, relative to untreated and unsized fibres (12K AU4, Hexcel Coorperation, USA). No decrease in the tensile properties of the fibres was observed; however, it was found that surface roughness increased slowly for treatments under 3 minutes (by less than 15%), but then dramatically after 5 minutes (55.8%). Interestingly, XPS data suggests the sample exposed for 3 minutes showed the highest level of oxygen content, despite having only marginal adhesion gain. Thus, the authors concluded surface roughness played the dominant role for adhesion in this study.

Ma *et al.*[74] investigated low-pressure (13.33 Pa) oxygen plasma sources and reported similar results. After two minutes, a maximum increase of up to 28% in ILSS was observed, using a room temperature oxygen plasma. Treatment times ranged from 1 to 5 minutes and plasma power from 50 – 200 W. Additional findings concluded that as plasma power and exposure time grew, fibres began to degrade. SEM data showed an increase in surface roughness as treatment time continues, although no quantitative roughness data was available. FTIR spectroscopic data of the fibres show a very slight increase in carboxyl and carbonyl stretches, though this may be attributed to background fluctuation.

Borooj and co-workers performed a thorough investigation of low-pressure oxygen plasmas (13.3 Pa) under various operating parameters, including oxygen flow rate, power and treatment time.[71] Maximum adhesion gains were observed within the first minute of treatment time; from 65.57 MPa of the control, to 85.92 MPa (31% improvement). However, as treatment time progressed after 5 minutes, ILSS decreased by around 19% from the peak measurement to 68.62 MPa (Figure 8). Faster oxygen flow rates improved ILSS; increasing from 20 standard cubic centimetres per minute (sccm) to 100 sccm improved ILSS by 8%. The study concluded that power has a marginal effect on ILSS while lower energies providing the optimal improvement. Plasma treatment increased the surface roughness as high as 65% relative to pristine fibres, which is believed to improve wettability and mechanical interlocking with polymer resins.[75] As treatment time and power increased, so too did the risk of partially destroying the surface of the fibre, and a decrease in roughness/wettability was observed, alongside a reduction in ILSS.

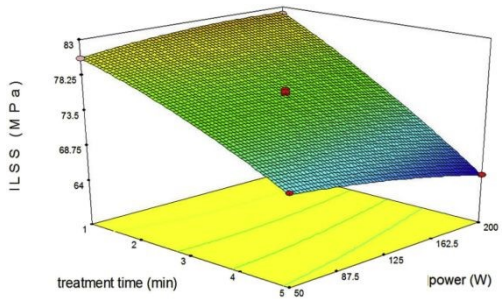

Figure 8 Effect of treatment time vs power (W) on carbon fibre adhesion (ILSS) from Borooj and co-workers. Adapted with permission from reference.[71] Copyright, 2016, Elsevier inc.

Zhang and co-workers obtained an 18% IFSS improvement in epoxy by using a 1:5 oxygen/argon plasma source under atmospheric pressures.[76] Discharge power was 120 W, and the fibres were exposed for 90 seconds at ambient temperatures. The authors further increased fibre adhesion by performing a post-polymerisation step with maleic anhydride. This was achieved by submerging the fibres in maleic anhydride for 30 minutes at 60 °C, then curing at 170 °C for 5 minutes. After post-polymerisation, a 38% improvement in shear strength was observed. Wettability increased after plasma treatment, together with a subtle improvement in oxygen content, determined by XPS (17.1% for control, 20.1% for plasma modified), though no data on surface roughness was reported.

Similarly, Sun *et al.* used an atmospheric helium plasma as a form of pre-treatment before pyrolytically depositing carbon

fragments *via* chemical vapor deposition (CVD), with ethanol as the carbon source.[77] Using 100 W of RF power for generation, the plasma was applied to the carbon fibre tow for a duration of 1 min, with the tow pulled through the plasma *via* a step-motor setup 1 mm from the plasma source. A 10% improvement in IFSS, *via* SFFT, was observed in epoxy resin, though the improvement is attributed to the increase in surface roughness (increasing from 33 nm to 39 nm). XPS analysis showed a slight decrease in oxygenated content relative to unmodified fibres. After pyrolytic deposition (using CVD conditions) a 15.7% improvement in tensile strength as well as a 27.9% improvement in ILSS, obtained via short beam shear testing, was observed. XPS data showed slight increases in oxygen content after deposition of pyrolytic carbon (PyC), as well as a decrease in water contact angle (Wilhemy model, from 79.8° to 73.2°). Diiodomethane contact angle data was dramatically decreased (from 54.5° to 32.1°) after PyC deposition.

Montes-Morán *et al.* exposed pristine, pitch-based, ultra-high modulus (UHM) fibres to an oxygen plasma source under low pressures (10 Pa). A significant improvement of 600% in fibre-to-matrix adhesion was obtained (6 MPa to 42 MPa in epoxy resin).[78] XPS data highlighted that after exposure to an oxygen plasma source, the oxygen count rose dramatically from 1.7% to 6.9%. In addition to this, Scanning Tunnelling Microscopy (STM) and Scanning Electron Microscopy (SEM) acquisitions revealed a similar roughness profile of plasma treated fibres to that of untreated carbon fibres.

3.2 Ammonia based plasmas

Interestingly, one study showed that carbon fibres exposed to an ammonia plasma source had little improvement on adhesion in epoxy resins. In that work, Moosburger-Will *et al.* exposed SIGRAFIL® C30 T050 carbon fibres (directly after carbonization) to a 90 W ammonia plasma source over a variety of treatment times and low-pressures (50 Pa).[69] XPS analysis highlighted a dramatic increase in nitrogen content, about a factor of 2 greater than the oxygen content, which showed little change when compared to the oxygen content of unmodified carbon fibres. Capillary rise contact angle experiments showed an increase in fibre wettability, with the maximum hydrophilicity obtained after 16 minutes exposure (11°, *cf.* 49° for untreated). No difference in the surface roughness was observed, as determined *via* AFM.

Despite this increase in wettability and nitrogen content, no discernible difference in adhesion (within error) was obtained in epoxy, measured *via* single fibre push out tests. The authors propose that the presence of nitrogen based functional groups serve little role in the improvement of interfacial adhesion.

That conclusion is challenged somewhat by Lew and co-workers, who treated pristine carbon fibres with an ammonia/ethylene blended plasma as a pre-treatment step for depositing SiO_2 nano particles under low pressures (~10 Pa).[79] The authors performed SFFT on these plasma treated fibres and reported a 141% improvement in adhesion in epoxy resin. After SiO_2 deposition this adhesion rose to as high as 217% relative to control. Plasma power was maintained at between 60-68 W for 20 minutes, followed by a NH_3 gas purge for 5 minutes. Interestingly, no decrease in tensile properties was observed, even after the extended plasma exposure time. The variances between Lew and Horn may originate from differing surface roughness, particularly caused by the polymerisation of ethylene in the latter. However, no data on surface roughness was published by Lew, and so the exact reason for the observed improvements remains inconclusive.

3.3 Plasma polymerisation

A number of polymer deposition techniques have been demonstrated on carbon fibres; including magnetron sputtering, pulsed laser deposition and plasma enhanced chemical vapor deposition (PECVD) to name a few.[80-82] In general, these treatments lead to dramatic alterations in the surface morphology and chemistry, with the deposition of polymer films up to 1 mm thick.

Plasma polymerisations are widely utilized in the surface treatment industry, particularly due to their low operating cost, low operating temperatures (in the case of atmospheric plasmas), rapid treatment times and low environmental waste. Recent applications of plasma polymerisation include film deposition for chip fabrication, solar cells, and surface treatments for medical implants.[83]

3.4 Plasma enhanced chemical vapor deposition (PECVD).

Wei and co-workers fabricated graphene nano-walls (GNW) onto the surface of M55j carbon fibres (Toray, Japan) using a radio frequency plasma-enhanced chemical vapor deposition (RF-PECVD) technique under low pressures.[84] This process involved the desizing of the carbon fibres using an acetone reflux method before placing them in a quartz tube filled with a H_2:CH_4 gas mixture (1:1). A 250 W RF was applied at 750 °C to grow GNWs that increased surface roughness dramatically, creating wall heights of up to 0.618 µm (Figure 9a).

The GNW's were grown over different treatment durations, five in total at 15 minute intervals ranging from 0 minutes to 60 minutes, and an extended 90 minute treatment. It was found that the nano-wall height has an almost linear growth rate, however the length of graphene walls plateaued at ~300 nm after 60 minutes. The authors reported IFSS improvements of up to 222.8% (peaking at 30 minutes exposure time) and ILSS gains upwards of 41.1%. However, they also noted a 9.5% reduction in tensile strength after 15 minutes of treatment, which was within error for the values obtained from the proceeding treatment intervals.

Taking these results in hand, Wang *et al.*[85] grew GNW under slightly different operating conditions. Firstly, the authors selected lower temperatures (480 °C vs 750 °C), hoping that lower temperatures will inhibit the fibre degradation events reported by Wei and co-workers.[84] Secondly, the authors opted for a higher RF Power (1000 W *vs* 250 W). This allowed wall growth to form within 10 minutes, and as high as 8 µm (Figure 9b).

Surface roughness increased dramatically; from 15.9 nm for control fibres, to 191 nm for coated fibres. Surface wettability also increased as a function of wall height; with an observed contact angle of 51.8° for control, to 28.7° for surface coated

fibres. Tensile strength was unaffected after treatment, suggesting that lower temperatures are ideal for fibre preservation. IFSS data was obtained *via* SFFT, with the highest performing wall height (4.2 µm) peaking at 112.4 MPa (118.7% improvement *vs* control). This result is significantly lower than that obtained by Wang and co-workers (222.8% improvement *vs* control). The authors suggested that this could be attributable to the formation of voids from within the GNW, degrading the physical properties of the GNW wall and hence its ability to adhere to epoxy resin.

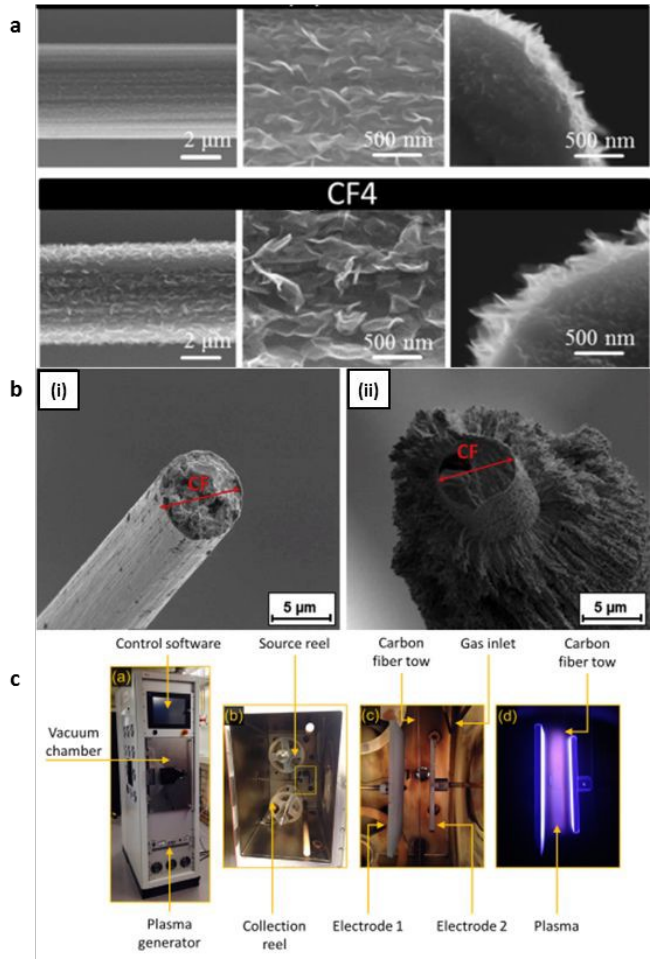

Figure 9 a) Graphene nano-walls (GNW) grown onto the surface of carbon fibres. Adapted with permission from reference.[84] Shared under creative commons licence. **b)** (i) untreated carbon fibres, (ii) High density graphene nano-walls (GNW) grown onto the surface of carbon fibres. Adapted from reference.[85] **c)** Reel-to-reel instrumentation for the manufacturing of carbon fibres endowed with graphitic petals (GP) and graphene nano-walls (GNW). Adapted with permission from reference.[86] Copyright 2018, Wiley-VCH GmbH, Weinheim

Interestingly, a similar treatment using radio-frequency plasma-enhanced chemical vapor deposition (RF-PECVD) was reported by Fisher and co-workers that achieved reel-to-reel surface modifications at low pressures (10-20 mbar).[86] In this work, the authors produced graphitic petals (GP) on the surface of plasma-treated carbon fibres, as well as GNW, using a mixture of gases (Ar, H_2, CH_4, N_2 & O_2) (Figure 9a).

Virtually no GNW or GP was observed in the cross-sectional centre of the tow; however, consistent film morphologies were obtained up to around 20 fibres deep. This suggests that for this treatment method to be effective on scale-up, the carbon fibres would need to be 'fanned out' for consistent surface modification throughout the tow.

Zhang *et al.* grew carbon nanotubes (CNT) on the surface of carbon fibres using a tube-furnace and microwave generated plasma discharge within a H_2/CH_4 mixture. This microwave assisted plasma enhanced chemical vapor deposition (MPECVD) allowed for the growth of CNTs onto T700 carbon fibres (Toray) at low pressures (500 Pa).[82] MPECVD Treatment durations of 0, 5, 10 and 15 minutes were applied to carbon fibres, which had been desized *via* refluxing in acetone at 80 °C for 48 hours. The MPECVD treatment used a 9.15 MHz microwave frequency at 450 °C and resulted in a decrease in fibre mechanical properties for treatments exceeding 15 minutes. Nevertheless, the highest IFSS measured (129.92 MPa) was for the fibre subjected to an exposure of 15 minutes; realising a 153% IFSS improvement relative to desized carbon fibres (51.35 MPa). It is worth noting that the authors modified only around 100 fibre filaments at each time interval for this study, and thus scale up would provide significant challenges.

Recently, Karakassides and co-workers grew graphitic flakes on the surface of sized carbon fibres and investigated the adhesion properties in epoxy resin.[87] These flakes were deposited on the surface using MPECVD under very low pressures (~ 1 Pa), with the applied power varied at 500, 800 and 900 W. Exposure time was kept constant at 5 minutes, and the methane carbon source was introduced at a rate of 20 sccm, and at temperatures ranging from 300 °C to 600 °C. Prior to CNT deposition, the fibres were treated with a nitrogen plasma for 2 minutes. Additionally, the fibres were cooled under a constant flow of nitrogen after deposition (flow rate of 50 sccm). However, only one sample had its IFSS evaluated (800 W at 600°C) in epoxy resin, showing an IFSS increase of 102% IFSS, from 15.10 MPa (control) to 30.43 MPa (treated sample).

3.5 Wet Chemical Modification

In this section we will focus on the use of more traditional approaches to modify carbon fibres, where they have been treated more like a chemical, rather than a material upon which to deposit another substance. Typically, these fibres have undergone a surface reaction while submerged in solution or similar medium. A very common means of undertaking this approach to surface modification is to first prepare the surface for derivatization. The oxidation of desized carbon fibres by emersion in concentrated nitric acid at reflux is routinely used. This process installs a range of functional groups on the fibre surface that can be assessed immediately for interfacial benefits. Alternatively, the installed chemical functionalities (e.g., COOH, PhOH, CH_2OH, etc.) can be used for molecular elaboration of the carbon fibre surface via esterification or carbodiimide chemistries.

Extensive research has been conducted to identify the effects of acid surface treatments on carbon fibre and its ability to interact at the fibre-resin interface. In general, oxidation is seen to improve the adhesion of carbon fibres to a range of polymers, though, as mentioned above it can also result in deleterious

effects on the original strength and stiffness of the carbon fibres. There is a large amount of conflicting data regarding the point at which the trade-offs shift from the benefits gained from functional group installation to physical properties dominated by the deterioration of the underlying fibre.

In one study,[88] the effects of treatment time in concentrated nitric acid were analysed over varying intervals (0 to 160 minutes). Initially, the tensile strength, degree of surface oxidation, and surface energy all increased before the tensile strength and surface oxidation stabilised after 20 min by no longer show obvious improvements. The fibre diameter was seen to rapidly decrease after 40 minutes of treatment, coinciding with a decline in fibre strength, thus 20 minutes was identified as the optimal treatment duration. Another publication indicated similar trends, whereby exposing carbon fabric to nitric acid for extended periods of time decreases the properties of the material. In this study, Tiwari *et al.*[89] found that treatment beyond 90 minutes was detrimental to the properties of the fibre.

Further attention was given by Tiwari *et al.*[90] toward finding the optimum length of time for nitric acid treatment to achieve an increase in adhesion with the matrix without inflicting strength reducing damage to the fibres. Rather than use a bundle (or tow) of fibres, the nitric acid treatment in this case was applied to a carbon fabric for various time intervals (15-180 minutes). The interfacial adhesion was conducted using a polyetherimide matrix and evaluated for mechanical and abrasive wear properties. Like their previous work, it was observed that a 90-minute treatment time was most ideal to achieve maximum possible enhancement in adhesion and tribological properties. Analysis by FTIR revealed adhesion was improved due to the inclusion of oxygenated functional groups combined with increased surface roughness, assessed via SEM. Furthermore, the ILSS and flexural strength were maximised using a 90-minute treatment (71% and 29% improvements, respectively) though the tensile strength, showed maximum strength after a 60-minute treatment.

Similar work was carried out by Vautard *et al.*[91] whereby IMS 5000 fibres were subjected to a series of oxidation times, from minutes to hours in boiling nitric acid, and the surface chemistries were examined. In this work, it was found that a rapid increase in oxygen was observed in the first few minutes, though after 60 minutes the oxygen content of the surface plateaued. This plateau was attributed to the alcohol and acid groups undergoing conversion to esters and ethers etc., thereby giving no net gain in oxygenated species. Though, it should be noted though that this conclusion remains speculative as no supporting spectral or physical data was provided.

The work by Vautard et al.[90] also included the IFSS of the oxidised fibres in an acrylate derived resin cured by either UV or electron beam (e-beam) irradiation. Oxidised fibres in UV cured resin showed up to a 20% improvement in IFSS, but the same samples in e-beam cured resin were all significantly lower. This suggests that the mechanism of curing influenced the adhesion, and characterisation of nano-roughness did not correlate to adhesion further supporting a chemical interaction at the interface. This effect is potentially due to the presence of persistent radical species on the surface of the carbon fibres, stabilized due to the extensive conjugated aromatic network, but again, this remains speculative.

The effect nitric acid treatment duration has on surface heterogeneity of the resulting oxidized carbon fibres has also been examined,[92] with treated fibres characterised by SEM, AFM, XPS, and Raman spectroscopy. These analyses indicated that the longest exposure (180 minutes) resulted in the most heterogenous surfaces. Notably, fibres treated for 120 and 180 minutes show an increase in the overall nitrogen content. This excess nitrogen was at a higher binding energy in the N1s XPS spectra (*c.f.* ~405 eV) suggesting the incorporation of oxidized nitrogenous species onto the surface via aromatic ring nitration or possibly anion intercalation. The Raman and AFM data indicates the etching process removes surface-bound amorphous carbon and/or weakly bound graphene surface sheets. This latter point is consistent with the previously discussed reports of reduced fibre diameter after extended etching periods.

Older reports have similar findings,[93] suggesting the strength of the fibre increases with initial nitric acid treatments, but eventually decreases for prolonged duration of treatment. Collectively, this indicates that prolonged treatments of both concentrated and dilute nitric acid can etch pits on the fibre surface, decreasing fibre strength, also longer treatment times correspond to a more significant weight loss. Nevertheless, the authors suggest that both mechanical properties and fracture behaviour are improved with physical interlocking and chemical bonding of fibres and matrix.

Another report,[94] identifies that nitric acid oxidation treatments can be used to generate acidic functional groups on the fibre surface, with that the acid capacity (typically determined by titration with an hydroxide base) of the carbon fibres increasing linearly with increasing oxidation time. Of the functional groups found to exist on the fibre surface, the majority were carboxylic acids, though it should be noted that phenolic alcohols may also react with hydroxide anions and thus contribute to these data. This work found both tensile strength and weight decrease with extended treatments, as is consistent with previous and later reports. Following this, subjecting the fibres to a second treatment of refluxing in sodium hydroxide, was found to remove partially oxidised graphitic fragments.

Conversely, Yusong *et al*.,[95] also using a nitric acid treatment, proposed that fibre-matrix, adhesion gains observed in ultra-high weight polyethylene was due to the treatment increasing the morphological features of the fibre surface only, and not due to the installed chemistry. This was primarily attributed to the striations along the fibre axis and little focus was placed by the authors on the fibre surface chemistry.

Nitric acid treatment on short fibres (< 5 mm) has also been conducted.[96] These fibres were treated with ethanol and concentrated nitric acid prior to their addition to an epoxy resin used to generate laminates by infusion into carbon fabrics. The effects of oxidized short fibre content and treatment time were examined and the ILSS of composites comprising of oxidised fibre was consistently higher than the ILSS of untreated fibre. This effect was observed at very low short fibre loadings of 0.07

wt%. Interestingly, the introduction of ethanol to the oxidation solution extended the optimal treatment time to 4 hours for improvements in ILSS of the composite. SEM indicates that the surface of treated fibres feature deep gullies and a large number of punctate spots and bumps in comparison to the untreated fibre. Whether or not the introduction of the organic solvent influenced the optimal treatment time by diluting the etchant or if it facilitated additional reactions (e.g. Fischer esterification) with functional groups on the fibre surface were not discussed.

Similarly, oxidation of meso-phase pitch-based carbon fibres using nitric acid showed intercalation of the nitrate anion into the graphitic structure. This was after passing a current through the material and submerging in nitric acid, followed by heating at 100 °C. XRD was used to examine interlayer spacing which was consistent with ion intercalation,[97] and is consistent with the reports of oxidised nitrogen being present on the fibre surface, described above.

In a study by Fei *et al.*[98] carbon fabric was treated with nitric acid for 2 hours under hydrothermal conditions (100, 120 and 140 °C). The introduction of oxygenated functional groups was supported by FT-IR analysis and an increase in hydrophilicity was confirmed via the measurement of contact angle. While adhesion was not explicitly examined in this work, the friction and wear behaviours of the fibres were evaluated. The carbon fabric treated by hydrothermal oxidation led to changes in the surface morphology of fibres and the appearance of carbonyl groups. The authors made a composite with the modified fibres that showed improved physical properties, attributed to enhanced interfacial adhesion, though ILSS was not measured. Hydrothermal oxidation treatment of 100-120 °C improved the tribological properties and would be beneficial for abrasive wear performance, though increasing the hydrothermal temperature to 140 °C decreased the fibre strength.

A similar approach was taken by Zhang *et al.*,[99] but the oxidation and thermal processes were carried out separately. Carbon fibres were examined after being soaked in nitric acid for a set time (30, 60, 90, 120, and 720 min) before subjecting them to elevated temperatures in a muffle furnace (350-550 °C). The authors state that soaking for 90 minutes and heating at 420-430 °C gave an optimal ratio of micromechanical interlocking via surface etching and minimal property degradation.

The previous two articles highlight a persistent inconsistency within the literature, whereby similar fibre treatments result in variable outcomes. While some variation would be expected between reports, this example shows a stark contrast between optimal treatments. This is to say that the research has been conducted diligently and thoroughly, though the fibre origin, processing conditions, and precursor are all unknowns and thus provide an uneven foundation to compare results.

Around a similar time, Ozcan *et al.*[100] examined only thermally treating carbon fibres (up to 900 °C) under a nitrogen atmosphere. Monitoring the C, N, and O percentage by XPS showed rapid losses in oxygen content (18% down to 13%) when heating from room temperature to 100 °C, possibly via the loss of surface bound water. Further to this, heating from 400-900 °C resulted in almost complete removal of oxygenated species (11% to 2%) via the release of CO_2, analogous to the thermal reduction of graphene oxide. The fibre-matrix adhesion within a vinyl ester resin was improved for thermally treated fibres, coinciding with a change in failure mode suggesting changes to the interfacial interactions of the thermally treated carbon fibre samples. The authors postulate that the heating process results in the formation of radicals on the surface that can react with the vinyl ester groups, thereby increasing adhesion.

As noted above, the oxidation of carbon fibres can lead to a reduction in the physical properties of carbon fibres via overoxidation. This effect seems to be enhanced by sulfuric acid, as supported by work carried out by Wang *et al.*[101], where fibres were acid treated (3:1 v/v H_2SO_4 and HNO_3, respectively) for different durations. The optimum treatment time was 15 min, as determined by improvements in interfacial shear strength, fracture toughness and tensile strength. However, prolonged exposure (after 30 mins) to the surface treatment resulted in the introduction of surface flaws which lead to a reduction in properties. These times are significantly reduced from those reported in nitric acid solutions alone and are possibly due to the enhanced formation of nitrous acid (HNO_2), the 'active' oxidative species.

Studies have been conducted to compare the chemical and physical impact of various chemical treatments.[102] Carbon fibres were treated with hydrochloric acid and nitric acid as well as argon and oxygen cold plasmas. To evaluate the changes imparted to the CF surface, AFM, SEM, XPS, tensile strength and Raman techniques were used. These analyses found that the nitric acid treatment (durations of 5, 10 and 20 minutes) caused the most pronounced chemical changes to the surface, introducing the most extensive chemical functionality and increased surface roughness. However, the nitric acid samples observed a larger decrease in tensile strength compared to fibres treated with hydrochloric acid, again consistent with the oxidative nature of the solvent, the proposed etching, and the observation of increased surface roughness.

An alternative approach to oxidative surface modification was taken by Koutroumanis *et al.*[103] that focused on using a mild chemical process to functionalised CFs via an epoxidation reaction at room temperature. Their treatment consists of immersing the fibres in a solution *meta*-chloroperoxybenzoic acid (*m*CPBA) to epoxidise the fibre surface, installing chemical groups which can be used as reactive synthetic handles towards nucleophiles. Presumably this is targeting isolated alkenes in non-aromatic systems, as this approach typically does not work for the epoxidation of aromatic rings due to their stability imbibed by resonance. The authors used XPS analysis to quantify the carbon and oxygen presence on the fibre surface. These results indicate a significant increase in oxygen, including oxygen species attributed to epoxides on the carbon fibre surface. Furthermore, a 2.3-fold increase in the maximum interfacial shear stress was observed for the treated fibres in an epoxy resin, being 3.3 MPa for untreated fibre, 4.7 MPa for a 2-minute treatment, and 7.7 MPa for a 5-minute treatment. These increases were attributed to the additional chemical bonding by cross linking reactions between the epoxy resin and the oxygen moieties.

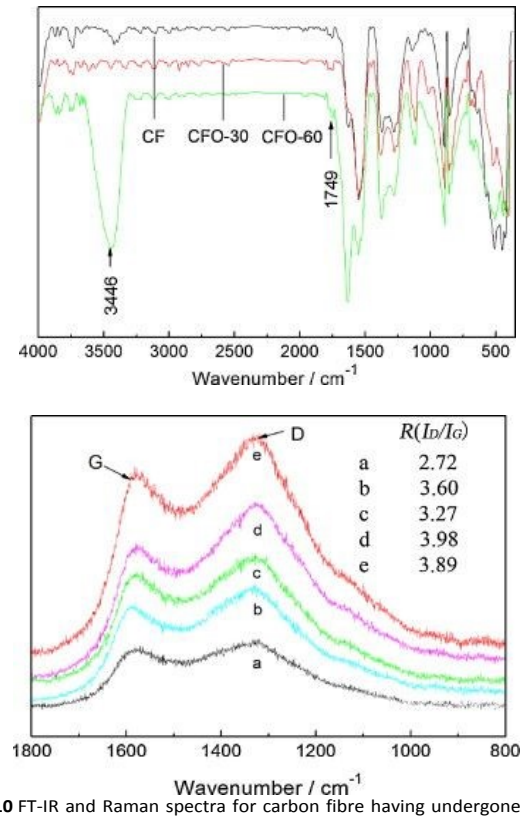

Figure 10 FT-IR and Raman spectra for carbon fibre having undergone chemical oxidation. Reproduced with permission from reference.[104] Copyright 2012, Elsevier Ltd.

Objectively, the ring opening of the surface bound epoxides by a *bis*-amine hardener in an epoxy resin is not likely, as epoxides typically react via an S_N2 reaction requiring the nucleophile to approach the epoxide from 180° behind the oxygen atom. In this instance, this reaction scenario is not possible as the fibre itself prevents this orientation of nucleophile. It is possible, however, that the epoxidation has been carried out on isolated alkenes, plus there is also the possibility that hydroxy and phenolic groups have been oxidised to the corresponding aldehyde or ketone which can react with the amines in the epoxy resin formulation. Additionally, this approach benefits from no notable alterations to the surface morphology of the fibres observed by SEM.

In other work,[104] CF was modified by oxidation in a mixture of H_2SO_4 and $KClO_3$, followed by subsequent treatment with a silane coupling agent (γ-aminopropyltriethoxysilane, APS). The intention behind this strategy was to increase chemical reactivity at the fibre surface while simultaneously increasing the fibre surface area and roughness. When the carbon fibres were oxidised, the oxygen content increased, expressed by an increase in the O/C ratio. Further treatment of these fibres with APS increased the C-O-R content, while concurrently decreasing the presence of O-C=O groups. The surface characteristics and morphological changes of these treated fibres were investigated by SEM, XPS, Laser Raman Spectroscopy (LRS), and FT-IR (Figure 10). These showed that significant changes to the graphitic/amorphous structure of the carbon fibres was not significantly changed due to acid treatment, shown by D/G band ratios. The minor changes in the I_D/I_G ratios of the treated fibres did suggest a small increase in the disorder of the aromatic surface, consistent with the installation of sp^3 hybridised carbons. This was consistent with the FT-IR spectra of these fibres, where the progressive growth of peaks at 3446 cm^{-1} and 1749 cm^{-1} was attributed to the installation of OH and COOH groups, respectively.

ILSS was examined in a phenolic resin matrix, and the APS treatment improved ILSS (12%) compared to the acid-only pre-treatment. The authors concluded this improvement is due to an increase in chemical bonding, rather than the enhanced mechanical interlocking gained when fibres were subjected solely to an acidic pre-treatment. The choice of a phenolic matrix to examine ILSS is unusual, as the presence of amino terminated small molecules on the fibre surface would not, theoretically, interact favourably with the highly aromatic resin. Though, it is possible that hydrogen bonding (or acid-base interactions) may occur between the acidic phenolic protons and the basic amine groups.

The use of oxidation followed by molecular elaboration of carbon fibre surfaces with silicon containing materials has been used as a strategy to install chemical compatibility with specific resins, and to nanotexture the fibres for enhanced mechanical interlocking. This has been demonstrated with the use of Polyhedral Oligomeric Silsesquioxanes (POSS®). For example, amino-terminated POSS was introduced to chemically oxidised carbon fibre surfaces via carbodiimide chemistry (Figure 11a).[105] By repeating the final grafting process the fibre surface chemistry could be tuned through extended dendrimer generation.

Both the polarity and roughness of the carbon fibre surface increased with generation number, supporting the sequential installation of dendritic surface species. The IFSS, ILSS and dynamic mechanical properties of composites made from these functionalized fibres was also examined. Composites with the highest enhancement showed an improved IFSS (87.9%) and ILSS (8.7%), relative to untreated fibres and increasing surface roughness correlated to increased interfacial enhancement.

Similar effects were observed by Wu and co-workers, by investigating hydrothermal aging of silicon resin composites.[106] The use of a POSS-epoxy hybrid was also successfully carried out by Guo *et al.*,[107] showing improvements in both ILSS (45-57%) and fracture toughness, attributed to the energy dissipative mechanisms of the POSS at the fibre-matrix interface. It was shown that the POSS chemistry itself has potential to tailor the fibre-matrix interface to thermoplastics such as polyester. The surface roughness after grafting methacryl POSS or methacrylisobutyl POSS was almost the same at 131.6 nm and 129.6 nm, respectively. Similarly, dynamic contact angle analysis revealed similar surface energies, and both treated samples exhibited values higher than that of the as-received carbon fibres. The methacrylolsobutyl derivative increased ILSS by 31.9% and the methacryl-POSS increased ILSS by 42.6%. The IFSS of methacryl-POSS grafted CFs was significantly increased (102.2%) compared to pristine fibre. The toughening effect of POSS is well known, and in this report the total absorbed impact energy for the methacryl-POSS sample was 1.72 J, higher than

the as received (1.00 J) and methacryoylisobutyl POSS grafted carbon fibres (1.43 J).

An alternative approach to surface functionalisation of CFs by Zhao and Huang saw an oxidation-EDC grafting approach to attach POSS units bearing tethered epoxides, afforded by reacting POSS with octaglycidyldimethylsilyl.[108]

Unsurprisingly, the surface energy (determined by dynamic contact angle) showed significant increases to the polar component, consistent with the intended surface modification. When IFSS was determined by single fibre pull-out, increases of over 70% were realised for the treated fibres. Comparison of cryo-fractured specimens using SEM showed significant differences in fibre debonding, with the POSS grafted fibres showing obvious improvements in interfacial adhesion through a pull-out fibre decrease and no observed interfacial debonding.

A potential shortcoming of nanomaterial deposition approaches is the extended time needed to modify the fibre surface. These processes often involve multi-step sequences ranging from hours to days in duration making their application challenging at a large scale or by a continuous process. Nevertheless, these types of studies provide useful insight into the interface mechanics and effects to improve fibre-matrix adhesion.

In a bid to improve the mechanical properties of the engineering plastic polyoxymethlene (POM), composites (POM/CF) containing nitric acid treated (25 °C for 24 hours) carbon fibres have been investigated (Figure 11b).[109] Polyoxymethylene thermoplastics contain acetal, polyacetal, and poly(fomaldehyde) motifs, and are used in applications requiring low friction and high stiffness, such as gears and seals. The resultant POM/CF composites were analysed using SEM, Raman spectroscopy, FTIR, fibre length distribution measurement, and unnotched Izod impact test, plus wear testing to evaluate their tribological behaviour. Analysis of the nitric acid treated fibres revealed the roughness of the surface increased along with an increase in disorder, and FTIR suggested the introduction of OH and C=O groups. The modified fibre also improved flexural strength and modulus of POM/CF composites by up to 40% in each instance.

Further insight into the changes of the fibres' surface after nitric acid treatment was gained using Raman spectroscopy, revealing that the acid treatment reduced crystallite size at the fibre surface increasing the percentage of disorder.[109] This would be consistent with the etching of carbon edge planes away from the fibre surface and the installation of hydroxyl and carbonyl groups, as supported by FTIR. Together, the evidence supports that the nitric acid treatment increases the number of flaws, roughness of the surface and disorder of carbon atoms on fibre. Furthermore, the treated fibres had superior adhesion to the POM matrix, which may be attributed to the grafting of functional groups to the fibre surface that are able to hydrogen bond with the highly oxygenated resin.

Similarly, the use of nitric acid as a pretreatment for further surface modification was conducted by Kang and co-workers,[110] where oxidation by HNO_3 was followed by global chemical reduction using $LiAlH_4$, giving an alcohol rich surface. Subsequent exposure of those fibres to APS ((3-aminopropyl)triethoxysilane)) conjugated an exposed terminal amine to the fibre surface.[110]

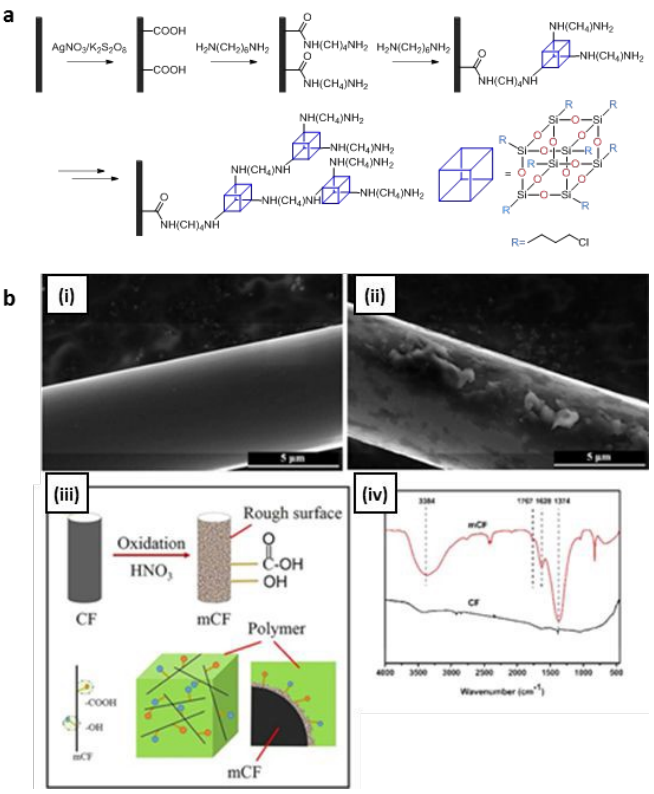

Figure 11 a) The structure of octa(γ-chloropropyl) POSS and the functionalisation procedure. Reproduced with permission from reference.[105] Copyright 2019, Elsevier Ltd. **b)** SEM images of the surface of CF before nitric acid treatment (c) and milled CF after nitric acid treatment (d); FTIR spectroscopy of CF and mCF (f); changes of fibre after acid treatment (g). Reproduced with permission from reference.[109] Copyright 2015, Wiley Periodicals, LLC

The tensile strength of the silanised fibres increased, attributed to the potential countering of defects formed during nitric acid oxidation by the introduced silcate layer. The IFSS for silanised fibres increased from 20.3 MPa (for untreated CF) to 30.0 MPa. The oxidation pre-modification step alone increased IFSS to 23.7 MPa, and the $LiAlH_4$ reduced surface gave an IFSS of 22.9 MPa in a polyurethane matrix.

This approach of APS surface modification has seen routine use in the literature and is typically a direct adaptation of glass substrate surface modification. It is far less effective on carbon fibres, due to the lack of alcohol groups in very close proximity to each other, thus the tethering mechanism is less stable and even less likely to occur considering the heterogeneity of the CF surface and the dispersity of any hydroxy groups present. Though, as outlined in the previous report, this surface modification approach can be promoted via harsh oxidative treatments.

Such an approach was used in 2016 by Jin and co-workers[111] to deposit mesoporous silica nanoparticles (MCM-41) that had been modified to include vinyl groups on the silica nanoparticle periphery. The deposition of these particles was undertaken by a simple dipping procedure at 0.5, 1, and 1.5% colloidal solutions of MCM-41, and interfacial adhesion was determined in vinyl ester resin.

The presence of the vinyl groups was identified as the critical factor in the IFSS improvements (55%) relative to non-functionalised silica particles. Examination of fracture surfaces showed less fibre pull out and more fibre breakage for the vinyl-modified silica, supporting the participation of the surface grafted vinyl groups in the polymerisation process.

The use of silica-based chemicals as surface and interface modifiers has been extensive in the literature with the previous instances being the most pertinent examples.

3.6 Carboxylate derived post-functionalisation.

This section is focused on the attachment of small molecules, polymers, and other species to carbon fibre surfaces decorated with carboxylate groups. Given the extensive literature and high synthetic versatility of carboxylic acids to be tailored to give a myriad of chemistries, it is easy to see why oxidative pretreatment to install such groups on the fibre surface is a popular starting point for many researchers.

The formation of esters and amides with carboxylic acids is a procedurally simple process, often involving Fischer esterification via the catalytic addition of a strong acid (e.g., H_2SO_4) to an alcoholic solution. Alternative methods including conversion to acid chlorides or using a carbodiimide coupling agent such as dicyclohexylcarbodiimde (DCC) have also been used.

In a recent report by Rahmani *et al*.,[112] this carboxylate modification approach was used to tether a common epoxy hardener (diaminephenylsulfone, DDS, Dapsone®) to the surface of carbon fibres via an acid chloride intermediate. The differences between aliphatic and aromatic compounds, both featuring an amine functionality, were examined in this work. The fibres were functionalised with 4,4-diaminodiphenyl sulfone, ethylenediamine, and *p*-aminobenzoic acid, as a control sample (Figure 12 top i) and ii), respectively).

The installation of the aromatic and aliphatic amide groups was undertaken at elevated temperatures for 4 and 24 hours, respectively. The authors did not reveal why the difference in reaction procedure was used, as this timeline is counter intuitive. The aliphatic amine is far more nucleophilic than the aryl amine moiety of DDS, especially considering the deactivating presence of the sulfone group. Nevertheless, examining the IFSS for each of the samples showed that the aromatic amines outperformed the aliphatic. It is worth noting that, in this work, a final surface ligation was undertaken using an anhydride group as the anchoring functional group (Figure 12, ii). This is unusual as anhydride groups are not stable in the presence of amines, as they are often used in acylation chemistries, which would remove the group from the surface.

Han *et al*.[113] analysed the mechanical properties of epoxy-based composites after treating fibres with acid (3:1, v/v mixture of concentrated H_2SO_4/HNO_3 at 60 °C) followed by a titanate coupling agent (LICA38). It is not clear what reaction the coupling agent facilitated, as the fibres were simply dipped in a solution of LICA38 and then washed with 2-propanol. Characterising the treated samples by SEM, XPS and single filament tensile testing showed that fibres that underwent acid treatment for 3 hours appeared to have deep grooves and a significant amount of damage on the surface resulting in a 45.3% reduction in tensile strength. The fibres then underwent subsequent titanate treatment which coincided with a 14.6% increase in tensile strength, but this was not statistically significant. Moreover, the titanate treated CF (without acid pre-treatment) increased IFSS by 34% in an epoxy resin compared to that of untreated fibres.

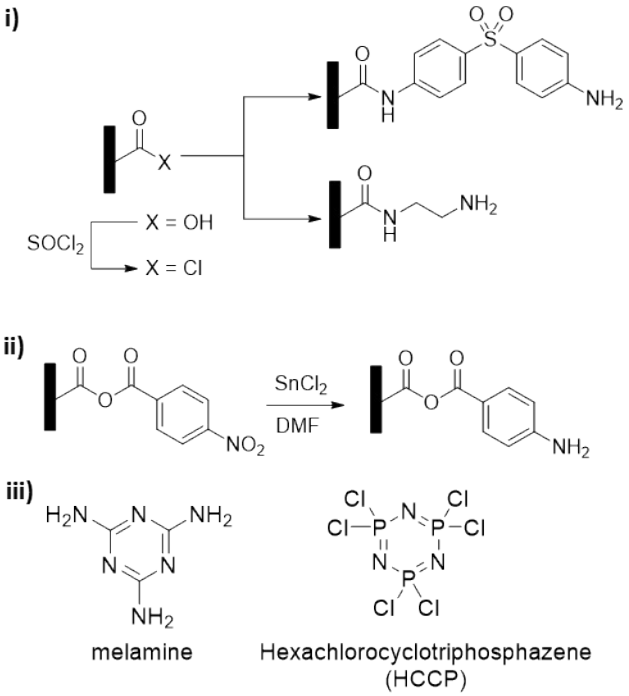

Figure 12 i) and **ii)** Scheme adapted from the original report containing the surface modification approach taken by Rahmani *et al*. Adapted with permission from reference.[112] Copyright 2016, John Wiley & Sons Ltd. **iii)** Chemical structures of melamine and HCCP resulting in significant increases in ILSS and flexural strength. Adapted with permission from reference.[114] Copyright 2017, Elsevier Ltd.

Melamine (Figure 12, iii)) in supercritical methanol has been used to functionalise desized carbon fibre surfaces furnished with acid chloride groups, before assessing their interfacial properties within CF reinforced epoxy composites.[115] Grafting was supported by FTIR, XPS, and Raman spectroscopy. A uniform surface graft was suggested by SEM, resulting in increased surface roughness. Dynamic contact angle revealed significant increases in both polar and dispersive surface energies, suggesting improved wet out in epoxy. Evaluation of IFSS showed improvements of 41.3%, relative to untreated samples, and was attributed to chemical bonding between the melamine and epoxy resin. When scaled up, and ILSS improvements of 36.4% were observed suggesting good translation to large scale composites. Significant toughening improvements were also observed (up to 23.7%), which was attributed to the melamine inducing some small cracks at the interface, thus deflecting them away from the interface.

Extending on this concept, Li and co-workers[114] enriched the carbon fibre surface with phenolic groups to which Hexachlorocyclotriphosphazene (HCCP) was then ligated.

The HCCP rich surface was then reacted with melamine, in a similar manner to the previous report, to give a highly aminated

surface. In this work, the resin of choice was a poly(ethersulfone) that incorporated a phthalazinone unit, which was accessed via *in situ* polymerisation.

XPS analysis was consistent with the expected surface chemistry and the surface energy was shown to increase in polar component after functionalisation. This modification technique had no impact on the single filament tensile strength and when examined in a composite, improvements in ILSS of 23% were observed. Further to this, the flexural strength was also seen to increase by 29%, relative to untreated fibres.

These improvements were attributed to the complementary between surface polarity and their novel thermoplastic resin, thus influencing the infiltration of the polymer into the fibrous reinforcement. It was proposed that the grafted layer of molecules was able to arrest crack tip growth upon the initiation of failure, leading to better performing composites (Figure 13).

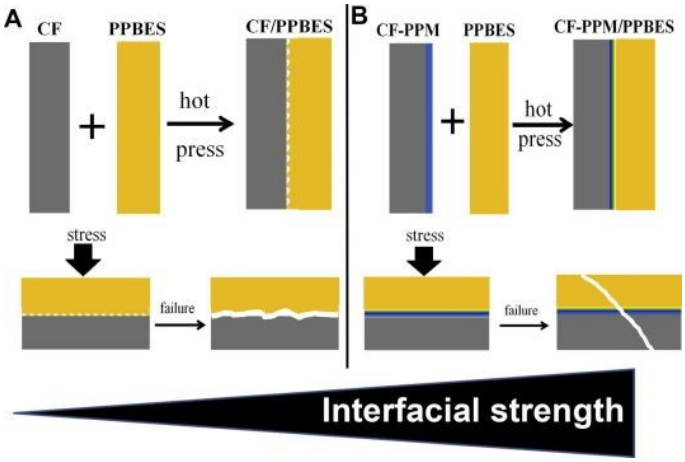

Figure 13 Proposed failure mechanism of composites, reproduced with permission from reference.[114] Copyright 2017, Elsevier Ltd. (To assist in the interpretation of this figure, the reader is referred to the coloured web version of this article.)

Ehlert *et al.*[116] used the innate presence of hydroxyl groups on carbon fibres , reacting them with isopropylidene malonate to graft terminal malonic esters, effectively creating a carboxyl functionalised surface. Surface grafting was quantified by XPS showing the relative surface coverage by carboxylic acid group increased from the initial 5.2% to 9.2%. Two concentrations (0.01 M and 0.05 M) were used with various treatment times (30 - 240 mins) and temperatures (50, 80, 110 °C). However, these parameter changes didn't present any trends to the final surface coverage. SEM revealed no roughening, pitting or change in surface topology, though no mechanical analysis was reported.

Other work using activated carbon fibres bearing surface carboxyl groups provides a method to improve the low interfacial adhesion between carbon fibres and polyetheretherketone (PEEK).[117] First the PEEK underwent nitration in HNO_3/H_2SO_4 followed by reduction to afford PEEK-NH_2. Dynamic mechanical analysis (DMA) and scanning electron microscopy (SEM) (Figure 14, a) confirmed that the properties of the modified CF/PEEK composites interface were enhanced by this process. Then, the activated fibres were tied to a glass frame and placed into PEEK-NH_2/dimethylformamide solution (with different degrees of amination), and the reaction proceeded under nitrogen atmosphere at 50 °C for 48 hours to install PEEK-NH_2 to the fibres' surfaces (Figure 14, b). After grafting, the interlaminar shear strength (ILSS) was improved by 33.4% due to the covalent bonds in the interface region.

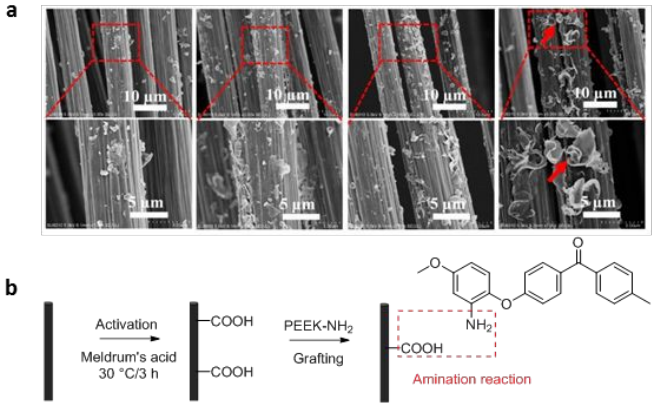

Figure 14 a) SEM images (A) PEEK-NH_2-1@CF, (B) PEEK-NH_2-2@CF, (C) PEEK-NH_2-3@CF, and (D) PEEK-NH_2-4@CF. Reproduced with permission.[117] Shared under creative commons licence. **b)** Grafting of amino-PEEK by derivatization of carboxylic acids on the fibre surface. Adapted with permission from reference.[117] Shared under creative commons licence

3.7 Post functionalisation of single molecules

The use of carbon fibres as a substrate for chemical derivatization using small molecules has also been extensively investigated. In an example of this approach, Servinis *et. al.*[118] successfully grafted complex molecules bearing a pendant primary amine group to react with an epoxide based resin, forming a chemical bonded carbon-matrix interface. Surface grafting was accomplished by *in situ* generation of reactive diazonium species aryl amine that was then cleaved releasing dinitrogen gas and the radical species responsible for forming the covalent bond between the molecule and the fibre surface (Figure 15, a). No change in the tensile modulus and strength of the fibres resulted, showing that this approach enables the retention of the critical physical properties that carbon fibres are valued for. Additionally, the surface topography and microscopic roughness, when compared to control unsized oxidised fibres, were unchanged, suggesting that changes in adhesion were due to the chemical manipulation of the interface and not mechanical interlocking and keying effects. As such, the increased IFSS (15%) of the functionalised fibres was attributed to the chemical compatibility and bonding between the pendant amine and epoxy matrix.

In a similar approach to improving compatibility with an epoxy resin at the interface, Beggs *et al*. also modified carbon fibres to introduce a small organic molecule with amine functionality. However, in this case, the process involved low power microwave irradiation in ionic liquid and organic solvent. The ionic liquid treatment installed a higher density of surface grafted material to the fibres, resulting in an interfacial adhesion improvement of 28% (relative to untreated fibres), somewhat higher than the fibres treated in a conventional organic solvent, which gave an improvement of 18%.[119]

Grafting of molecules bearing BOC (*tert*-butyloxycarbonyl) protected pendant amines to carbon fibre surfaces has also been carried out using azomethine 1,3-dipolar cycloaddition (Figure 15, b).[120] The surface modification process involved the *in situ* formation of a reactive azomethine ylide in DMF at 140 °C. The temperature of the reaction was maintained for 92 h, to allow the 1,3-dipolar cycloaddition of the ylide at the carbon fibre surface, which was subsequently confirmed by XPS analysis. A second step, BOC deprotection using HCl, revealed a pendant amine group. Evaluation of the interfacial mechanics, using single fibre fragmentation, showed improved adhesion between amine decorated fibre and the epoxy matrix, this was not quantified.

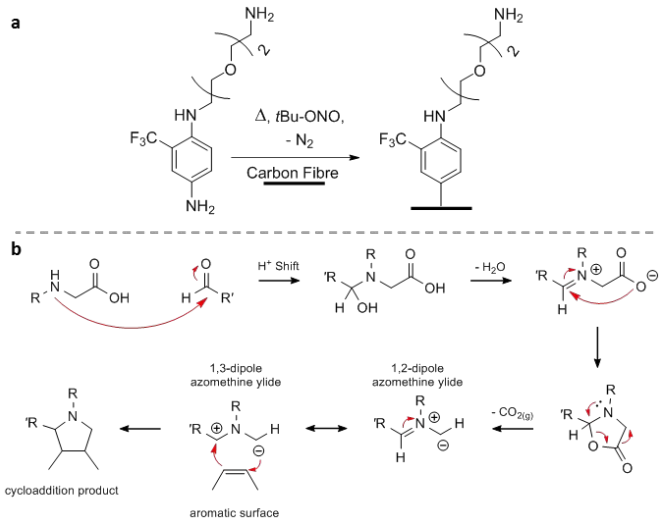

Figure 15 a) The *in situ* formation of aryldiazonium species to modify carbon fibres. Reproduced with permission from reference.[118] Copyright 2015, The Royal Society of Chemistry **b)** Using 1,3-dipole azomethine ylide formation as a strategy to tether small molecules to the carbon fibre surface. Adapted with permission from reference.[120] Copyright 2015, CSIRO Publishing

The optimisation of aryl diazonium grafting methodology was undertaken using a series of reagent concentration studies.[121] The fibres functionalised at each concentration were characterised physically (tensile strength, modulus, coefficient of friction and AFM) and chemically (XPS). The IFSS of all treated fibres was determined, the authors reporting increases in IFSS between 28-47%.

The functionalisation of oxidized and unoxidised carbon fibre has also been facilitated by using an aziridine linking group derived from reactive nitrenes.[122] These nitrenes were formed by the thermal degradation of alkyl azides, which results in the release of nitrogen gas. The functionalisation was supported by XPS and the fibre performance was compared to fibres functionalised using amide chemistry. The process of amide coupling involved two-steps: first, a reaction with thionyl chloride to give surface bound acid chloride groups, and second, *N*-acylation with ethylene diamine.

Of the functionalised fibres obtained, increases in the coefficient of friction (23% compared to untreated control) was observed for fibres with just thionyl chloride surface groups, and this was maintained after addition of ethylene diamine. Both oxidized and unoxidized fibre which had been functionalised using nitrenes showed a 40% and 66% increase in friction, respectively. This nitrene based approach demonstrates how the electron rich aromatic groups of carbon fibre can be exploited to successfully graft functional groups to its typically unreactive surface by aziridine formation.

A common biological adhesive, polydopamine, was used as a fibre coating/sizing and its effect on interfacial adhesion was explored in 2015 by Liu *et al.*[123] Submersion of fibres in a solution of dopamine, followed by spontaneous self-polymerisation, adhered poly(dopamine) to the fibre surface (Figure 16, a). Micro-droplet testing of these materials showed an 88% increase in IFSS for a polypropylene matrix and an impressive 284% increase within a maleic anhydride grafted polypropylene (MAPP) matrix. While a more polar and hydrogen bonding rich surface does not seem compatible with polypropylene alone, the increase in MAPP adhesion was attributed to the reaction of the phenols and nitrogenous species with the anhydride groups of the polymer backbone. Larger scale testing of properties in this instance was undertaken using short carbon fibres (1 mm) in MAPP, that showed a 109% increase in flexural strength and a 223% increase in impact strength. Again, these benefits are thought to arise due to the interaction of the polydopamine with the anhydride moiety of the modified polymer.

Building on the approach of using poly(dopamine), a 'rigid-and-soft' structure was developed by Zhu *et al.*[124] Using a core of poly(dopamine) directly grafted to the fibre surface as the rigid component, followed by addition of polyetheramines (Jeffamine®) as the soft component in a layer-by-layer approach.

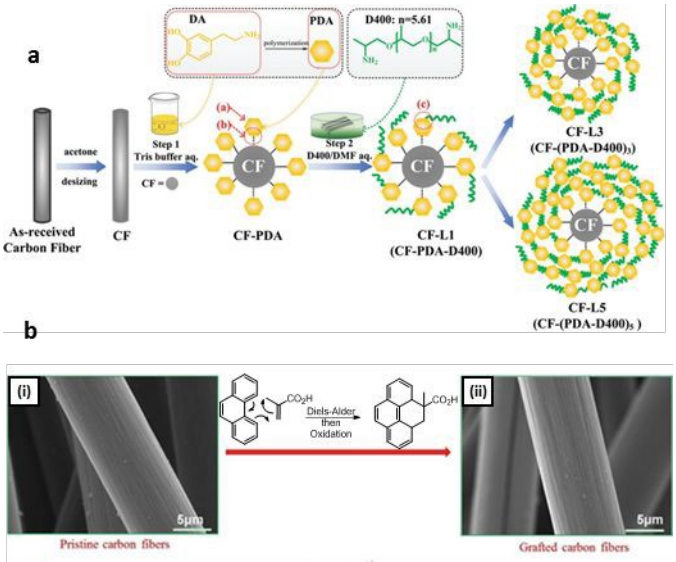

Figure 16 a) Schematic illustration of dip coating assembly of PDA/D400 multilayers onto surface of carbon fibre. Reproduced with permission from reference.[124] Copyright 2019 Wiley-VCH GmbH, Weinheim **b)** SEM Images of the carbon fibres (a) before and (b) after modification using a Diels Alder reaction approach. Adapted with permission from reference.[125] Copyright 2018, Elsevier Ltd.

Three layers of PDA/polyether amine achieved an improvement in interfacial strength and toughness, 39.2% and 99.8% respectively, compared to untreated fibre. The authors concluded that the alternating "rigid" and "flexible" interphase deflects the crack path and induces plastic deformation and viscoplastic energy dissipation.

A similar approach[126] involves the covalent attached of lignin to carbon fibres, making use of a potential waste stream from the paper and pulp industry. Successful surface grafting was confirmed by cyclic voltammetry, XPS and field emission scanning electron microscopy coupled with energy dispersive X-ray spectroscopy. Evaluation of IFSS using the microdroplet test showed 27% and 65% increases in interfacial shear strength for epoxy and cellulose propionate matrices, respectively.

Methyl acrylate was surface grafted to carbon fibres, via a Diels-Alder reaction, by Fei and co-workers,[125] creating an ester functionalised surface. The effect of grafting temperature on the surface morphology and functional groups of carbon fibres was investigated by FTIR, Raman spectroscopy, XPS and SEM. The optimal grafting temperature was determined to be 80 °C, resulting in surface coverage of carbonyl groups increasing from 5.16% to 19.30%, as determined by XPS. The authors claim the shear and tensile strength increased by 90.3% and 78.7%, respectively, and this treatment also imbued a high and stable coefficient of friction with the wear rate decreasing significantly by 52.7% (Figure 16, b).

The inherent carbonyl groups on untreated carbon fibre surfaces have been proven to be reactive towards Meldrum's acid to create carboxylic functionalised surfaces.[127] The grafting process, needing only 1 hour to complete, involved simply dipping the fibres in a solution of Meldrum's acid. Fibres modified by this process were evaluated using SEM, AFM and TGA. Also, XPS revealed that the carboxylic acid groups increased from the initial 1.4% to 7.8%, while the carbonyl groups decreased 23% to 13%. This apparent conflict in results suggests that the ester groups of the Meldrum's acid remain as esters rather than ring opening to the corresponding dicarboxylate. SEM showed no evidence of etching or the generation of a homogenous coating, though this approach resulted in an ILSS increase of 74%.

The grafting of small molecules to carbon fibres has shown significant benefits in the optimization of interfacial adhesion, as outlined above. The natural extension of this concept is to graft larger molecules to the fibre surface to enhance and magnify any benefits observed.

An example of an amine rich macromolecule grafted carbon fibre was examined by Ma and co-workers in 2014.[128] In that work, oxidized carbon fibres ($AgNO_3/K_2S_2O_8$) were esterified using DCC and 3-bromoethanol. The pendent bromide served as an anchoring point for reaction with hexamethylenetetramine (HMTA). The generational growth of the dendrimer was undertaken by subsequent reaction with 1,2-dichloroethane, then again with HMTA. This sequence was repeated until the desired dendrimer was generated.

Interestingly, the authors do not take into consideration the potential disassembly of the HMTA unit in the presence of HCl, which is generated upon reaction with 1,2-dichloroethane. This little-known reaction (Delépine reaction)[129] has been used to access primary amine groups, as the HMTA will degrade to formaldehyde and ammonia. Nevertheless, XPS analysis of the fibres was consistent with the desired surface chemistry and SEM showed a good coverage of the fibre surface.

Dynamic contact angle showed an increase in fibre surface energy, increasing by 148%, and IFSS was increased by 81%. It is difficult to gauge how much of these benefits were due to mechanical interlocking, as the modification approach here significantly increased fibre roughness.

A similar polyamine surface chemistry was reported by Meng *et al.*[130] though the modification with triethyl tetramine (TETA) was carried out in supercritical water and ethanol. The system required the use of an autoclave to heat the solution to 400 °C. XPS results revealed an increased nitrogen content on the surface, with peaks corresponding to amino and imino groups. AFM showed the treatment process had roughened the fibres, though no physical damage could be observed (Figure 17).

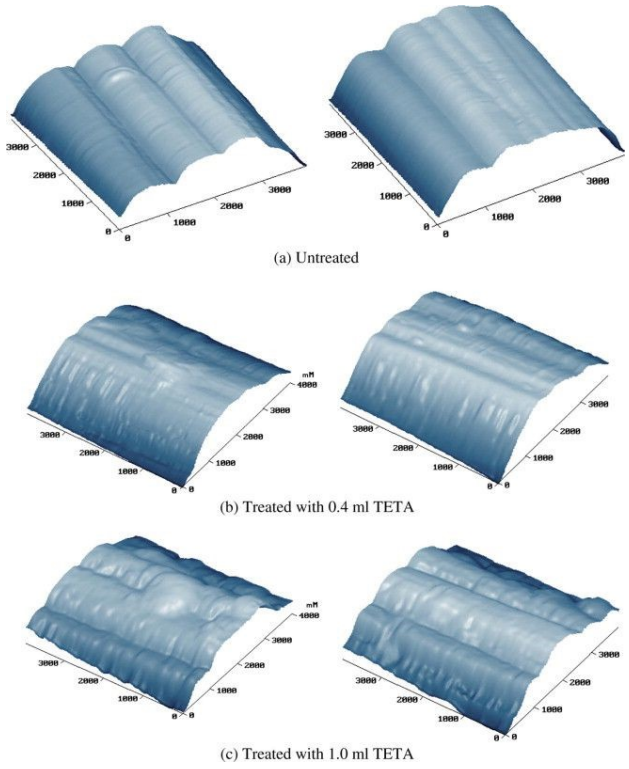

Figure 17 AFM images of untreated and aminated carbon fibres as reported by Meng and co-workers. Reproduced with permission from reference.[130] Copyright 2018, Elsevier Ltd.

IFSS of the best performing treatment (0.4 mL of TETA in 50 mL of the supercritical solvents) gave increases of up to 22.9%, relative to untreated fibres, and when scaled up the ILSS of treated fibres increased 19.2%, compared to untreated samples. Notably, XPS also indicated that the accumulation of the polymerised TETA onto surfaces was unfavourable when more than 1.0 mL TETA was used in the parent solution.

A very common dendrimer, used in a similar manner to the above examples, is poly(amido amine) (PAMAM). Again, the aim of this process is to install a nitrogen rich surface to increase the

degree of cross-linking from the fibre surface to the interphase of the resin.

In the work by Zhang *et al*.[131] the dendrimeric species was grown from the surface by oxidizing the fibre (HNO_3) followed by conversion to the acid chloride with $SOCl_2$ and subsequent reaction with ethylenediamine (Figure 18). This amine rich surface was then reacted with methylacrylate via Michael addition, followed by amidation with ethylenediamine. This process was repeated to generate the desired dendrimer. Visualising the fibre using SEM showed a roughened surface, and XPS was consistent with the installation of a highly nitrogenous surface chemistry. When IFSS was determined, via micro debonding in epoxy, improvements of 34.7% were observed for the treated fibres. This seems significantly lower than would be expected considering that the IFSS gains with much smaller, and less nitrogen rich, molecules seem to be higher.

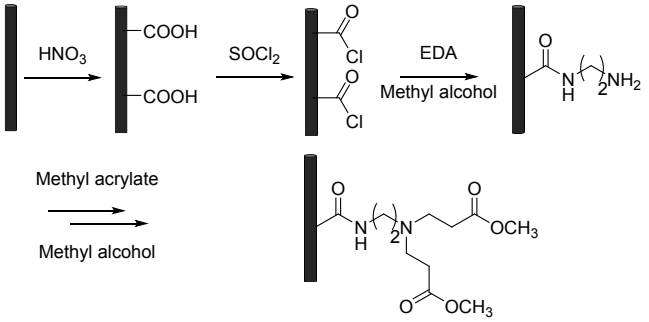

Figure 18 Schematic outlining PAMAM functionalisation process. Adapted with permission from reference.[131] Copyright 2017, SAGE Publishing.

A tipping point may exist at the CF-matrix interface, whereby excessive cross-linking and adhesion may lead to an interface which is very brittle. While initial adhesion would be high, the generation of micro-cracks would lead to debonding, causing catastrophic failure at lower than anticipated stress.

An additional approach to this was taken by Ma and co-workers who employed a similar grafting method in supercritical methanol.[132] After oxidation and acid chloride formation, Ma and co-workers deviated from previous works by using a pre-synthesised PAMAM dendrimer (Figure 19).[133]

Notably, the functionalisation time is significantly reduced to 10 minutes in an autoclave. XPS showed the presence of several nitrogenous species on both the oxidized and grafted materials which included a significant peak at ~406 eV. This indicates that there is a significant presence of N-oxides, potentially as NO_2 and related species which may not assist in fibre-matrix adhesion. Additionally, XPS indicated that the supercritical methanol distributes the dendrimer more homogenously than conventional methanolic solution. Further improvements of IFSS were also observed for supercritical methanol grafting (82.6%) over the conventional method (53.6%). However, this method has small negative effects on single fibre tensile strength.

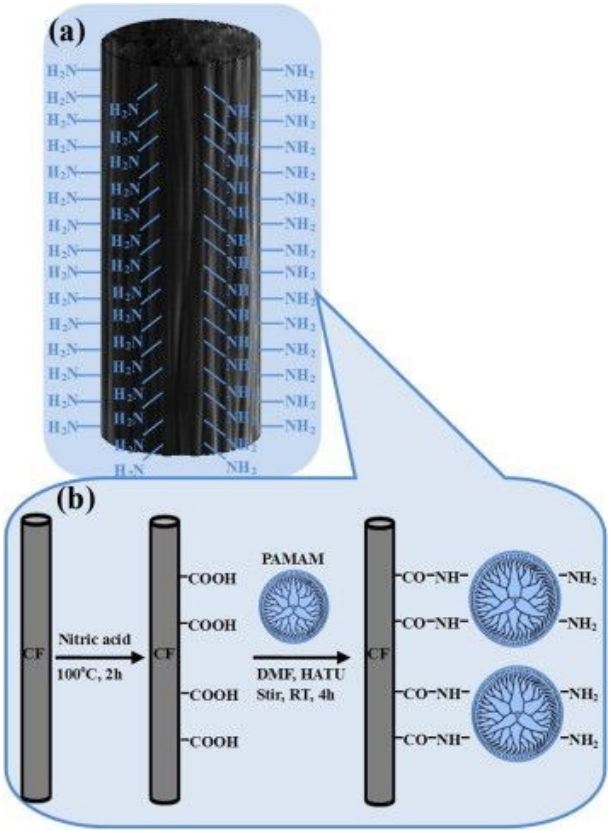

Figure 19 The installation of PAMAM onto carbon fibre, using a surface oxidation and coupling agents for amino-terminated carbon fibres. Reproduced with permission from reference.[133] Copyright 2013, Elsevier Ltd.

3.8 Post functionalisation polymerisations

Extending on the current work of grafting macromolecules, there has been some work in using living polymer synthesis, such as RAFT or ATRP, and uncontrolled radical polymerisation to grow polymers from the surface of carbon fibres.

In 2015, Wu and co-workers used ATRP to grow poly (glycidyl methacrylate) (PGMA) from carbon fibres to improve the interaction between carbon fibre and epoxy matrix.[134] This is a stark counter to the previously discussed approaches where a common approach is to attach amines to the fibre surface to mimic the hardener in the epoxy resin. Here the epoxy grafted to the surface is aimed to interact with the hardeners in the epoxy formulation.

Notably, in that work, the authors use a combination of TGA, FT-IR and XPS to determine a grafting content of polymer, found to be 10.2%. It is difficult to determine if this is a high or low number as this type of quantification is not usually carried out. This is not due to any lack of diligence on behalf of other authors, but because of the notoriously inhomogeneous CF surface, any grafting quantification is likely fraught with error and high variance.

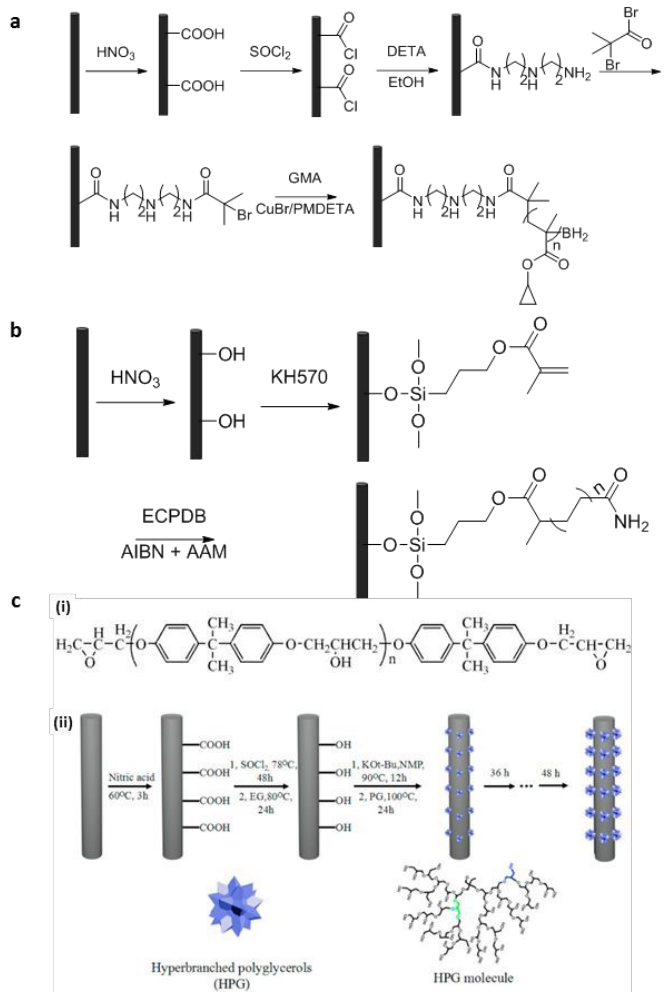

Figure 20 a) Synthesis of CF-PGMA *via* ATRP. Adapted with permission from reference.[134] Copyright 2015, IOP Publishing. **b)** The procedure of grafting PAAM onto CF surface via an acrylate tethered to the fibre surface using a silane anchor. Adapted with permission from reference.[135] Copyright 2017, Society of Plastics Engineers. **c)** Using and oxidative pre-treatment to install hyperbranched polyglycerols. Reproduced with permission from reference.[136] Copyright 2017, Elsevier Ltd.

As with all ATRP 'grow from' approaches, the process required an α-bromocarbonyl unit to be installed on the fibre surface. This was done, as previously described, via oxidation of the fibre and subsequent amide formation with a polyamino linking unit. This was then amidated with α-butylrylbromide from which the radical polymerisation can take place (Figure 20, a). No physical or adhesion characterisation was undertaken in this work, though the process has been included here to demonstrate the possibility of using controlled polymerisation for interface tailoring.

Similarly, RAFT polymerisation has been employed to attach acrylate-derived polymers from carbon fibre surfaces, in this instance poly(arylamide) (PAAM). In this interesting approach Xiong *et al.*[135] use surface oxidation and silanation to install a terminal acrylate on the fibre surface (Figure 20, b). The modified fibre is then placed into a solution in which poly(acrylamide) is being synthesized using RAFT.

In this way, the polymer is neither grown from the surface nor grafted to the surface in any targeted way, such as cycloaddition or thiol-ene type chemistry. It is more the goal that the pendant acrylate will be incorporated into the polymer backbone being generated in the solution phase. Analysis of this modification approach using XPS was consistent with the presence of poly(acrylamide), and the original silicon-based anchoring moiety was also observed.

Using TGA, the surface grafting density was estimated to be around 18-19% for PAAM, and the IFSS, determined via micro bonding, was shown to increase by 107%. Fractography comparison between pristine and modified fibres showed a marked reduction in fibre pull-out for the samples in which PAAM had been grafted to the surface.

Hyperbranched polyglycerol (HPG) has been grown from the carbon fibre surface via anionic ring-opening polymerisation (Figure 20, c) by Shao *et al.*[136] The anchoring approach was via oxidation then esterification of the installed carboxylic acid with ethylene glycol.

This was followed by ether formation using an iterative reaction with glycidol, to increase the free hydroxyl content and increase the compatibility of the fibre surface with the intended epoxy resin. The interfacial and interlaminar shear strengths were increase by 90.6% and 49.8%, respectively. Further to this, the authors used AFM for nanomechanical mapping to examine the interphase, which after anionic polymerisation saw significantly increased breadth. This change in modulus between fibre and bulk polymer has been attributed to the effective blending of the surface grafted material and the resin. The gradient modulus, in this instance, is reported to make the interphase act as a stress transfer medium and the load can be transferred from matrix to carbon fibres uniformly and effectively.

The work by Giebel *et al.*[137] involved using free radical polymerisation of vinylic monomers to graft polymers to the fibre surface. Interestingly, the authors evaluate two methods of desizing the commercially obtained T700 fibres, one thermal and one based on a common acetone washing procedure. In this work both approaches resulted in decreased tensile strength of the desized material; though, this was more significant for the thermally desized material.

This approach is similar to that taken by Xiong *et al.*[138] discussed previously, whereby the fibres were placed in a solution phase polymer synthesis reaction. A proof of concept, whereby poly(styrene) was grafted to the fibre surface, showed increasing surface-bound material with increasing radical initiator (AIBN) (Figure 21, a). In a similar process, but under aqueous conditions, the monomer 2-hydroxyethyl methacrylate (HEMA) was polymerised with $K_2S_2O_8$ as the initiator. Again, surface bound material, as observed by SEM, increased in with initiator concentration. At high initiator concentrations the fibres were seen to fuse via the coalescence of surface bound polymer.

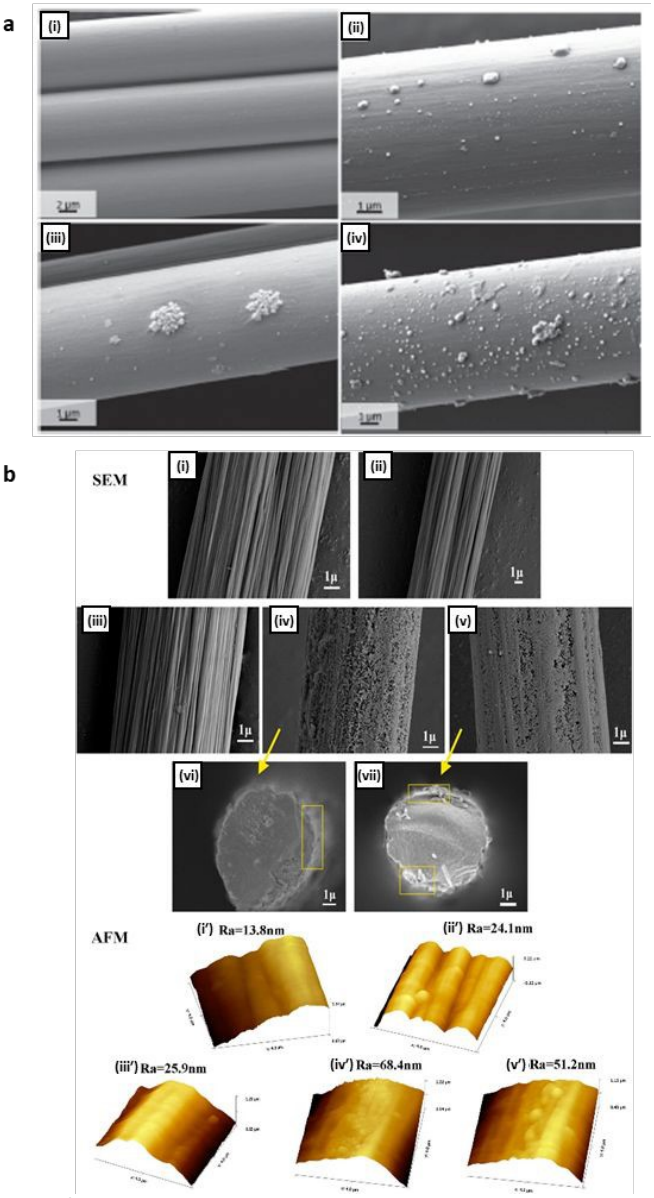

Figure 21 a) SEM images of CF surfaces i) – iv) prior to treatment and B-D) after treatment with styrene using B) 0.01 equiv. of AIBN C) 0.025 equiv. of AIBN and D) 0.05 equiv of AIBN for 1 hour at 50 °C. Reproduced with permission from reference.[137] Copyright 2017, Wiley-VCH GmbH, Weinheim **b)** SEM and AFM images of carbon fibres: (I, i') Pristine CF; (ii, ii') CF-COOH; (iii, iii') CF-OH; (iv, iv') CF-IA; (v, v') CF-IA-EDA; (vi) the transverse cross-section of CF-IA; (vii) the transverse cross section of CF-IA-EDA. Reproduced with permission from reference.[139] Copyright 2019, John Wiley & Sons Ltd

Analysis by XPS was consistent with the expected surface chemistry, and exposure of the hydroxyl-rich surface to the epoxy resin was proposed to interact favourably. Determination of ILSS of the modified fibres showed up to a 22% improvement relative to the commercial material. However, the majority of the treated samples were indistinguishable, or reduced by up to 12%, compared to the parent material.

Ao *et al.* used a similar approach of polymer growth from the carbon fibre surface though using itaconic acid as the monomer of choice.[139] The original fibre surface was oxidized then the installed functional chemical groups surface were globally reduced using $LiAlH_4$ to give a hydroxyl rich surface. Itaconic acid was then polymerized in the presence of this fibre and spontaneous esterification was assumed. The net result was a fibre surface enriched with carboxylic acids, to which ethylene diamine was attached using EDC. Analysis of the fibres at each modification phase was consistent with the expected surface chemistry installed. The polymerisation step resulted in a porous coating on the fibres' surface (Figure 21, b), which persisted after amide formation.

Measurement of surface roughness via AFM reflected observations from the SEM images (Figure 21, b), with the increase roughness proposed to provide more contact points with the resin thereby enhancing adhesion. When IFSS was determined, increases of 89.5% were observed via microdroplet testing, and fractography showed significantly reduced fibre debonding and pull-out for the poly(itaconic acid) functionalised and the subsequent aminated sample.

In other work to enhance the interfacial adhesion strength, hyperbranched aromatic polyamide (HBP) was grafted to carbon fibres using solution polymerisation.[140] The fibres were desized, oxidised, reduced, and then subjected to silanisation prior to polymer functionalisation. Chemical grafting involved mixing the treated CFs with 3,5-diaminobenzoic acid (DABA) and *N*-methyl-2-pyrrolidone under sonication for 30 minutes. Pyridine and TPP were added and the mixture heated to 100 °C and stirred under N_2 for 6 hours. The surface morphologies of the fibres were characterised by SEM after each step.

Analysis by XPS verified the surface chemistries at each stage, with peaks at 287.9 and 285.8 eV for the CF-HBP C-N and O=C-NH bonds, respectively, indicating that the poly(aryl amide) was successfully grafted. FTIR spectroscopy was employed by the authors to assess the functional groups of the untreated carbon fibre, CF-OH, CF-APS, and CF-HBP (Figure 22). The peaks at 1656 and 1374 cm^{-1} were assigned to amide C=O stretching, indicating that the HBPs were successfully grafted.

A reduction in contact angle and the increase in the surface energy was reported, demonstrating the effectiveness of the HBP modification. The incorporation of the HBP on the fibre surface resulted in significant increases in both IFSS (65.3%) and flexural strength (34.3%) of the corresponding composite.

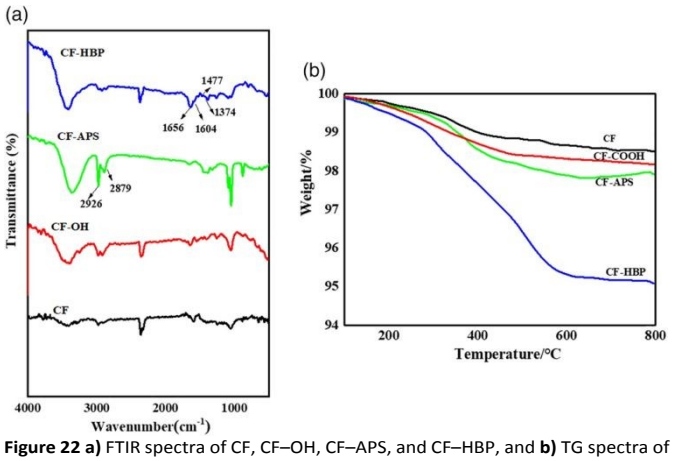

Figure 22 a) FTIR spectra of CF, CF–OH, CF–APS, and CF–HBP, and **b)** TG spectra of CFs, Reproduced with permission from reference.[140] Copyright 2019, Wiley Periodicals, LLC.

4.0 Electrochemically mediated surface modifications

Commercial production of carbon fibre incorporates the use of electrochemical oxidation to modify the functional groups on the fibre surface. It is thought that this oxidation increases the amount of surface-bound oxygen containing groups that are proposed to influence the adhesion between the fibre and the supporting polymer matrix of the final composite. Notably, commercial carbon fibre is coated with a sizing to prevent fibre damage during textile processing and improve the ability to handle tows of fibre. Sizing has been shown to decrease wettability, smoothing the surface and mask surface functional groups.[49] Due to this, many research groups perform surface modification on unsized samples of carbon fibre, or remove the sizing (desize) prior to surface modification.

Along with providing a means of chemical modification, electrochemistry can also characterise carbon fibre and its graphitic analogues. Early reports demonstrate the formation and reduction of quinone-like functional groups on low-porosity graphite electrodes and the effect of pretreatment.[141, 142] XPS analysis of carbon fibre after electrochemical oxidation shows the correlation between the increased presence of surface oxides with increasing potential.[143] Furthermore, the electrolyte used influences the oxide groups; H_2SO_4 provides increased oxygen species, while NH_4CO_3 (which is more commercially relevant) increases the amount of nitrogen species as well as oxygen. Also, the applied current is an additional variable which may influence the ratio of surface oxide groups.[144]

Analogous work on glassy carbon electrodes gives support to the effect increasing current and time has on the surface oxygen groups observed.[145] However, applying such treatments to glassy carbon results in porous structures due to inefficient packing in an isotropic assembly of stacked, graphite-like crystals resulting in a low density of oxygen species.[146, 147] Indeed, the graphite edges of the glassy carbon electrode have been shown to be the active sites for electron transfer.[148]

The electrochemical response of PAN-based carbon fibres is suppressed following reduction in an H_2 environment at elevated temperature (950 °C).[149] In contrast, oxidation of those fibres with ammonium persulfate ($(NH_4)_2S_2O_8$, 50 °C, 24 h) increases the surface oxygen content, resulting in greater interaction with the aqueous electrolyte and better electrochemical reactions at the carbon fibre-liquid interface.[149] Subjecting PAN-based carbon fibres to anodic oxidation in KNO_3 (1 wt%) caused a decrease in fibre weight (up to 30% loss) with increased oxidation.[19] Subsequent heat treatment (550 °C, 30 min) resulted in further mass lost (15%, control showed no mass loss), attributed to the release of volatiles via decarboxylation of the generated oxygen-rich surface groups. The oxidation of these fibres resulted in micropores, which expanded following decarboxylation.

The surface functional groups of commercial CF (subjected to the full suite of manufacturing surface treatments) can be modified through electrochemical treatment, though not in the same way as these same fibres that have undergone '*de-treatment*' (*i.e.* thermal removal of surface chemistry installed by previous surface treatments). Analysis via XPS, demonstrates that the results of surface treatment may be strongly influenced by the initial surface chemistry installed on the fibre during manufacture.[150]

Also relevant is the method of surface treatment for different types of carbon fibre. The anodic polarization of highly graphitised PAN-CF (following heat treatment >1500 °C) has been shown to result in more efficient oxidisation by electrochemical methods (2.0 V, 30 min, 0.5 M H_2SO_4) compared to chemical processes.[151,152] Furthermore, these samples exhibited greater capacitance values than high heat-treated samples exposed to chemical oxidation.

Georgiou *et al.*[153] attempted to isolate the effects of cyclovoltammetric surface modification by first subjecting commercial carbon fibres to pyrolysis (up to 1000 °C) to remove any surface bound oxygen-containing groups. These fibres were then electrochemically treated in aqueous H_2SO_4 (5-50% w/w) in both narrow (-1.0 V to +1.5 V, *vs.* SCE) and wide (-3.0 V to +3.0 V, *vs.* SCE) potential windows within a range of 1-20 cycles. The surfaces were characterised via XPS. Also, the adsorption of dyes (methylene blue and alizarin yellow) from solution was used to indicate the greater degree of oxidation at higher concentrations of H_2SO_4 after exposure to a wide potential window. A possible downside to this approach is, at peak electrolyte concentration and cycles (50% w/w; 20 cycles), the surface may become over-oxidised leading to degradation of surface structures. It was noted that whilst XPS gives excellent insight into the type of surface groups present, quantification is difficult. Conversely, the degree of surface oxidation may be indirectly estimated through the uptake of the dyes without identifying the surface groups. Still, when considered together, these data can accurately indicate the surface chemistry. Similarly, the adsorption of linear alcohols (1 to 4 carbons chain length) has been demonstrated as a method to identify surface oxidation trends (Figure 23).[154]

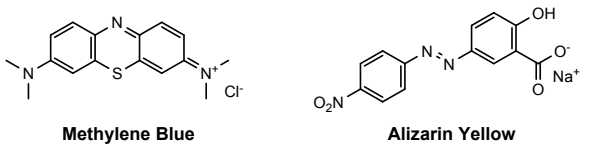

Figure 23 Structure of the dyes to determine the degree of surface oxidation.[153]

Other reports suggest the electrolysis of water may lead to increases in surface oxygen functional groups when using wide potential windows for cyclovoltammetric treatments.[155] This is suggested to lead to the formation of electron donor and acceptor groups on the surface, thereby improving interfacial interactions or the adsorption of dyes.[155]

Oxidation of PAN-based CF in air has also been shown to improve the electrodeposition of Cu from a $CuSO_4$ solution.[156] Treatment at 400 °C resulted in an increase of surface carbonyl groups, leading to the deposition of more Cu able on the CF surface. The use of metals to coat carbon fibres, such as copper and nickel, has implications for multi-functional composites including EMI shielding applications.

Anodic oxidation in H_sSO_4 (0.5 M) demonstrates an increase in interlaminar shear strength (52 MPa, *cf.* 23 MPa for the control)

without compromising fibre physical properties.[157] An increase in polymer reinforcement has also been demonstrated with fibre oxidised in acidic or alkaline mediums, but reported fibre degradation.[158, 159] Furthermore, the structure of the resulting fibre is effected by the electrolyte used. Employing H_2SO_4 (1 M) resulted in cracking the fibre 'skin' at higher potentials, whilst NaOH (1 M) caused pitting of the fibres.[160] These findings may give some information on carbon fibres' internal 'core' structure, though the idea of a skin/core configuration is debated in the literature.[43]

Electrochemical oxidation of PAN derived carbon fibre in either NH_4CO_3 or H_3PO_4 demonstrates an increase in ILSS (95-100 MPa *vs.* ~87 MPa control), though the former outperformed the use of H_3PO_4 in terms of transverse flexural strength at higher levels of oxidation.[161] This was attributed to the formation of defects on the surface of the fibres, despite increased oxygen to carbon ratios. Other reports indicate the presence of oxygen functional groups to have a greater influence on composite strength than nitrogen-containing groups.[162] This was evaluated with the anodic oxidation (70 μAm^{-2}) of PAN-based carbon fibre in phosphoric acid (10 wt%) demonstrating an increase in ILSS to 64 MPa from 56.5 MPa.

The use of NH_4HCO_3 (0.5 M) has also been investigated in a continuous process at a range of current densities (1-4 A m^{-2}) for its effect on the interfacial adhesion of CF to epoxy resin using the microbond test.[163] A treatment time of 1.4 minutes using a treatment speed of 0.7 m min^{-1} was employed, with the finding that the greatest increase in IFSS (~36 MPa *vs* ~25 MPa, +14.4%) was achieved at the highest current density (4 A m^{-2}) with minimal degradation in tensile strength (-14%). The authors reported that the increase in IFSS was due to increase surface roughness following electrochemical surface oxidation.

A similar study conducted by Park *et al.*[164] demonstrated the anodization of untreated/unsized PAN-based carbon fibre in $NaHCO_3$ (5 wt%, 1 m min^{-1}) in a continuous line (Figure 24). A range of current densities were investigated with the peak ILSS achieved at 6 A m^{-2} (~100 MPa *vs.* 60 MPa of control). Higher current densities resulted in samples with lower fibre-matrix adhesion due to etched micropits.

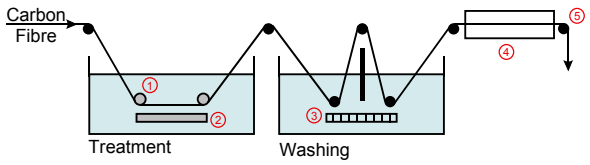

Figure 24 Example of a continuous process line for carbon fibre surface modification. 1) Anode Rollers; 2) Cathode Plate; 3) Bubbler for agitating solution; 4) Drying oven; 5) Collection. Adapted from reference.[164]

This is echoed in PAN fibres electrochemically oxidised in KNO_3 (1 wt%) showing increased surface acid groups with increased oxidation, though extensive treatment produced porous carbon fibre.[165] Further, this porosity was not limited to the surface, but extended beyond the depth of XPS profiling. In this work there was no investigation into composite performance for the treated fibres.

A statistical optimisation of electrochemical treatment conditions on PAN-CF has also been performed.[166] It was found that the optimal conditions included nitric acid as the electrolyte (15 wt%), 10 minutes of oxidation time (+3.0 V *vs.* SCE) at 20 °C. These conditions were then experimentally employed, preserving tensile strength, and increasing ILSS compared to control samples.

XPS analysis of carbon fibre surfaces with polyvinyl alcohol (PVA) following electrochemical oxidation in nitric acid (1 M) were shown to have improved interaction with increased oxidation.[167] Again, extensive oxidation was seen to damage the fibre rather than improve interactions with PVA. This interaction may be analogous to the application of sizing to the surface of carbon fibres during commercial production.

4.1 Covalent Surface Modification

The success of grafting small molecules to the surface of carbon fibre is difficult to conclusively ascertain. This is often because the carbon-based structure of the small molecule is difficult to discern from the carbonaceous substrate it is bound to. One useful method is to use a small molecule with an atom or functional group that is not native to carbon fibre. The use of fluorine-containing molecules is a good option as this atom is readily identifiable through XPS and is not (typically) observed in unmodified carbon fibres. The attachment of 4-fluorophenylacetic acid to the surface of PAN-CF has been achieved using oxidative electrochemistry via the Kolbe decarboxylation reaction (Figure 25).[168] This modification is facilitated by using a constant potential of +1.75 V (*vs.* Ag/AgCl) in acetonitrile with a tetrabutylammonium hydroxide electrolyte. This process shows no reduction in tensile strength or tensile modulus after a 30-minute treatment time. Interestingly, a 10-minute treatment time was determined to be optimal as quantified by the presence of Fluorine and Oxygen signals in the XPS spectra.

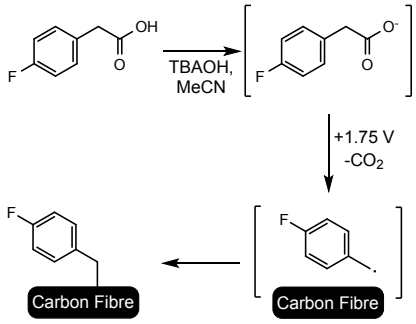

Figure 25 Demonstration of the Kolbe decarboxylation reaction to modify the surface of carbon fibre.[168]

In terms of composite performance, this modification resulted in a 114% increase in IFSS (38.1±2.8 MPa *vs* control 17.8±1.1 MPa).[168] It is important to note that these types of covalent surface modification are not easily removed from the CF surface, and have undergone extensive washing procedures to remove any adsorbed material.

4.2 Diazonium Salts

The use of aryl diazonium salts allows tailoring of surfaces, opening an avenue for the post modification of grafted groups including amide formation, click chemistry, and methods of polymerisation such as ATRP.[169]

Early reports of electrochemical modification of carbon surfaces through attachment of organic molecules focussed on the reduction of diazonium salts.[170, 171] This method is reliable and rapid (<1 hour), allowing CF surfaces to be tailored to an application. It is perhaps more elegant than simple oxidation in an acidic or alkaline medium, though this makes it more delicate. Notably, this modification is enabled by the application of a reductive potential to the carbon fibres, in contrast to most other methods that use oxidative approaches. The reduction of diazonium salts and their covalent attachment to carbon fibre was reported by Delamar *et al.*[172] That work explored the attachment of a nitrophenyl moiety to the carbon fibre surface via the reduction of the corresponding 4-nitrobenzenediazonium salt. When performed in an aprotic solvent, the nitro functional group was maintained, and could subsequently be electrochemically reduced to an amine group. Alternative means of reaching this amine group include the concurrent attachment and reduction of the nitro group when performed in a protic solvent, or the hydrolysis of the acetyl group of the grafted 4-acetamidobenzenediazonium tetrafluoroborate. Grafting compounds bearing two diazonium moieties resulted in attachment of one, then hydrolysis of the second to a phenol group, as seen with the commercially available bis-diazonium dye, Fast Blue B.[172] In this case, the presence of the grafted aromatic compound could be confirmed through oxidation of the diazo to a nitro group ($NaNO_2$, Cu) or through electrophilic substitution (H_2SO_4, HNO_3). This was necessary for characterisation due to the instability of the second diazo group once bound to the surface. The post modification of the attached surface groups also served as a demonstration of their availability for typical chemical reactions. Indeed, that report also demonstrated the reaction of the amine or phenol moieties with epoxides, identical to the reactive functional group of many commercially used resins. Further, a ~60% increase in interfacial shear *stress* was observed for fibres functionalised with an amine group (compared to unfunctionalised, determined by single fibre pull out test).[172]

Recent work focusing on the reduction of diazonium salts investigated the use of cyclic voltammetry compared to chronoamperometry.[173] Using aryl diazonium salts with different substitutions on the aryl ring allows for simple manipulation of carbon fibre surface to exhibit the desired chemistry (Figure 26, a).

The use of potentiostatic control (-1.0 V, 10-30 min) has been reported to allow the formation of multilayers and showed greater increases in resistivity (up to +250%). The greatest increase in resistivity was found to be the phenyl derivative (Figure 26, a, bottom right), with this sample exhibiting an IFSS of 38±1 MPa, a 19% increase over the control (32±2 MPa).[173] (Note: The sodium-carboxylate sample (Figure 26, a, bottom middle) in this body of work was achieved through submersion of the carboxylic acid derivative in a NaOH solution for 1 min).

The IFSS can largely be influenced by the types of functional groups grafted to the CF surface. Servinis *et al*. [174] examined the effect on IFSS after grafting of surface bound amine, carboxylic and lipophilic amide groups. These modifications were achieved using cyclic voltammetry (-1.0 V to +1.0 V, vs. Ag/AgCl, 0.02 V s^{-1}, 10 scans), and resulted in significant improvements to IFSS. Samples bearing anilinic nitrogenous groups, able to form crosslinks in an epoxy resin, showed the greatest improvement (49±2 MPa, +172%) compared to control (18±1 MPa), as determined by SFFT in an epoxy resin. Despite the beneficial effects of covalent interactions between fibre and resin, non-covalent interactions, with no crosslinking, also showed improved IFSS (carboxylic, 21±4 MPa; lipophilic amide, 24±2 MPa).

To minimise the occurrence of multilayers, the cyclic voltammetry process was reduced to 6 scans at a scan rate of 0.02 V s^{-1} (from -1.0 V to +1.0 V *vs* Ag/AgCl). Again, a variety of functional groups were studied, and all modifications demonstrated an increase in fibre resistivity (up to +202%, compared to control), indicating attenuation of the exposed graphitic surface.

Also reported, was the improvement in IFSS when these samples were tested *via* the micro-pullout method in maleic anhydride grafted polypropylene. Again, the aniline derivative showed the greatest response, manifesting as a 67% increase in IFSS (25±3 MPa *vs* 15±1 MPa control). This was attributed to the reactive crosslinking between the amine rich fibre surface and the maleic anhydride co-monomer in the polymer backbone.[174] The successful grafting was supported via physical analysis (XPS and TOF-SIMS) together with the effect on IFSS in an epoxy matrix, which was consistent with insights provided by molecular dynamic (MD) simulations.[174]

The effect of aniline groups increasing interfacial adhesion has also been observed on a larger scale.[175] Stojcevski *et al.*[175] demonstrated that fibres bearing this same aniline moiety showed improvements in IFSS using the SFFT method (39.6±5.6 MPa compared to control 19.5±0.5 MPa). This gain translated well to a larger scale, resulting in increased failure loads. Important findings in that work were that the orientation and placement of surface modified fibres was extremely influential in the composite's overall strength. For instance, a composite made entirely of functionalised fibre was outperformed by a hybrid mixture of functionalised and control fibre. This was due to the strategic manipulation of local interphase properties of the composite in areas that would benefit most, rather than a globally modified composite which could potentially lead to a brittle interface.

Molecular dynamic (MD) simulations have also informed the design of molecules to be bound to the surface. In a report by Demir *et al.,*[176] MD simulation was used to estimate the interfacial shear *stress* (ISS) of compounds with either *para*- or *meta*- substitution patterns around an aryl ring. This work also included a small molecule possessing functionality at both *meta*- positions of the aryl ring. The carbon fibre surfaces were decorated with these compounds, again with the electrochemical reduction of diazonium salts (Figure 26, b).

The ISS that resulted from MD simulations exposed very consistent trends with the experimentally determined IFSS,

with *para*- and *bis-meta*- substitution giving the best performance, though all modifications resulted in improvement (compared to control, ISS: 0.04±0.11; IFSS: 34.4±1.4 MPa). Interestingly, the introduction of a second reactive group in the *bis-meta*- sample did not result in an interface twice as strong.

Further use of MD simulations to influence design has been reported for bolo-amphiphilic compounds.[177] In that work, the mechanical interlocking of a long, amphiphilic chain within a resin matrix was simulated and correlated with experimental work.

The increase in interfacial adhesion was observed via IFSS, from the control (18.1±0.9 MPa) to the amphiphilic surface (69.2±7.5 MPa), representing an increase of +283%. This structure consisted of 6 ethylene oxide groups, terminated by a C18 alkyl tail. The compound was imparted onto the surface through the initial grafting of 4-ethynylbenzenediazonium, leading to protruding alkyne groups, which were then subjected to click chemistry conditions to form the 1,2,3-triazole with desired functionality (Figure 26, c, top). MD simulations suggested that a similar gain in IFSS could be achieved through a significantly smaller arch-like structure that anchored to the CF surface through two attachment points.[177] This would allow the epoxy matrix polymer chains to thread through the arch, thus locking the two in a non-covalent interaction and improve interface interactions (Figure 26, c, bottom). This threading was encouraged by the hydrophilic linking unit of the two anchoring points.

Insert Figure 26 here

Figure 26 a) Examples of the surfaces that can be accessed through diazonium chemistry.[173, 174] **b)** Structures of compounds evaluated for interfacial shear *stress* (ISS) through computational chemistry and interfacial shear *strength* (IFSS) determined experimentally.[176] **c)** Example of post-modification strategy using click chemistry (top) and the attachment of more complex, arch-like architecture on the surface of carbon fibre (bottom).[177] **d)** Hydrophobic surfaces prepared through diazonium grafting, including water contact angles of each samples and their IFSS.[178] **e)** Surface modification of the carbon fibre surface using an aryl diazonium salt with different methods of stimulus.[179] **f)** The application of click chemistry to tailor a surface integrated with alkyne groups, with increase in IFSS of each sample relative to control.[180]

Indeed, a similar IFSS gain of 276% (68.1±9.3 MPa) in IFSS was observed compared to the control (18.1±0.9 MPa).[177] It is also worth noting that all treatments investigated in this work had no deleterious effects on the fibre's mechanical properties. In several instances some improvements in these properties actually coincided with increased tensile strength.

The use of electrochemical reduction of diazonium salts serves as an operationally simple method of tailoring carbon fibre surfaces to tune the polarity or hydrophilicity (Figure 26, d). Arnold *et al*.[178] demonstrated the reduction of aryl diazonium salts bearing a nitro group in the presence of a perfluorinated alkyliodide compound to induce an extremely hydrophobic surface (WCA up to 139.9±1.0°, from control 98.4±0.6°).

The carbon fibres could be prepared with surface groups such as aryl-nitro, aryl-amine (from electrochemical reduction of nitro groups), combinations of both of these with perfluorinated alkyl chains, and a surface with only perfluorinated alkyl chains. The attachment of alkyl chains was achieved through the use of a sacrificial diazonium species (2,6-dimethylbenzenediazonium), which is unable to attach to the CF surface, but able to initiate homolytic cleavage of the carbon-iodide bond resulting in attachment.

The introduction of different functionality on the carbon fibre surface largely influenced the measured water contact angle, and the IFSS (Figure 26, d). Reduction of the nitro group to a more hydrophilic amine group showed a decrease in WCA, and an increase in IFSS for samples both with and without the perfluoroalkyl chains, compared to the nitro analogues. This is due to the ability of the amine to crosslink to the epoxy network, and the combination of aryl amines bearing hydrophobic groups allows for increased IFSS with a hydrophobic surface. This is the first report of its kind, as interfacial adhesion is usually linked to hydrophilicity and fibre wettability with the epoxy matrix.

Producing a surface with only hydrophobic groups resulted in a very high WCA, and very similar IFSS (18±5 MPa) as the control (18±1 MPa), suggesting there is no loss in composite strength with the introduction of these hydrophobic groups.[178] Tensile strength of the carbon fibre was preserved throughout these modifications, though there was a slight increase in Young's modulus.

The use of diazonium salts have proved to be a very effective and reliable method of modifying the CF surface, especially in the fidelity of grafting compounds produced through multistep synthetic pathways. The electrochemical reduction of these salts has been shown to be an advantageous method when compared to other radical-forming methods (e.g. UV light exposure, heat).[179]

To further develop diazonium based processes, a compound with a fluorine-based XPS tag was synthesised and attached to the surface of the carbon fibre using this diazonium chemistry (Figure 26, e). The goal of this work was to develop a means of carbon fibre surface modification in situations where electrochemical stimuli could not be employed. The properties of the samples produced, including IFSS, tensile strength, and Young's modulus, were evaluated after treatment. The study consisted of submersion of a carbon fibre tow in a solution of diazonium salt then forming the reactive radical species through heating (100 °C, 1 h) or exposure to UV light (1 hr). A control of submerged fibre in diazonium solution was produced with no stimuli.[179] These samples were compared to electrografting of the diazonium using cyclic voltammetry (-1.0 v to +1.0 V, 0.02 V s^{-1}, 10 sweeps).

Electrochemical reduction of the diazonium, unsurprisingly, proved to have the greatest increase in IFSS (54.0±3.7 MPa, compared to control 17.8±1.1 MPa), though heat treatment was similar (44.8±2.5 MPa). The sample exposed to UV light also increased in IFSS (21.8±2.0 MPa), though this was not statistically significant relative to the pristine fibre. Most interestingly, the sample not exposed to any stimuli also saw a slight increase in IFSS (26.4±1.8 MPa), due to random radical formation on the carbon fibre surface. The tensile strength and Young's modulus was preserved (except in the case of the UV treated fibres), and the increase in IFSS was attributed to drag effects of the surface-bound compound through the epoxy

matrix suggested by MD simulations of the interface and interphase regions.[179]

4.3 Post modification

Other reports of the electrochemical reduction of diazonium salts onto the carbon fibre surface incorporate the use of 4-ethynylbenzenediazonium tetrafluoroborate to provide an additional pathway to install further functionality.[180] Employing cyclic voltammetry (-1.0 V to +1.0 V (*vs* Ag/AgCl), 0.02 V s^{-1}, 6 sweeps) using a 15 cm tow of carbon fibre as the working electrode, resulted in a surface decorated with alkyne groups. The alkynes serve as facile chemical handles allowing further elaboration of the CF surface in solution using click chemistry (e.g. $CuSO_4$, ascorbic acid, DMF). The reliable and rapid formation of a triazole through copper catalysed azide-alkyne cycloaddition (CuAAC) allows introduction of a broad range of functional groups under mild conditions, which has seen CuAAC exploited in many areas of chemistry and biology.[181, 182] In the report outlining this process, the installation of surface chemistries was analysed using conventional XPS and also, more notably, through CuAAC using ferrocene-azide derivative. Following attachment of the ferrocene group, the fibres were analysed by cyclic voltammetry revealing the diagnostic redox couple of ferrocene. Using CuAAC, Servinis and co-workers tethered a range of variable chemistries to the surface of carbon fibres and examined their mechanical properties and interfacial adhesion in an epoxy resin through the SFFT method. The results from this study showed that all modified samples had increased IFSS compared to the pristine fibre (with no treatment at all) (18±1 MPa) including the alkyne-bearing surfaces (30±3 MPa, 67% increase compared to the control). Notably, amine functional groups, that are able to crosslink with the epoxy resin, demonstrate elevated IFSS values compared to compounds that are only able to interact mechanically. This manifests as increased IFSS for the aliphatic amine (53±4 MPa, +192%) and aromatic amine (58±3 MPa, +220%) compared to aryl (39±5 MPa, +116%) and nitro aryl (48±2 MPa, +167%), compared to the control sample.

Interestingly, this study also showed that an aryl amine compound maybe installed on the CF surface through use of 4-azidoaniline•HCl or reached in two steps by reduction of a nitro group. The former method ensures pendant surface modification bears an amine group, whilst the latter relies on further electrochemical reduction to access the aryl amine (Figure 26, f). Differences in these two processes can be seen in the IFSS as the reduction of nitro group to amine increases IFSS by 100% (36±1 MPa), as opposed to 220% compared to the control when using the amine-hydrochloride method.[180]

Using this triazole forming click-chemistry approach, larger functional groups have been explored to formulate a carbon fibre surface decorated with long PEO groups.[183] Azide-terminated PEO chains of varying molecular weight (1 kDa -10 kDa, Table 3) were attached to a carbon fibre surface bearing alkyne groups and the effect on interfacial adhesion evaluated. These chains are highly hydrophilic, which was reflected in the wettability of the carbon fibre surface, and the size of the chains also promoted a high degree of molecular entanglement with the epoxy matrix. This work set out to determine if surface density of grafted compounds or interphase penetration was more influential toward increasing the IFSS.

The largest of the PEO groups (10 kDa) showed the greatest increase in IFSS (46.3±4.4 MPa, compared to control 17.8±1.1 MPa) using the SFFT method. Perhaps contrary to logical progression, the second greatest increase was seen for the 1 kDa sample (41.0±2.3 MPa, +130% increase). MD simulations demonstrated a significant drag effect due to molecular entanglement of the PEO chains with the epoxy matrix. The absence of a clear trend between increased PEO length and improved performance was attributed to the increased penetration of long-chain PEO being offset by lower grafting densities. As the PEO groups became larger, the grafting density of PEO groups decreased due to limited diffusion.[183] Another contributing factor is the exclusion zone created when a large substrate attaches to a surface. The radius of gyration for the ligated polymer decreases the accessibility of adjacent alkyne groups, and they may be blocked by the steric bulk of the larger PEO chains. The conclusion from this work was that both extensive surface coverage and interphase penetration are viable means to dramatically increase fibre-matrix adhesion, but they are typically competing effects.

Table 2 – Diffusion coefficients and IFSS of samples grafted with PEO groups of various molecular weights.[183]

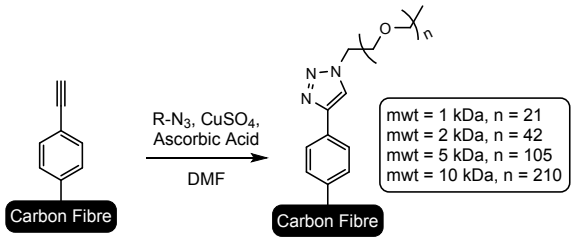

Sample	Diffusion Coefficient (m^2 s^{-1})	IFSS (MPa)	Gain (%)
Control	-	17.8±1.1	-
1 kDa	2.02×10^{-9}	41.0±2.3	+130
2 kDa	1.75×10^{-10}	32.5±0.6	+84
5 kDa	5.80×10^{-11}	38.6±3.7	117
10 kDa	4.78×10^{-12}	46.3±4.4	+160

Carbon fibres modified to bear these same large PEO compounds have also been evaluated in other polymer matrices, using a range of IFSS determination techniques.[184] The polymer matrices evaluated included epoxy, vinyl ester, polycarbonate, nylon 6, and nylon 6,6. Generally, surfaces with PEO functionality demonstrated increases in IFSS (single fibre pullout method). This was true for all PEO molecular weights (1 kDa, 2, kDa, 5 kDa and 10 kDa), presumably due to the same mechanism of mechanical entanglement as previously described.[183]

One interesting finding was the increase in IFSS (microbond method) for the pre-CuAAC fibre, bearing the terminal alkyne, with a vinyl ester resin. The 1 kDa sample returned an IFSS of

21.3±0.9 MPa (compared to control 16.2±0.1 MPa), though this was significantly lower than the IFSS of the alkyne bearing surface (37.4±0.2 MPa). This observation was attributed to the radical curing method of vinyl ester resin and the ability of the exposed alkyne group to participate in this reaction.[184]

A similarly robust 'click' reaction has been shown to impart functionality on the carbon fibre surface, offering an alternative to the copper catalysed click reaction. The sulfur-fluorine exchange (SuFEx) click reaction utilises the sulfone groups bearing a fluorine atom for coupling with silyl ether groups. This reaction takes advantage of the strong affinity of silicon and fluorine bonds, allowing fast reaction times and high fidelity of attached compounds. Randall *et al.*[185] demonstrated a comparison between traditional CuAAC click chemistry and the SuFEx reaction. Functionalised surfaces were analysed by XPS and the attachment of a ferrocene moiety was used to observe the success of the reaction, similar to previous reports.[180]

This study also demonstrated the possibility of using both forms of click reaction sequentially, to construct bespoke surface chemistries. In support of this idea, an azide dervivatised arylsufonyl fluoride group reacted, via CuAAC, with surface bound alkynes. Then, using SuFEx and a ferrocene-silyl ether derivative, ferrocene was covalently attached to the sulfonyl group, and the presence of the ferrocene was confirmed by cyclic voltammetry. Although the diagnostic redox couple of ferrocene was observed initially, the signal disappeared upon successive potential sweeps. This suggests that the triazole group is electrochemically unstable under the conditions used for the cyclic voltammetry, resulting in the cleavage of ferrocene from the carbon fibre surface.[185]

Using SuFEx to attach an aryl-amine group, pendant to the surface resulted in no loss in the mechanical properties of the CF, and a substantial gain in IFSS (+130%, 47.0±4.4 MPa *vs* 20.4±0.8 MPa, control) in an epoxy matrix (SFFT method).

Polymer attachment using post-modification approaches

Other carbon surfaces can be used as an analogue for carbon fibre to explore the grafting of various substrates. These surfaces, such as glassy carbon or highly oriented pyrolytic graphite (HOPG), are often easier to analyse than carbon fibre bundles or single filaments. This is due to the curved and inhomogeneous surface of carbon fibres making simple measurements, such as FTIR, water contact angle, and Raman spectropscoy, difficult and unreliable.

To illustrate the use and applicability of other carbon surfaces, thiophene-based conductive films have been electrochemically copolymerised on glassy carbon with potential application in energy-storage devices.[186] This type work has also been carried out on carbon fibre, clearly demonstrating the transferability of techniques between these types of carbon surfaces.[187]

Similarly, a copolymer system of poly(3,4-ethylenedioxythiophene) and pyrrole, and 3,4-ethylenedioxythiophene (EDOT) were each electrochemically deposited on a carbon fibre microelectrode (CFME, a single carbon fibre filament) surface in a polycarbonate solution of $LiClO_4$ (0.1 M), using a potential sweep of -1.5 V to +1.5 V (*vs.* SCE) at a scan rate of 0.01 Vs^{-1} for 10 cycles and a monomer concentration of 0.01 M. A very homogenous coating was reported, synthesised using an EDOT copolymer at a mole fraction of 0.925. The resulting coated CFMEs had well defined electro-activity and electrochemistry. Potential use in bio-applications was suggested, as these microelectrodes are often used to probe brain function.[188] Furthermore, the installed PEDOT polymer was very stable to over-oxidation, demonstrating limited degradation of electro-activity at potentials 1.2 V above the half-wave potential.

Similarly, the electrochemical polymerisation of 2,2-dimethyl-3,4-propylenedioxythiophene on the surface of carbon fibre has been demonstrated to produce a micro-supercapacitor.[189] Generated by using cyclic voltammetry in MeCN ($TBAPF_6$, 0.1 M; 0.0 V to 1.6 V (*vs.* Ag wire reference), using approx. 100 CF filaments as the electrode), this film was characterised by FTIR-ATR (Fourier-Transform Infrared Attenuated Total Reflectance), EIS (Electrochemical Impedance Spectroscopy), SEM, and EDX. The resulting surface-modified carbon fibre filament showed high capacitance behaviour as was demonstrated by the Nyquist, Bode phase relationship (Figure 27, top 3 panels).[189]

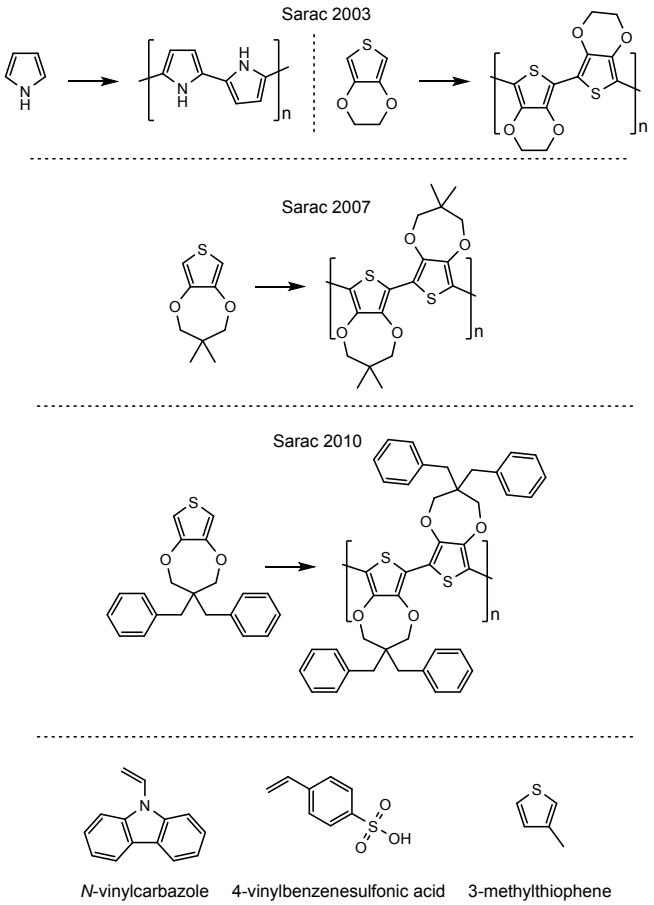

Figure 27 top 3 panels Development of conductive polymers for modification carbon surfaces.[188] **Bottom panel** Conductive monomers used to produce polymers or co-polymers.[190]

Exchange of the two methyl groups for benzyl moieties also served as an advanced avenue to carbon fibre capacitors, due to increased surface area.[190] Employing 2,2-dibenzyl-3,4-propylenedioxythiophene in electrochemical polymerisation

from the surface of a single carbon fibre generated nanofibre networks, able to efficiently transport and collect charge.

In terms of energy applications, electrochemical pretreatment of CFMEs at positive potentials improve the efficiency of vanadium flow batteries.[191] This improvement is reversible (through application of significant reductive potentials) and reproducible, indicating that the advantage lies in the change of surface states rather than alterations to surface area. This result highlighted the importance of surface chemistry in the context of broader applications based on enhanced surface interactions.

Saraç *et al.*[192] further explored the electrochemical deposition of conductive films on PAN-based carbon fibre as polymers or copolymers. This was achieved galvanostatically, with a constant electrolysis current applied by maintaining the current density constant (10 or 20 mA cm^{-2}). The monomers examined included *N*-vinycarbazole, 4-vinylbenzenesulfonic acid and 3-methylthiophene, each of which resulted in drastically different morphologies, as seen by SEM, when used neat or in combination (Figure 27, bottom panel). For example, the polymerisation of neat 3-methylthiophene resulted in a non-homogenous coating on the carbon fibres, but when combined with *N*-vinylcarbazole the resulting film manifested as linear rods. The use of *N*-vinylcarbazole strongly influences the formations of the grains of the linear rods grown from the surface. When copolymerised with 4-vinylbenzenesulfonicacid the coating was observed to self-organise in linear rods, with deep steps between grains (2 μm). These different morphologies may induce different topological effects and could positively influence physical strength if they were used in a carbon fibre composite materials. The conductive nature of the films also lends itself for use in carbon fibre devices, such as, sensing, structural health monitoring, and the adsorption of proteins in biological applications.

Conductive polymers are also attractive as solid supports for catalysis. The growth of polyaniline has been achieved on carbon fibre paper potentiodynamically, galvanostatically or potentiostatically, facilitating spontaneous Pd deposition on these surfaces.[193] It was found that the electrochemical method chosen for grafting greatly affected the morphology and particle size of the deposited Pd. This in turn affected the electro-catalytic activity, evaluated by the activity of the deposited Pd towards formic acid oxidation. Galvanostatically deposited polyaniline demonstrated better outcomes than films grown under controlled potential. The results highlight that not only the installed surface chemistry is important, but also the method of installation and resultant surface morphology.

Using electrochemistry to form polymer layers on the surface of carbon fibre has also been shown to improve the physical properties of the carbon fibres themselves. Kainourgious *et al*.[36] found that the polymerisation of vinylic monomers such as acrylic acid, methacrylic acid, acrylonitrile and *N*-vinylpyrrolidone improved the wetting properties of carbon fibres as well as their tensile strength (Table 3). The conditions leading to these improvements include the use of H_2SO_4 (0.4 M) as the electrolyte, a 0.3 M concentration of monomer and a 1 hour treatment time. It was also found that following polymerisation, substantial gains in specimen weight (up to 10%) were observed. Polymers were characterised using FT-IR, micro-droplet contact angle, micro-CT scanning, SEM, and Raman spectroscopy.

Table 3 – properties of carbon fibre samples with different monomers polymerised on the surface.[36]

Sample	Tensile strength (GPa)
Pristine (control)	50±3
Acrylic acid	81±4
Methacrylic acid	112±6
Acrylonitrile	97±5
N-vinylpyrrolidone	67±4

Other examples of polymers grown on carbon fibre include the electro polymerisation of acrylic acid onto the surface of carbon fibre fabrics.[194] The fabrics were pretreated using cyclic voltammetry (H_2SO_4, 5 wt%, -2.0 V to +2.0 V, 0.01 V s^{-1}, multiple sweeps, no reference electrode provided) to increase the surface oxygen content. This was followed by polymerisation under potentiostatic control in an aqueous media (acrylic acid 0.3 M, ZnCl 0.4 M). A crosslinking agent in the form of *N,N*-methylene-*bis*(acrylamide) (10 mM) was also employed and the resulting polymer films analysed by IR, XPS, SEM, and AFM.

Following treatment, samples exhibited a 3% gain in mass and a 36% increase in ILSS (92 MPa *vs* 68 MPa, control). This result came with no compromise in the ductility of the composite and the authors propose that the production of the polymer film improved the interactions occurring at the interface, thereby increasing the composite performance.

Wen *et al.*[195] was also able to grow different polymer film from the surface of carbon fibre and investigate their effect on the IFSS (Table 4).

Table 4 – properties of carbon fibre samples after surface polymerisation of the listed monomers.[195]

	IFSS (MPa)	
Monomer	CF	CF-GO
-	45.63	-
Diacetone acrylamide	47.71	55.83
Acrylic acid	57.38	72.54
Phenol	50.54	60.73

Carbon fibres were grafted with graphene oxide before polymerisation of either acrylic acid, phenol or diacetone acrylamide. The polymerisation was achieved in a continuous process using a range of current densities (1 A m^{-2}, 1.5 A m^{-2}, 3 A m^{-2}) and resonance times (60 sec, 120 sec, 300 sec). The treated samples exhibited decreases in the water contact angle and tensile strength varied with according to the monomer used. Despite this, increases in IFSS was observed for all samples compared to control, though carbon fibres grafted with graphene oxide showed the greatest improvement across all modifications relative to samples without graphene oxide present.

4.4 Solution Electro-Initiated Emulsion Polymersation (SEEP)

The reduction of aryl diazonium salts can be used for more than just single molecule attachment to the carbon fibre surface. Deniau *et al*.[196] demonstrated the use of diazonium salts as initiators for Surface Electro-initiated Emulsion Polymerisation (SEEP) on glassy carbon surfaces. This technique uses cyclic voltammetry to reduce a diazonium salt in aqueous sulfuric acid, forming an aryl radical. This radical may then attach to the electrode surface, to form a priming layer, or diffuse into the bulk and initiate polymerisation of acrylate-derived monomers.[197] Once polymerisation has begun, oligomeric chains may then diffuse to the fibre surface, attaching to existing surface bound aryl units allowing continued polymer growth from the surface. One note about this method is the difficulty in managing polymer length or polymer film thickness, and for water insoluble monomers, a surfactant is needed to form an emulsion. Originally, only three monomers were explored including acrylic acid, acrylonitrile and *n*-butylmethacrylate; though, recent investigations show that a broad range of monomers have been successfully polymerised using this process.[198]

The SEEP technique has been employed on PAN-CF with great success using acrylic acid and 4-nitrobenzenediazoium tetrafluoroborate as the initiator.[199] Treated carbon fibre resulted in IFSS gains of 311% together with substantial improvements in tensile strength and modulus. The improved tensile strength was attributed to the polymerisation of acrylic acid in defect sites on the surface of the fibre, effectively gluing together weaker sections of the fibre filament.

Following treatment, these carbon fibre samples were imbued with a rich metallic blue colour, which persisted after simple washing, sonication or mild heat, though the colour did temporarily disappear with the application of organic solvent. The colour was attributed to the occurrence of thin film interference caused by the growth of a polyacrylic acid film, measuring approximately 200 nm thick.[199] The colour disappearance was attributed to the swelling of the polymer film in solvent, with subsequent evaporation of solvent allowing the polymer film morphology to return to its previous state resulting in the return of the blue colour.

Other notable attributes of these samples was that the treated fibres were stiff and a single tow could be set in complex shapes through the same addition and evaporation of organic solvent. These self-supporting tows could hold many times their own weight without any extra support or reinforcement, and their shape could be immediately reversed with the addition of solvent.[200] With respect to scaling this procedure to industrially meaningful scales, this method of surface modification was optimised in a recent report by Eyckens and co-workers.[200] In that work, the electrochemical treatment time was reduced to 2 minutes, like that of a currently used surface treatment bath in carbon fibre manufacture. Moreover, the concentration of the monomer solution was reduced from 1.0 M to 0.2 M that will facilitate a reduction in cost for this type of surface enhancement approach.

5.0 Molecular modelling

Computer simulation techniques are now an invaluable part of the modern materials science and engineering toolbox. A broad range of computational techniques allows investigation of structure-property relationships at the molecular level, giving insight into the mechanistic origins of macroscopically observed behaviour previously inaccessible by traditional experimental methods due to time- and length-scale resolution limitations. Regarding carbon fibre reinforced polymer composites, simulation techniques have been used on a variety of size regimes. At an atomic level, first principles in quantum chemistry using density functional theory (DFT) calculations allow the modelling of chemical reaction pathways on carbon fibre surfaces (e.g., oxidation processes and oxygen group stability on graphitic carbon surfaces).[201-203] At the macro-scale, finite element analysis (FEA) allows simulations showing stress propagation to inform the design of structural composite components.[204-207] In particular, the interaction between the carbon fibre and the polymer matrix has been studied at the nano-scale using molecular modelling, or molecular dynamics (MD) simulations. MD simulations are a computational method in which the classical equations of motion for individual atoms or groups of atoms are propagated in accordance with Newton's equations of motion, subject to forces that describe inter-atomic interactions. Such simulations can complement traditional experimental techniques that characterize the carbon fibre composite interface and help elucidate the molecular-level mechanisms that drive interactions between the fibre and matrix and, ultimately, the mechanical integrity of the fibre-matrix interface.

At the nano-scale, the CF surface is understood to be a complex, highly graphitic arrangement of mostly sp^2 carbon atoms. However, the atomic-scale traits and features of the CF surface remain unknown. Typically, the CF substrate is approximated as a few layers of graphene or graphite in the simulation literature. With this picture of the CF-matrix interface in mind, there are many analogous carbon polymer composite systems that are relevant to understanding the CF-matrix interface, e.g., carbon nanotube-polymer interfaces[208-213] or graphite nanoparticle-polymer composites.[214]

A vital component of these interface simulation efforts is the structural model of the amorphous polymer network, specifically the polymer located at the interface with the CF surface. The task of capturing the true complexity of these networks in the vicinity of the carbon fibre interface has only become practical via fully atomistic MD simulations within the last decade or so. Many computational polymerisation strategies have been proposed, most of which can be applied to interfacial simulations in one of two distinct ways: "pre-packed" polymerisation, where the polymer network is crosslinked independently and subsequently interfaced with the substrate, or in situ crosslinking where the polymer network is crosslinked in the presence of the CF substrate. Of these methods, only the in situ approach is, in principle, able to capture the influence of the substrate on the polymerisation process, which is currently

considered capable of producing a more faithful structural model of the interphase. Therefore, discussion of simulations that employed the "pre-packed" crosslinking method will be limited to historically significant reports. A detailed overview of MD simulations of thermoset polymers in general can be found in the literature.[215]

In the following sections, focus is placed on simulation reports that have explicitly studied either the CF-matrix interface, or similar carbon-polymer composites and interfaces. It is noted that first principles simulations can and have previously been used to study reaction pathways relevant to surface modification of the carbon fibre, however, here focus is placed on simulations that aim to study the thermomechanical response of the composite and CF-matrix interface explicitly.

5.1 Pristine Carbon Fibre

Despite its common use throughout the simulation literature, graphite as a CF model should be regarded as being more representative of an idealized and pristine, i.e. unsized, CF surface, in contrast to commercially available carbon fibre subjected to the surface treatments outlined above. Regardless of the simplicity of the graphite carbon fibre surface model, simulations of graphite-polymer composite interfaces have been employed in partnership with experiment to elucidate the molecular-level mechanics of the carbon fibre-matrix interface that underpin thermomechanical properties. Aromatic carbon rings are a common feature in many thermoset epoxy resins (e.g., diglycidylether of bisphenol A) used in structural composite applications. The interaction between aromatic carbon molecules benzene, anthracene, pyrene, and tetracene, and pristine graphene surfaces has been studied using both DFT and semi-empirical density functional tight binding (DFTB) pull-off simulations.[216]

Zhe authors reported that adhesion energies increased with increasing molecule size, and that the adhesive force required to remove the absorbate aromatic molecule is affected by the pulling method, even for small rigid molecules such as benzene. As expected, the forces required to remove the absorbate molecules was ascribed to non-bonded dispersion interactions. The pristine CF-matrix interface has been extensively investigated and characterized using MD- and multiscale-simulation approaches, for a verity of polymer systems, both thermoset and thermoplastic. In particular, the mechanical response of the interface may be assessed using non-equilibrium pull-out MD simulations, where the CF substrate is pulled-out of the polymer matrix and the change in total system potential energy is monitored. The change in potential energy is directly proportional to the interfacial shear stress (ISS), which forms one part of the total interfacial shear strength (IFSS)[217] that can be experimentally measured. The IFSS additionally includes contributions effective over time- and length-scales that are practically inaccessible to atomistic simulations, such as the plastic flow of the matrix and the residual stress within the matrix. Nonetheless, the ISS provides a qualitative proxy for the IFSS, and has been successfully used to recover relative trends in simulation versus experimental findings.

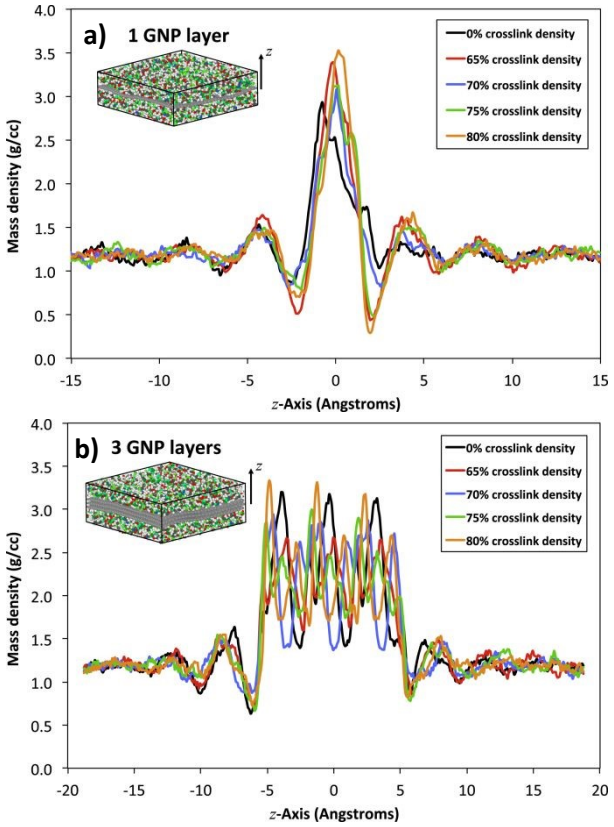

Figure 28 Mass density distributions normal to graphite nano particle (GNP) surface for a) one-layer, and b) three-layer composites. Reproduced with permission from reference.[218] Copyright 2015, Elsevier Ltd.

Yarovsky and Evans[219] were amongst the earliest pioneers to model computationally cross-linked resins interfaced with a solid surface. In terms of specific carbon substrates, some of the earliest work on simulating similar carbon-epoxy resin matrix interfaces were reported by Gau *et al.*,[208] where MD simulations of a carbon nanotube substrate embedded in a commercial resin EPON 862 (diglycidyl ether of bisphenol F, DGEBF) and diethyltoluenediamine (DETDA) epoxy resin were used to calculate the ISS of debonding. In this early effort, among others, the polymer matrix was computationally cross-linked prior to the introduction of the carbon substrate, in the so-called "pre-packed" manner, and hence does not fully capture the influence of the substrate on the polymer interphase.

The advent of more sophisticated polymerisation techniques within the traditional non-reactive (i.e. fixed topology) MD simulation framework enabled *in situ* polymerisation of the matrix in the presence of the carbon substrate, e.g the crosslinking methods of Grissinger *et al.*,[220] Demir and Walsh,[221] Tam and Lau,[222] Khare and Khare,[210] Li and Strachan,[223] and Yarovsky and Evans.[219] These contributions made substantial advances in composite interface modelling, as the effect of the substrate on the polymer interphase during crosslinking could be fully captured using these techniques. Hadden *et al.* reported MD simulations of a three-layer graphite substrate in the presence of an *in situ* cured DGEBF-DETDA polymer matrix, cured to various degrees of crosslinking, from 57% up to 85%.[214]

These authors found that the interphase thickness for the pristine graphite-epoxy system was approximately 10 Å, independent of crosslink density. MD simulations that investigated substrates with a shallow angle shingle-like graphite sheet stacking were reported by Nouranian *et al.*[224] These authors investigated the wetting of this surface with a precursor liquid of vinyl ester (VE) resin comprising bisphenol A based methacrylate, and styrene monomers, finding that styrene was enriched at this liquid interface, which suggested potential implications for the hypothetical structure of the polymerized interface. A later study reported by Hadden *et al.*[218] used a combined MD simulation and micromechanical simulation approach to investigate the influence of the number of layers in graphite layer the polymer interphase for DGEBF-DETDA resin. The authors reported that three-layers were sufficient to fully capture modified mass density distribution of the polymer of the interphase. Figure 28 presents the total mass density distributions for both single sheet and three-layer graphite composites.

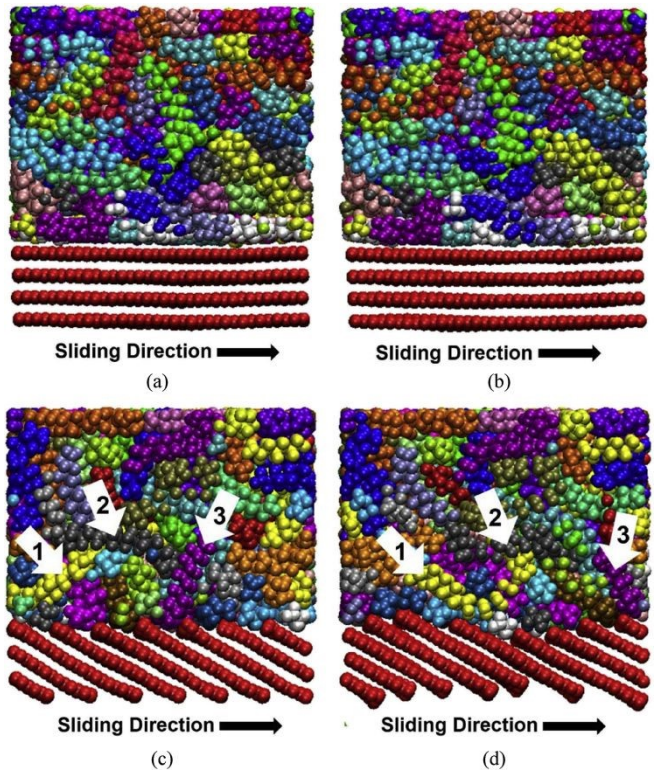

Figure 29 Snapshots of molecular structures during sliding MD simulations. Panels a) and b) show snapshots of before and after sliding for the basal exposed interface (θ = 0°), respectively. Panels c) and d) show images before and after sliding for the shingle stacked substrate (θ =30°) case, respectively. For panels c) and d) numbered arrows indicate the movement of the polymer structures in the shingled composites due to sliding, whilst no such movement can be seen in the basal exposed case. Reproduced with permission from reference.[225] Copyright 2016, Elsevier Ltd.

The effect of substrate orientation with respect to the polymer matrix has also been investigated. Li *et al.*[223] reported MD simulations of two orientations of graphite substrate, basal-exposed and edge-exposed, within two epoxy resin formulations: diglycidylether of bisphenol A (DGEBA) with a 3,3' diamino-diphenyl Sulfone (33DDS) hardener, and a diglycidyl ether of bisphenol C (DGEBC) with the same 33DDS hardener. The authors reported that the edge-exposed case resulted in a reduced interfacial energy and failed at the interface via debonding under shear loads, whereas the basal-exposed composite failed in the polymer matrix after yield. However, this early work did not report the edge termination state of the substrate and assumed the graphite edges to be charge neutral. Hu and Ding,[225] reported MD simulations of carbon-nanofiller morphologies in polyethylene (PE) polymer networks that investigated the impact of nanofiller orientation on the thermomechanical properties of the composite. The authors used non-equilibrium shear and tensile deformation MD simulations of a graphite substrate (hydrogen edge termination) arranged in a shingle like stack interfaced with the PE (modelled as amorphous, comprising 40-unit oligomeric chains). A range of stacking angles from 0° (basal-exposed) through to 90° (edge-exposed), were tested in increments of 10°, and sliding shear was applied in both in the positive and negative stacking direction (examples for the 0° and 30° cases shown in Figure 29). A maximal shear stress transfer was identified for a stacking angle of 30°, whereas the 90° case resulted in around half of this amount, and the basal exposed case of 0° was effectively zero.

The impact that defects and vacancies within the sp^2 carbon lattice substrate have on the interfacial bond with the matrix has also been explored. Peng and Meguid[226] reported MD simulations of carbon nanotubes featuring vacancy, adatom, and Stone-Wales (SW) defects interfaced with a DGEBA and triethylene tetramine (TETA) epoxy resin. When this system was subjected to pull-out simulations, the authors report that the ISS decreased, reflecting a weaker interface, with an increase in the number of vacancy, and conversely the ISS increased for an increase in SW defects resulting in a stronger shear response. Adatom defects were reported to have a negligible effect on the ISS. The molecular mechanisms behind these results were not completely clear. Likely, the defects in the carbon nanotube surface induced some nanoscale surface roughness which resulted in modest mechanical interlocking between the epoxy and substrate under pull-out conditions. Similar results have also been reported for MD simulations of graphene/DGEBA-TETA interfaces.[227]

Recent MD simulations have been reported, alongside experimental characterisation, on the effect of carbon nano-pores and grooves on the wetting of the liquid polymer pre-cursor. Xu *et al.*[228] reported MD simulations of two-dimensional nano-grooved surfaces, of various geometries, where the substrate was modelled as frozen atoms on an FCC lattice and non-bonded interaction parameters between the liquid TGDDM-44DDS resin and CF substrate were obtained via contact angle experiments of pristine, oxidized, and sized high modulus CFs. The simulations indicated that both oxidized and sized CF surfaces were able to fully wet the nano-grooves for all geometries. However, nano-grooves in pristine CF surfaces were only able to fully wet shallow grooves. Zhang *et al.*[229] reported fully atomistic MD tensile loading simulations of nano-grooved CF substrates interfaced with a polypropylene thermoplastic matrix. In these simulations, the polymer matrix was deformed via a tensile deformation while the substrate was

held fixed (i.e., atomic positions frozen) during tensile loading. The authors reported a competing effect of enhanced mechanical interlocking which improves the tensile strength of the interface, and a reduced interfacial interaction between matrix and CF for deep groove geometries (summarized in Figure 30). Two distinct failure mechanisms were reported: interfacial debonding and failure of the matrix. All grooved substrates exhibited larger interfacial interaction energies relative to the flat CF surface. However, the authors did not report the charge state of edge carbons or the termination state of the edges. Clearly a complex interplay between surface chemistry and topography is a major factor in the quality of the interfacial bond between CF and the matrix and has been shown to influence the interface prior to resin cure.

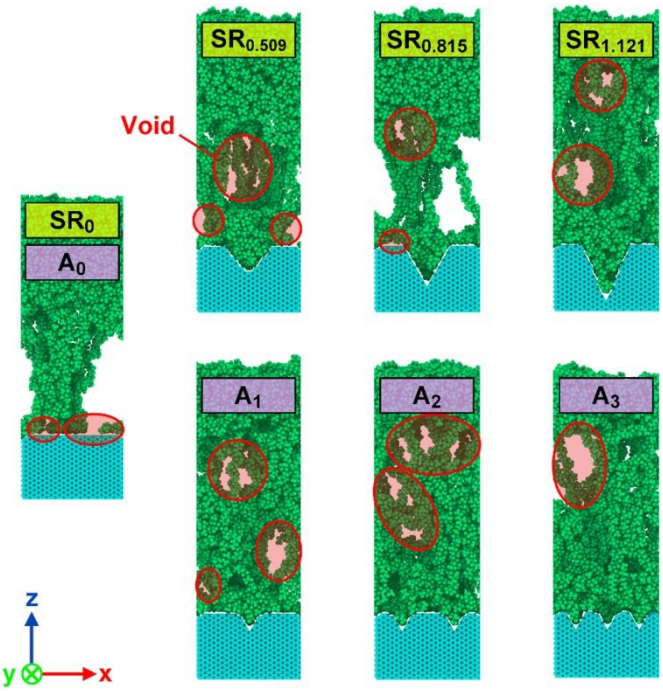

Figure 30 Tensile deformation MD simulation snapshots of a polypropylene-CF interface featuring nano-grooves, where the red regions indicate voids formed during tensile deformation. Reproduced with permission from reference.[229] Copyright 2020, Elsevier Ltd.

A key aspect of the interfacial interaction at the CF-matrix interface is the effect of resin chemistry. However, due to the enormous range of resin systems available, a complete summary of all systems explored through simulation is beyond the scope of this review. However, focus is placed here on previous simulation efforts regarding these effects of matrix chemistry on the substrate-matrix interfacial response. Recent MD simulations reported by Patil *et al.*[230] summarized studies of so-called 'flattened carbon nanotube' stacks, modelled as graphitic bi-layers, interfaced with two different aromatic polyimide systems: NASA Langley Research Center's Colorless Polyimide 1 (LaRC CP1), and Hunstman's Matrimid 5218 (M5218), where LaRC CP1 is fluorinated and M5218 is not. The authors reported the fluorinated polyimide resulted in greater friction force when sliding over the substrate, as well as a greater peak adhesive strength, relative to the non-fluorinated polyimide. Figure 32 presents the calculated friction force as a function of sliding velocity for both the fluorinated and non-fluorinated polyimide-nanotube composites. This increase in friction and adhesive strength was attributed to greater steric effects between the carbon substrate and fluoride ($-CF_3$) groups, despite the lower interaction energy between the surface and polymer, which was also attributed to steric effects. Additionally, the authors highlighted the need for new potentials which are able to fully capture the corrugation of the graphitic sp^2 carbon surface, also known as a 'registry' effect, between polymer and carbon. Currently, only certain carbon-only potentials have this capacity (e.g., the Kolmogorov-Crespi Registry Dependent Potential).[231]

These select examples highlight simulation efforts to investigate the pristine carbon-polymer matrix interfaces via MD simulations.[22, 232-240] The results indicate that surface roughness and mechanical interlocking between the matrix and CF play a significant role at the substrate-matrix interface, and this has a bearing on the performance of the real CF-matrix interface. As such, the next generation of simulation efforts should account for the presence of features such as surface defects and intrinsic roughness in a holistic model of the CF surface, and therefore the interface, as a necessary step towards a fully atomistic model of the pristine CF-matrix interface.

Oxidised Carbon Fibre

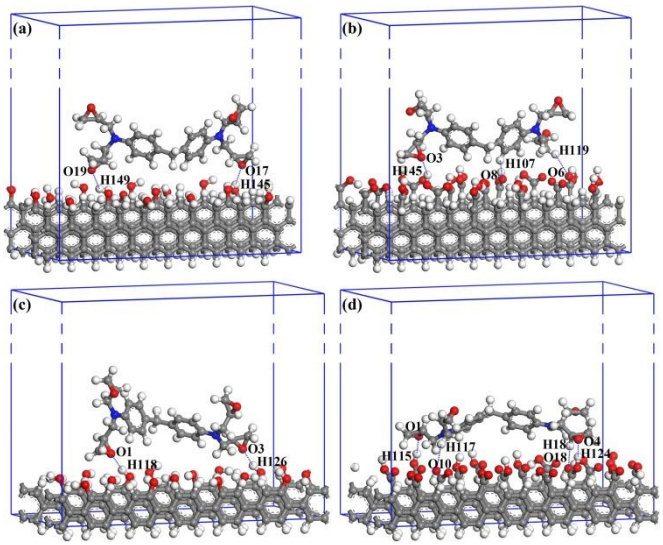

Figure 31 DFT optimized configurations of TGDDM-CF interactions for the following CF surface models: (a) (1 0 0) with hydroxyl, (b) (1 0 0) with carboxylic acid, (c) (1 1 0) with hydroxyl, (d) (1 1 0) with carboxylic acid. Hydrogen bonds are indicated with dash lines. Atom colours: white, grey, red and blue spheres denote H, C, O and N atoms, respectively. Reproduced with permission from reference.[241] Copyright 2013, The American Chemical Society.

The oxidation treatment of CF is an integral part of CF manufacturing that is known, from experimental evidence, to improve interfacial adhesion with the polymer matrix. It is thought that due to the inert chemical nature of the sp2 carbon basal plane, hydrogen bonding interactions between the electronegative sites in the polymer network and oxygen and nitrogen-bearing groups at sp^2 carbon edges present on the CF

surface may be a dominant factor in interfacial adhesion. Due to the wide scope of this topic, only a selection of computational studies are used herein to highlight key issues in this area. To study such scenarios, Semoto *et al.* reported DFT calculations on the interaction energy between graphite edges decorated with oxygen functional groups and a fragment of a diglycidylether of bisphenol A (DGEBA) polymer chain.[241]

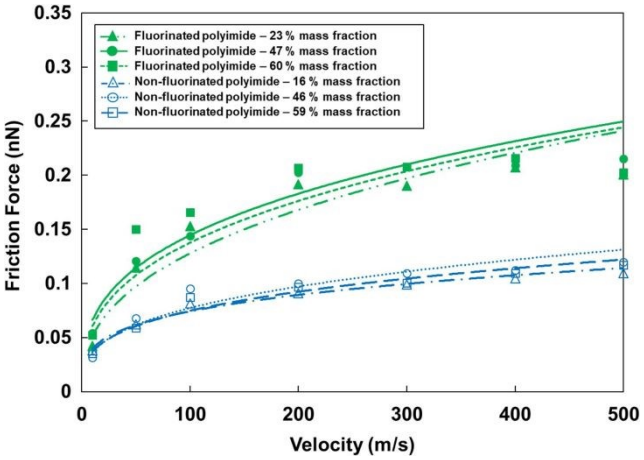

Figure 32 Calculated friction force as a function of sliding velocity for both fluorinated and non-fluorinated polyimide matrix interfaced with flattened carbon nanotubes. Reproduced with permission from reference.[230] Copyright 2020, Elsevier Ltd.

The authors also reported the adhesive force for two cases of CF edge oxygen functionalisation: one with hydroxyl groups only and another case carboxylic acid groups only. Their findings indicated slightly stronger interaction with the carboxylic acid functionalized CF compared with the hydroxyl counterpart. Li *et al.*[242] used a combined DFT and MD simulation approach to study interactions between a single tetraglycidyl diamino diphenyl methane (TGDDM) monomer and a graphite edge, considering both hydroxyl and carboxylic acid edge oxidation (Figure 31). These authors first used MD simulations to generate appropriate configurations that were used as input starting structures for geometry optimization using DFT. In line with previous studies, the authors reported that carboxylic acid edge termination produced both more, and stronger hydrogen bonds, predominantly interacting with the epoxide groups of the TGDDM monomer, relative to the hydroxyl terminated edge. This work explored two graphite edge terminations: (110) and (100), finding that the (110) case had a greater capacity for hydrogen bonding. The carboxylic acid functionalized (110) edge interface was found to confer the strongest interaction (Figure 31, d).

In a report by Jang *et al.*, *the* effects of surface oxidation on an interphase containing a vinyl ester resin liquid precursor of bisphenol A dimethacrylate and styrene were investigated via MD simulations.[243] The authors used a shallow angle shingle arrangement of two graphene sheets that were oxidized with epoxide, hydroxyl, carbonyl, and carboxylic acid groups to an O/C ratio of just under 0.02, featuring both edge and surface oxidation. They found that relative to the pristine shingled graphene case previously studied, which favoured the enrichment of styrene at the interface, this enrichment was somewhat suppressed at their oxidized interface. The enhanced co-location of both styrene and the monomers at the surface was suggested to possibly lead to increased interfacial cross-links in the hypothetical resin.

The effect of the spatial distribution of the oxygen-bearing functional groups has been studied via coarse-grained MD simulations via a related graphene oxide composite, reported by Li *et al.*[227] These authors considered a graphene oxide sheet decorated with various patchy oxidation structures, ranging from one large singular patch through to small randomly distributed patches, interfaced with a polybutadiene polymer matrix. The structure of the oxide patches directly affected the polymer interphase, both by introducing heterogeneity into the first monolayer of the polymer, which was concentrated at the oxide patch locations for the large size patch structures, and also the overall distribution of polymer in the interphase region above the graphene oxide sheet. The modified polymer interphase was reported to impact the storage and loss modulus of the composite along with interfacial energy, which reduced with increasing patch size.

5.2 Functionalized Carbon Fibre

Beyond the chemical oxidation of commercial CF production is the advent of chemical covalent CF surface functionalisation, which has been recently realized via novel “click-chemistry” functionalisation methods. Such functionalisation may be tailored to target specific design requirements of the composite, e.g., enhanced interfacial shear stress transfer or improved interfacial wetting by the resin precursor. Molecular modelling techniques such as MD simulation are uniquely positioned to provide molecular scale insights into the structure of the polymer upon interaction with CF surfaces at a functionalised interphase. These insights can advance understanding of the thermo-mechanical properties of the interface.

Khare *et al.*[210] reported MD simulations of both bare carbon nanotubes and nanotubes that were functionalized with amido-amine groups at the open nanotube ends, which were then embedded within a DGEBA and 4,4’-diaminodiphenylsulfone (44DDS) epoxy resin. The functionalised nanotube composites exhibited an increase in Young’s modulus of 50%, relative to the non-functionalized nanotube-epoxy composite. These simulations showed that significant gains in mechanical performance of composites could potentially be achieved by targeted modification of the surface attached groups of the composite substrate.

Gogoi *et al.*[244] reported MD simulations of graphite surfaces functionalised with amine, hydroxyl, and carboxylic acid, interfaced with a polypropylene thermoplastic. Coating of the graphite substrate in carbon nanotubes was also considered. The amine-functionalized case featured the highest interaction energy and increased the predicted ISS by ~125%, relative to the nanotube coated case. Similar small molecule functionalisation of CF surfaces was also explored by Sharma and Shukla.[211] These authors reported MD simulations of a graphite-carbon nanotube-epoxy composite, using a commercial LY556 (IUPAC name not specified) and DETDA hardener resin, where the carbon nanotubes were surface-functionalized with small

amine bearing groups. Mechanical properties predicated via MD simulation of the composites showed an increase in both transverse and longitudinal Young's modulus for the functionalised nanotube composites, relative to the graphite-epoxy only composites. However, this work did not provide the comparison with a control case (i.e., unfunctionalized nanotubes). Niuchi *et al.*[245] reported MD simulations of both pristine, fluorine substituted, and fluorinated (-CF_3 functionalised) graphite substrates interfaced with a coarse grained model of a phenolic resin polymer, where the resin was interfaced with the substrate in the "pre-packed" manner. The authors reported that the both the fluorine substituted, and the fluorinated CF supported lower predicted interfacial fracture stress via tensile pull-off MD simulations, with the fluorinated CF exhibiting the lowest interfacial stress.

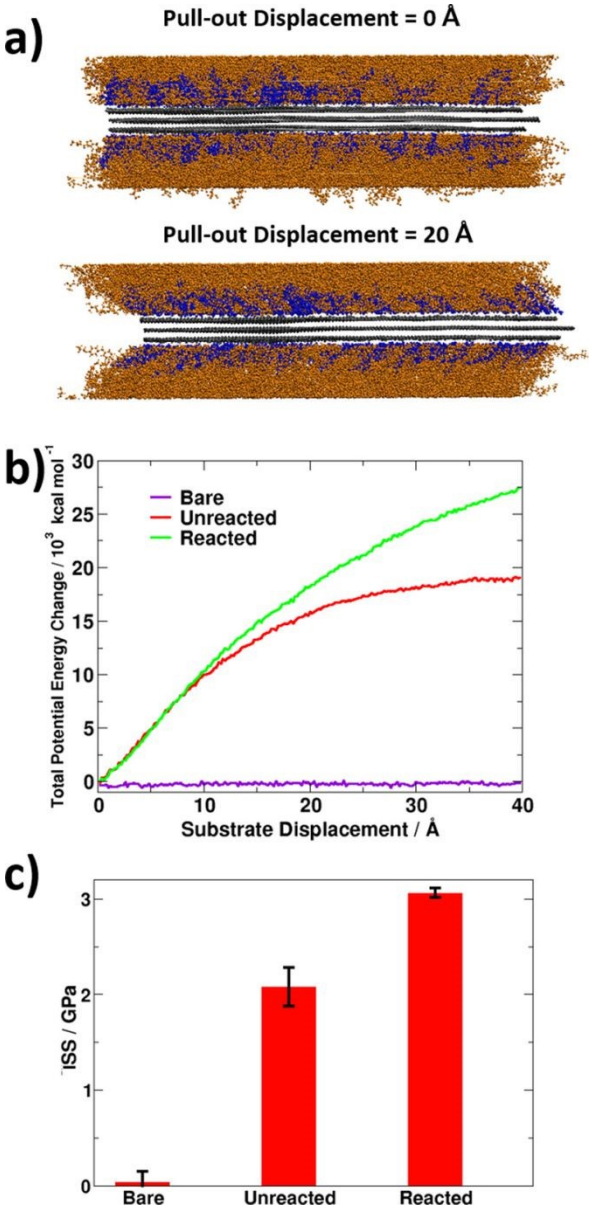

Figure 33 MD simulations of surface functionalized carbon fibre epoxy matrix interfaces under pull-out loading conditions. Panel a) Snapshot of pull-out MD simulations, b) total potential energy change during pull-out, and c) calculated interfacial shear stress. Reproduced with permission from reference.[216] Copyright 2017, The American Chemical Society.

Demir *et al.*[217] reported the first MD studies on the impact of CF surface functionalisation with larger, more complex molecules on interfacial mechanical response. Here, complex refers to molecules that are larger than groups such as amines, methyls, and the typical oxygen functional groups that result from fibre oxidation, such as carboxylic acid, epoxies, etc. The authors reported MD pull-out simulations and characterisation of composites consisting of a graphite substrate, both pristine and surface functionalized with long chain molecules with a terminus amine group, which was enabled to react with the EPON 862-DETDA polymer matrix to form crosslinks with the polymer. Figure 33 presents the images of the pull-out simulations, as well as the change in potential energy as a function of pull-out displacement and the total calculated ISS for these simulations. These authors reported that even if cross-linking between the surface-grafted molecules and the polymer matrix was suppressed, a substantial increase in ISS still resulted, relative to the un-functionalized interface. However, the crosslink-enabled functionalisation conferred the maximal increase in ISS of the three cases. It is noted that the control un-functionalized case yielded a markedly low ISS for the benchmark comparison. This low value is typical in the simulation literature in general and reflects the highly idealized character of the flat graphite interface in such simulations.

Later reports by Demir et al.[176] used a combination of MD simulation and experiment to map correlations between the design of the surface grafted molecules and the effects on the composite ISS. These authors reported MD pull-out simulations for three amine bearing surface grafted molecules: two that contain phenol rings with single meta- or para-substituted reactive amine terminated chains, and a third with two reactive amine terminated chains at both meta-substitution ring sites. The simulations suggested that a single para-substituted amine terminated chain would extend further into the matrix resulting in a similar ISS than that of molecule bearing two amines, which adopted a less extended conformation. The single meta-substituted amine group molecule resulted in the lowest mechanical interface performance. A combined MD simulation and experimental approach was reported by Arnold et al.,[246] studying the impact of both hydrophilic and hydrophobic surface functionalisation in CF-epoxy composite interfaces. The authors report that both hydrophilic and hydrophobic functionalisation resulted in increased IFSS, contrary to the common belief that surface polarity of the CF is directly related to the interfacial shear strength of the composite. Here, MD simulations were used to study the four surface grafted molecules considered: one terminated with un-reactive nitro groups, a second terminated with reactive amino groups, and two polyfluorinated alkyl chain molecules, one attached to a phenol groups and other attached to the surface. The functionalised CF surfaces were then interfaced with an EPON 862-DGEBA epoxy resin as reported in prior simulations. Both the nitro-terminated and the amino-terminated groups were predicted to predominantly adopt upright conformations perpendicular to the CF surface, engaging with the polymer

matrix. However, it was noted that a small fraction of amino-terminated molecules adopted a bent conformation, likely due to competing amino-CF interactions. In contrast, in the worst performing surface functionalisation, the majority of the non-reactive fluorinated carbon chains were found in a flattened conformation, reducing engagement with the polymer matrix.

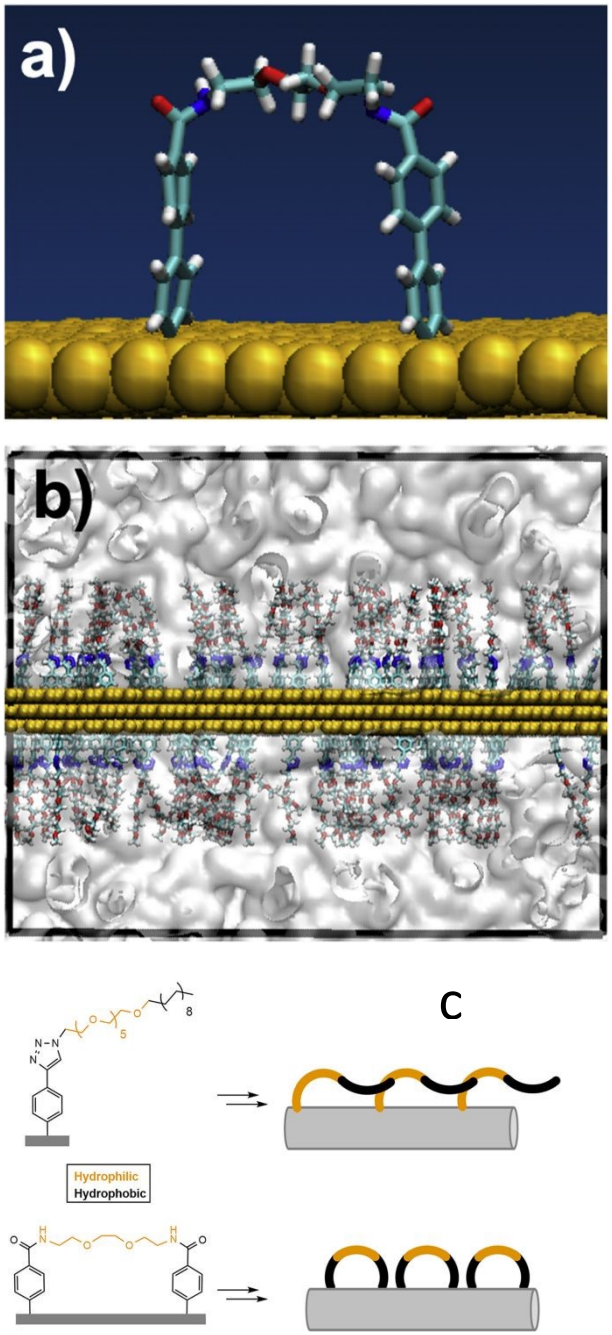

Figure 34 a) Snapshot of 'horseshoe' functionalisation on the CF surface. b) Snapshot of CF-polymer interface with amphiphile functionalisation. c) Schematic of both types of amphiphile functionalisation. Reproduced with permission from reference.[177] Copyright 2020, Elsevier Ltd.

In addition to the chemistry, the geometry and molecular conformation of surface grafted molecules have also been shown to affect the mechanical performance of the composite interface. Here, MD simulations can provide key insights into the molecular-level processes behind the macroscopically observed results.

MD simulations reported by Eyckens *et al.*[179] found that the engagement of the surface grafted molecules with the polymer matrix could lead to a dragging effect during CF pull-out, thereby substantially increasing the ISS despite the lack of chemical reactivity with matrix. This was further investigated in a study reported by Eyckens *et al.*[177] in which MD simulations of long amphiphilic molecules were covalently attached to the CF surface, and then interfaced with an EPON 862/DETDA epoxy matrix. This report illustrates the power of MD simulations in study of interfaces, as the long chain grafted molecules were predicted to adopt a bent-over or 'hooked' conformation at the polymer matrix interphase. These results prompted the synthesis and subsequent modelling of smaller grafted molecular chains which were attached to the CF surface at both ends, resulting in a 'horseshoe' like conformation (Figure 34). Simulations of both the dangling end, and horseshoe amphiphilic molecules resulted in an increase in ISS of 276%, relative to the bare CF-matrix interface. Experiments of both types of surface grafted molecule recovered similar increases in the measured IFSS of +280%.

Advancements in understanding arising from work reported in the functionalized composite simulation literature over the past few years has been substantial. Despite this, questions still remain regarding how the incorporation of more realistic CF surface models will impact the thermo-mechanical properties of the composite interface. To-date, all functionalisation efforts have considered basal plane functionalisation, however it is known that attachment to planar sp^2 is energetically less favourable relative to defect sites and edges. Hence, it is not yet understood what effect the edge carbon functionalisation will have on the mechanical response of the CF-matrix interface. Furthermore, the interplay between functionalisation, surface roughness, and varied topology has yet to be explored in the context of both functionalised and un-functionalised CF-matrix interfaces.

5.3 Sizing-modified Interfaces

The presence of a sizing layer on the CF surface adds considerable complexity in terms of molecular simulation of the CF-matrix interface. The thickness of the sizing layer is typically on the micron scale, which presents challenges of scale for all-atom simulations in tackling a complete description of the entire CF/sizing/matrix. Attempts at all-atom molecular simulations of this double interface have been recently reported.[247-249] However, all of these studies have approximated the sizing layer as a thin layer (nanometre or less) of oligomeric chains, which cannot capture much of the relevant phenomena which may control the structure/property relationships of these composite interfaces. For example, the diffusion of matrix precursor into the sizing layer (and vice versa) cannot be adequately represented with this structural model.

To address deficiencies in the processes outlined above, multiscale simulations that capture different regions of the interface at different levels of spatial and temporal resolution are ideally suited

to address these questions. However, these approaches typically sacrifice molecular level details out of necessity. Notably, Li *et al.*[250, 251] have previously applied such a multiscale simulation, incorporating mesoscale approaches including coarse-grained simulations and dissipative particle dynamics simulations to the CF/epoxy sizing/epoxy matrix sample. These authors were able to predict some mesoscale phenomena resulting from the interplay between the sizing thickness and degree of diffusion of hardener into the region between the sizing and the matrix.

Despite the impracticality of applying all-atom MD simulations to the entire CF/sizing/matrix interface(s), it would be possible to create all-atom structural models of the zoomed-in region between the sizing and the matrix. This would essentially entail MD simulation of a polymer-polymer interface, in which the matrix could be dynamically cross-linked in the presence of a cured sizing surface (modelled as a bulk polymer slab). Computational curing of epoxy resin in the presence of thermoplastic interfaces has been previously reported,[252] and could form the basis of future investigations in this area.

6.0 Conclusions and Outlook

There has undoubtedly been a large volume of experimental and theoretical work done on the modification of carbon fibres to promote adhesion, induce functionality, and enhance the compatibility of the fibre surface with the matrix. The mechanical and chemical nature of the interface both play a role at the fibre-matrix interface, though in the authors opinion, the modification of surface chemistry without detrimentally impacting the inherent value of the fibres is likely a route for maximising research impact.

The recent development of various capabilities to chemically control the surface chemistry and therefore interface/interphase of composite with high precision may provide the ability to engineer optimal hard-soft interfaces. There has been an historical desire to implement interphases which mimic those on naturally occurring composites such as bone, wood, nacre, etc. As these natural materials often possess contradictory properties, such as high strength and high toughness. A significant amount of work has already been conducted in this space but as fabrication techniques and chemical processes continue to advance, so too does the ability to tailor these properties and their functionality.

There exists conflicting motivation for the improvement of fibre-matrix interactions. The fundamental understanding of how and what chemistries impact the properties of a final composite, how they are balanced and optimised for each resin is an incredibly far-reaching goal that may not be satisfactorily realized even over the next few decades. Contrary to this motivation is the desire to develop novel, scalable, and rapidly deployable surface treatments that can have immediate impact. Thus, immediate deployment of technologies may be misplaced in the long run due to a lack of fundamental understanding about these interactions. These avenues of experimental investigation have, and will continue to be, conducted in parallel with one benefitting from the other, over time giving a more detailed picture of how the best performance and functionality can be designed into composite materials.

From a molecular modelling perspective, the past two decades has witnessed enormous progress in the capability to computationally describe the structure and properties of fibre-matrix interfaces, with increasing levels of sophistication and detail. At the heart of the molecular simulation approach is a pragmatic balance of rigour and relevance, which requires compromise between how faithfully the system is described in terms of structural models, how accurately the system is described in terms of the inter-atomic (or inter-particle) interactions, and how close to reality the simulation approaches are for determining the interfacial properties (e.g. strain rate or cooling rate). In the world of computer simulation, none of these can be expected to provide a 100% match with experimental scenarios. That said, simulation outcomes have been most meaningful in this field when comparing trends in predicted properties, rather than absolute values.

Several areas are ripe for development in molecular simulations of the fibre-matrix interface. First, the creation and use of more detailed structural models of the carbon fibre surface is a clear candidate. Past reliance on graphite surfaces has proven enormously useful, but as experimental characterisation breakthroughs continue, there is clear need for consideration of structural models of carbon fibre that can more realistically capture features such as fibre surface roughness, disorder, and the spatial distribution of relevant types of oxygen-bearing groups arising from surface oxidation. Second, great strides have been made in the modelling of surface-attached groups on carbon fibre and their impact on the structure and mechanical properties of the polymer interphase, specifically for epoxy resins.

Other types of resin, such as vinyl esters, phenolic resins, and so forth, are relatively under-studied in this context, and much more could be done in this area. In addition, expansion of molecular simulation approaches to model surface-initiated polymerisation processes such as SEEP are needed to keep pace with experimental developments and provide molecular-scale guidance into the design of these new interfaces, to enable the harmonization of the polymerised fibre matrix with a range of different resin types. Going further, the ability to model the effect of sizing and its impact on interfacial properties is an area where significant challenges remain. Specifically, new multi-scale modelling efforts, namely the ability to effectively couple across multiple length-scales while still retaining the required levels of molecular detail would be welcome developments. Finally, the search for appropriate surface functionalisation strategies that can optimise the desired properties of the fibre-matrix interface is hampered by relatively small datasets compared with massive datasets in other research areas e.g. the protein structure databank. This limits the ability to apply machine learning approaches for this purpose, and efforts could be taken to compile and strategically augment the fibre-matrix dataset, integrating both experimental data and simulation data. Together, the partnership of experiment and simulation has achieved significant progress, promising a bright future for

the rational design of multi-functional carbon fibre reinforced polymer composites.

Conflicts of interest

There are no conflicts to declare

Acknowledgements

The authors gratefully acknowledge Deakin University, the Australian Future Fibre Research and Innovation Centre (AFFRIC) and the Australian Research Council (DP180100094) and the ARC Research Hub for Future Fibres (IH140100018), the ARC centre for Automotive light weighting (IC160100032) this work was partially funded by the Office of Naval Research (N62909-18-1-2024) for funding this project.

Notes and references

1. E. Mäder, K. Grundke, H. J. Jacobasch and G. Wachinger, *Composites*, 1994, **25**, 739-744.
2. S. Zhandarov and E. Mäder, *Compos. Sci. Technol.*, 2005, **65**, 149-160.
3. M. Sharma, S. Gao, E. Mäder, H. Sharma, L. Y. Wei and J. Bijwe, *Compos. Sci. Technol.*, 2014, **102**, 35-50.
4. F. R. Jones, *J. Adhes. Sci. Technol.*, 2010, **24**, 171-202.
5. M. Maghe, C. Creighton, L. C. Henderson, M. G. Huson, S. Nunna, S. Atkiss, N. Byrne and B. L. Fox, *J. Mater. Chem. A*, 2016, **4**, 16619-16626.
6. D. Choi, H.-S. Kil and S. Lee, *Carbon*, 2019, **142**, 610-649.
7. S. H. Yoo, S. Park, Y. Park, D. Lee, H.-I. Joh, I. Shin and S. Lee, *Carbon*, 2017, **118**, 106-113.
8. E. Frank, L. M. Steudle, D. Ingildeev, J. M. Spörl and M. R. Buchmeiser, *Angew. Chem. Int. Ed.*, 2014, **53**, 5262-5298.
9. M. G. Huson, J. S. Church, A. A. Kafi, A. L. Woodhead, J. Khoo, M. S. R. N. Kiran, J. E. Bradby and B. L. Fox, *Carbon*, 2014, **68**, 240-249.
10. F. Stojcevski, T. B. Hilditch and L. C. Henderson, *Composites, Part A*, 2019, **118**, 293-301.
11. F. Stojcevski, T. Hilditch and L. C. Henderson, *Composites, Part A*, 2018, **107**, 545-554.
12. F. Stojcevski, T. B. Hilditch, T. R. Gengenbach and L. C. Henderson, *Composites, Part A*, 2018, **114**, 212-224.
13. F. Stojceveski, A. Hendlmeier, J. D. Randall, C. L. Arnold, M. K. Stanfield, D. J. Eyckens, R. Alexander and L. C. Henderson, *Materials*, 2018, **11**, 1786.
14. S. F. Zhandarov, E. Mäder and O. R. Yurkevich, *J. Adhes. Sci. Technol.*, 2002, **16**, 1171-1200.
15. E. Pisanova, S. Zhandarov and E. Mäder, *Composites, Part A*, 2001, **32**, 425-434.
16. S. Lee, S. Ham, S. J. Youn, Y. S. Chung and S. Lee, *Ind. Eng. Chem. Res.*, 2021, **60**, 9088-9097.
17. C. T. Chou and L. S. Penn, *The Journal of Adhesion*, 1991, **36**, 125-137.
18. A. Ishitani, *Carbon*, 1981, **19**, 269-275.
19. Z. R. Yue, W. Jiang, L. Wang, S. D. Gardner and C. U. Pittman, *Carbon*, 1999, **37**, 1785-1796.
20. Q. Ma, Y. Gu, M. Li, S. Wang and Z. Zhang, *Applied Surface Science*, 2016, **379**, 199-205.
21. J. Gulyás, E. Földes, A. Lázár and B. Pukánszky, *Composites Part A: Applied Science and Manufacturing*, 2001, **32**, 353-360.
22. K. Mori, N. Matsumoto, M. Yabe and Y. Konho, *Adv. Compos. Mater.*, 2020, **29**, 179-190.
23. D. He, V. K. Soo, F. Stojcevski, W. Lipiński, L. C. Henderson, P. Compston and M. Doolan, *Composites Part A: Applied Science and Manufacturing*, 2020, **138**, 106072.
24. A. Hendlmeier, L. I. Marinovic, S. Al-Assafi, F. Stojcevski and L. C. Henderson, *Composites Part A: Applied Science and Manufacturing*, 2019, **127**, 105622.
25. F. Stojcevski, L. C. Henderson and T. Hilditch, Doctoral Thesis (Engineering), Deakin University, 2018.
26. A. Kelly and W. R. Tyson, *Journal of the Mechanics and Physics of Solids*, 1965, **13**, 329-350.
27. L. Százdi, J. Gulyás and B. Pukánszky, *Composite Interfaces*, 2002, **9**, 219-232.
28. L. M. Manocha, *Journal of Materials Science*, 1982, **17**, 3039-3044.
29. C. U. Pittman, W. Jiang, Z. R. Yue and C. A. Leon y Leon, *Carbon*, 1999, **37**, 85-96.
30. C. U. Pittman, G. R. He, B. Wu and S. D. Gardner, *Carbon*, 1997, **35**, 317-331.
31. X. Qian, L. Chen, J. Huang, W. Wang and J. Guan, *Journal of Reinforced Plastics and Composites*, 2012, **32**, 393-401.
32. J. Jiang, X. Yao, C. Xu, Y. Su, L. Zhou and C. Deng, *Composites Part A: Applied Science and Manufacturing*, 2017, **95**, 248-256.
33. A. Fukunaga and S. Ueda, *Composites Science and Technology*, 2000, **60**, 249-254.
34. F. Severini, L. Formaro, M. Pegoraro and L. Posca, *Carbon*, 2002, **40**, 735-741.
35. Y. J. Kim, H. J. Lee, S. W. Lee, B. W. Cho and C. R. Park, *Carbon*, 2005, **43**, 163-169.
36. P. Kainourgios, I. A. Kartsonakis, D. A. Dragatogiannis, E. P. Koumoulos, P. Goulis and C. A. Charitidis, *Applied Surface Science*, 2017, **416**, 593-604.
37. B. Gao, R. Zhang, M. He, C. Wang, L. Liu, L. Zhao, Z. Wen and Z. Ding, *Composites Part A: Applied Science and Manufacturing*, 2016, **90**, 653-661.
38. F. Nakao, Y. Takenaka and H. Asai, *Composites*, 1992, **23**, 365-372.
39. J. Liu, Y. Tian, Y. Chen, J. Liang, L. Zhang and H. Fong, *Materials Chemistry and Physics*, 2010, **122**, 548-555.
40. J. Peng, W. Gao, B. K. Gupta, Z. Liu, R. Romero-Aburto, L. Ge, L. Song, L. B. Alemany, X. Zhan, G. Gao, S. A. Vithayathil, B. A. Kaipparettu, A. A. Marti, T. Hayashi, J.-J. Zhu and P. M. Ajayan, *Nano Lett.*, 2012, **12**, 844-849.
41. F. Stojcevski, T. B. Hilditch and L. C. Henderson, *Composites Part A: Applied Science and Manufacturing*, 2019, **118**, 293-301.
42. A. Hendlmeier, F. Stojcevski, R. Alexander, S. Gupta and L. C. Henderson, *Composites Part B: Engineering*, 2019, **179**, 107494.
43. J. D. H. Hughes, *Composites Science and Technology*, 1991, **41**, 13-45.
44. L. T. Drzal and M. Madhukar, *Journal of Materials Science*, 1993, **28**, 569-610.
45. J. Moosburger-Will, M. Bauer, E. Laukmanis, R. Horny, D. Wetjen, T. Manske, F. Schmidt-Stein, J. Töpker and S. Horn, *Applied Surface Science*, 2018, **439**, 305-312.

46. Michelman, Fiber Sizing, https://www.michelman.com/Industrial-Manufacturing/Reinforced-Plastic-Composites/Fiber-Sizing/, (accessed 10. Aug., 2020).
47. N. Dilsiz and J. P. Wightman, *Colloids and Surfaces A: Physicochemical and Engineering Aspects*, 2000, **164**, 325-336.
48. W. D. Bascom and L. Drzal, *The Surface Properties of Carbon Fibers and Their Adhesion to Organic Polymers*, 1987.
49. Y. Luo, Y. Zhao, Y. Duan and S. Du, *Materials & Design*, 2011, **32**, 941-946.
50. X. Yuan, B. Zhu, X. Cai, J. Liu, K. Qiao and J. Yu, *Applied Surface Science*, 2017, **401**, 414-423.
51. Y. Yang, Y. Zhao, Y. Li, Q. Dong and D. Chen, *Journal of Wuhan University of Technology-Mater. Sci. Ed.*, 2014, **29**, 483-487.
52. R. L. Zhang, Y. D. Huang, L. Liu, Y. R. Tang, D. Su and L. W. Xu, *Applied Surface Science*, 2011, **257**, 3519-3523.
53. F. Stojcevski, T. B. Hilditch, T. R. Gengenbach and L. C. Henderson, *Composites Part A: Applied Science and Manufacturing*, 2018, **114**, 212-224.
54. B. Fernández, A. Arbelaiz, A. Valea, F. Mujika and I. Mondragon, *Polymer Composites*, 2004, **25**, 319-330.
55. A. Kafi, M. Huson, C. Creighton, J. Khoo, L. Mazzola, T. Gengenbach, F. Jones and B. Fox, *Composites Science and Technology*, 2014, **94**, 89-95.
56. N. Dilsiz and J. P. Wightman, *Carbon*, 1999, **37**, 1105-1114.
57. A. Bhatnaga, Y. N. Liu, M. Muggli, T. C. Wardm, D. A. Dillard, H. Parvataveddy and J. E. McGrath, *Polymer Preprints ;*, 1997, **1**, 38.
58. Y. Luo, Y. Zhao, Y. Duan and S. Du, *Mater. Des.*, 2011, **32**, 941-946.
59. Z. Dai, F. Shi, B. Zhang, M. Li and Z. Zhang, *Applied Surface Science*, 2011, **257**, 6980-6985.
60. T. H. Cheng, J. Zhang, S. Yumitori, F. R. Jones and C. W. Anderson, *Composites*, 1994, **25**, 661-670.
61. F. Gnädinger, P. Middendorf and B. Fox, *Composites Science and Technology*, 2016, **133**, 104-110.
62. H. Yuan, S. Zhang, C. Lu, S. He and F. An, *Applied Surface Science*, 2013, **279**, 279-284.
63. S. Yumitori, D. Wang and F. R. Jones, *Composites*, 1994, **25**, 698-705.
64. A. Paipetis and C. Galiotis, *Composites Part A: Applied Science and Manufacturing*, 1996, **27**, 755-767.
65. W. Liu, S. Zhang, B. Li, F. Yang, W. Jiao, L. Hao and R. Wang, *Polymer Composites*, 2014, **35**, 482-488.
66. Q. Wu, M. Li, Y. Gu, S. Wang, L. Yao and Z. Zhang, *Polymer Composites*, 2016, **37**, 254-261.
67. E. M. Liston, *The Journal of Adhesion*, 1989, **30**, 199-218.
68. E. M. Liston, L. Martinu and M. R. Wertheimer, *Journal of Adhesion Science and Technology*, 1993, **7**, 1091-1127.
69. J. Moosburger-Will, E. Lachner, M. Löffler, C. Kunzmann, M. Greisel, K. Ruhland and S. Horn, *Applied Surface Science*, 2018, **453**, 141-152.
70. C.-M. Lee, Y.-H. Pai and F.-S. Shieu, *Journal of The Electrochemical Society*, 2009, **156**, B923.
71. M. Baghery Borooj, A. Mousavi Shoushtari, A. Haji and E. Nosratian Sabet, *Composites Science and Technology*, 2016, **128**, 215-221.
72. in *Atmospheric Pressure Plasma for Surface Modification*, 2012, DOI: https://doi.org/10.1002/9781118547519.ch2, pp. 27-53.
73. Y. Zhao, C. Zhang, X. Shao, Y. Wang and Y. Qiu, *Journal of Adhesion Science and Technology*, 2011, **25**, 2897-2908.
74. M. Baghery Borooj, A. Mousavi Shoushtari, E. Nosratian Sabet and A. Haji, *Journal of Adhesion Science and Technology*, 2016, **30**, 2372-2382.
75. J. Jang and H. Yang, *Journal of Materials Science*, 2000, **35**, 2297-2303.
76. H. Zhang and W. Li, *Applied Surface Science*, 2015, **356**, 492-498.
77. J. Sun, F. Zhao, Y. Yao, X. Liu, Z. Jin and Y. Huang, *Materials Letters*, 2017, **196**, 46-49.
78. M. A. Montes-Morán, A. Marťınez-Alonso, J. M. D. Tascón and R. J. Young, *Composites Part A: Applied Science and Manufacturing*, 2001, **32**, 361-371.
79. C. Lew, F. Chowdhury, M. V. Hosur and A. N. Netravali, *Journal of Adhesion Science and Technology*, 2007, **21**, 1407-1424.
80. M. Dietrich and L. J. Paterok, *Cryogenics*, 1984, **24**, 636-638.
81. A. Krämer, S. Engel, N. Sangiorgi, A. Sanson, J. F. Bartolomé, S. Gräf and F. A. Müller, *Applied Surface Science*, 2017, **399**, 282-287.
82. C. Zhang, L. Liu, Z. Xu, H. Lv, N. Wu, B. Zhou, W. Mai, L. Zhao, X. Tian and X. Guo, *Polymer Composites*, 2018, **39**, E1262-E1268.
83. N. R. Council, *Plasma Processing of Materials: Scientific Opportunities and Technological Challenges*, The National Academies Press, Washington, DC, 1991.
84. X. Wang, C. Li, Y. Chi, M. Piao, J. Chu, H. Zhang, Z. Li and W. Wei, *Nanomaterials*, 2018, **8**, 414.
85. Z. Sha, Z. Han, S. Wu, F. Zhang, M. S. Islam, S. A. Brown and C.-H. Wang, *Composites Science and Technology*, 2019, **184**, 107867.
86. K. R. Saviers, M. A. Alrefae and T. S. Fisher, *Advanced Engineering Materials*, 2018, **20**, 1800004.
87. A. Karakassides, A. Ganguly, K. Tsirka, A. S. Paipetis and P. Papakonstantinou, *ACS Applied Nano Materials*, 2020, **3**, 2402-2413.
88. T. A. Langston and R. D. Granata, *Journal of Composite Materials*, 2014, **48**, 259-276.
89. S. Tiwari, J. Bijwe and S. Panier, *Wear*, 2012, **274-275**, 326-334.
90. S. Tiwari, J. Bijwe and S. Panier, *Wear*, 2011, **271**, 2252-2260.
91. F. Vautard, P. Fioux, L. Vidal, J. Dentzer, J. Schultz, M. Nardin and B. Defoort, *Surf. Interface Anal.*, 2013, **45**, 722-741.
92. A. L. Woodhead, M. L. de Souza and J. S. Church, *Applied Surface Science*, 2017, **401**, 79-88.
93. L. M. Manocha, *Journal of Materials Science*, 1982, **17**, 3039-3044.
94. Z. Wu, C. U. Pittman and S. D. Gardner, *Carbon*, 1995, **33**, 597-605.
95. P. Yusong, M. Jiaheng and D. Jie, *Journal of Materials Engineering and Performance*, 2019, **28**, 1995-2005.
96. H.-J. Nie, X.-J. Shen, B.-L. Tang, C.-Y. Dang, S. Yang and S.-Y. Fu, *Composites Science and Technology*, 2019, **183**, 107803.

97. F. Stoeckli, C. Moreno-Castilla, F. Carrasco-Marín and M. López-Ramón, *Carbon*, 2002, **39**, 2235-2237.
98. J. Fei, W. Luo, J. Huang, H. Ouyang, H. Wang and L. Cao, *RSC Advances*, 2015, **5**, 64450-64455.
99. J. Zhang, H. Tang and S. Hao, 2012.
100. F. Vautard, H. Grappe and S. Ozcan, *Applied Surface Science*, 2013, **268**, 61-72.
101. C. Wang, X. Ji, A. Roy, V. V. Silberschmidt and Z. Chen, *Materials & Design*, 2015, **85**, 800-807.
102. L. B. Nohara, G. Petraconi Filho, E. L. Nohara, M. U. Kleinke and M. C. Rezende, *Materials Research*, 2005, **8**, 281-286.
103. N. Koutroumanis, A. C. Manikas, P. N. Pappas, F. Petropoulos, L. Sygellou, D. Tasis, K. Papagelis, G. Anagnostopoulos and C. Galiotis, *Composites Science and Technology*, 2018, **157**, 178-184.
104. H. Yuan, C. Wang, S. Zhang and X. Lin, *Applied Surface Science*, 2012, **259**, 288-293.
105. L. Ma, Y. Zhu, M. Wang, X. Yang, G. Song and Y. Huang, *Compos. Sci. Technol.*, 2019, **170**, 148-156.
106. G. Wu, L. Chen and L. Liu, *J. Mater. Sci.*, 2017, **52**, 1057-1070.
107. D. X. Jiang, L.; Liu, L.; Yan, X.; Guo, J.; Zhang, X.; Zhang, Q.; Wu, Z.; Zhao, F.; Huang, Y.; Wei, S.; Guo, Z., *J. Mater. Chem. A*, 2014, **2**, 18293-18303.
108. F. Zhao and Y. Huang, *Journal of Materials Chemistry*, 2011, **21**, 3695-3703.
109. Y. Zhang, S. Zhu, Y. Liu, B. Yang and X. Wang, *Journal of Applied Polymer Science*, 2015, **132**.
110. S. Jiang, Q. Li, Y. Zhao, J. Wang and M. Kang, *Compos. Sci. Technol.*, 2015, **110**, 87-94.
111. L. Jin, M. Zhang, H. Li, M. Li, L. Shang, L. Xiao and Y. Ao, *RSC Advances*, 2016, **6**, 80485-80492.
112. H. Rahmani, A. Ashori and N. Varnaseri, *Polymers for Advanced Technologies*, 2016, **27**, 805-811.
113. S. H. Han, H. J. Oh, H. C. Lee and S. S. Kim, *Composites Part B: Engineering*, 2013, **45**, 172-177.
114. N. Li, L. Zong, Z. Wu, C. Liu, X. Wang, F. Bao, J. Wang and X. Jian, *Composites Part A: Applied Science and Manufacturing*, 2017, **101**, 490-499.
115. M. Zhao, L. Meng, L. Ma, G. Wu, Y. Wang, F. Xie and Y. Huang, *RSC Advances*, 2016, **6**, 29654-29662.
116. G. J. Ehlert, Y. Lin and H. A. Sodano, *Carbon*, 2011, **49**, 4246-4255.
117. E. A. M. Hassan, T. H. H. Elagib, H. Memon, M. Yu and S. Zhu, *Materials (Basel)*, 2019, **12**, 778.
118. L. Servinis, L. C. Henderson, L. M. Andrighetto, M. G. Huson, T. R. Gengenbach and B. L. Fox, *J. Mater. Chem. A*, 2015, **3**, 3360-3371.
119. K. M. Beggs, M. D. Perus, L. Servinis, L. A. O'Dell, B. L. Fox, T. R. Gengenbach and L. C. Henderson, *RSC Adv.*, 2016, **6**, 32480-32483.
120. L. Servinis, T. R. Gengenbach, M. G. Huson, L. C. Henderson and B. L. Fox, *Australian Journal of Chemistry*, 2015, **68**, 335-344.
121. K. M. Beggs, L. Servinis, T. R. Gengenbach, M. G. Huson, B. L. Fox and L. C. Henderson, *Composites Science and Technology*, 2015, **118**, 31-38.
122. L. Servinis, L. C. Henderson, T. R. Gengenbach, A. A. Kafi, M. G. Huson and B. L. Fox, *Carbon*, 2013, **54**, 378-388.
123. Y. Liu, Y. Fang, J. Qian, Z. Liu, B. Yang and X. Wang, *RSC Advances*, 2015, **5**, 107652-107661.
124. Q. Wu, Q. Wan, Q. Liu, J. He, R. Zhao, X. Yang, F. Wang, J. Guo and J. Zhu, *Adv. Mater. Interfaces*, 2019, **6**, 1970131.
125. J. Fei, X. Duan, L. Luo, C. Zhang, Y. Qi, H. Li, Y. Feng and J. Huang, *Applied Surface Science*, 2018, **433**, 349-357.
126. L. Szabó, S. Imanishi, F. Tetsuo, D. Hirose, H. Ueda, T. Tsukegi, K. Ninomiya and K. Takahashi, *Materials (Basel)*, 2019, **12**, 159.
127. F. Cuiqin, W. Jinxian, W. Julin and Z. Tao, *Applied Surface Science*, 2015, **356**, 9-17.
128. L. Ma, L. Meng, D. Fan, J. He, J. Yu, M. Qi, Z. Chen and Y. Huang, *Applied Surface Science*, 2014, **296**, 61-68.
129. M. Delépine:, *Bull. Soc. Chim. Fr.*, 1895, 352-361.
130. L. Meng, D. Fan, C. Zhang, Z. Jiang and Y. Huang, *Composites Part B: Engineering*, 2014, **56**, 575-581.
131. B. Gao, W. Du, Q. Ma, R. Zhang, C. Wang and J. Zhang, *High Performance Polymers*, 2017, **29**, 808-815.
132. L. Ma, L. Meng, G. Wu, Y. Wang, M. Zhao, C. Zhang and Y. Huang, *Composites Science and Technology*, 2015, **114**, 64-71.
133. Q. Peng, Y. Li, X. He, H. Lv, P. Hu, Y. Shang, C. Wang, R. Wang, T. Sritharan and S. Du, *Composites Science and Technology*, 2013, **74**, 37-42.
134. Y. Wu, L. Xiong, X. Qin, Z. Wang, B. Ding, H. Ren and X. Pi, *IOP Conference Series: Materials Science and Engineering*, 2015, **87**, 012082.
135. L. Xiong, X. Qin, H. Liang, S. Huang and Z. Lian, *Polymer Composites*, 2017, **38**, 27-31.
136. B. Gao, J. Zhang, Z. Hao, L. Huo, R. Zhang and L. Shao, *Carbon*, 2017, **123**, 548-557.
137. E. Giebel, T. Herrmann, F. Simon, A. Fery and M. R. Buchmeiser, *Macromolecular Materials and Engineering*, 2017, **302**, 1700210.
138. L. Xiong, X. Qin, H. Liang, S. Huang and Z. Lian, *Polym. Compos.*, 2017, **38**, 27-31.
139. L. Shang, M. Zhang, L. Liu, L. Xiao, M. Li and Y. Ao, *Surface and Interface Analysis*, 2019, **51**, 199-209.
140. G. Wang, L. Ma, X. Yang, X. Li, P. Han, C. Yang, L. Cong, W. Song and G. Song, *J. Appl. Polym. Sci.*, 2019, **136**, 47232.
141. K. F. Blurton, 1973, **18**, 869-875.
142. R. C. Engstrom, *Analytical Chemistry*, 1982, **54**, 2310-2314.
143. A. Proctor and P. M. A. Sherwood, *Carbon*, 1983, **21**, 53-59.
144. A. D. Jannakoudakis, P. D. Jannakoudakis, E. Theodoridou and J. O. Besenhard, *Journal of Applied Electrochemistry*, 1990, **20**, 619-624.
145. T. Nagaoka and T. Yoshino, *Analytical Chemistry*, 1986, **58**, 1037-1042.
146. G. M. Jenkins and K. Kawamura, *Nature*, 1971, **231**, 175-176.
147. F. Rousseaux and D. Tchoubar, *Carbon*, 1977, **15**, 63-68.
148. R. J. Rice, N. M. Pontikos and R. L. McCreery, *Journal of the American Chemical Society*, 1990, **112**, 4617-4622.
149. Y. V. Basova, H. Hatori, Y. Yamada and K. Miyashita, *Electrochemistry Communications*, 1999, **1**, 540-544.
150. Y.-Q. Wang, H. Viswanathan, A. A. Audi and P. M. A. Sherwood, *Chemistry of Materials*, 2000, **12**, 1100-1107.
151. F. Vautard, P. Fioux, L. Vidal, J. Schultz, M. Nardin and B. Defoort, *Composites, Part A*, 2011, **42**, 859-867.
152. D. A. L. Almeida, A. B. Couto, S. S. Oishi and N. G. Ferreira, *Journal of Solid State Electrochemistry*, 2018, **22**, 3493-3505.
153. P. Georgiou, J. Walton and J. Simitzis, *Electrochimica Acta*, 2010, **55**, 1207-1216.

154. S. Osbeck, S. Ward and H. Idriss, *Applied Surface Science*, 2013, **270**, 272-280.
155. J. C. Simitzis and P. C. Georgiou, *Journal of Materials Science*, 2015, **50**, 4547-4564.
156. W. Li, L. Liu, C. Zhong, B. Shen and W. Hu, *Journal of Alloys and Compounds*, 2011, **509**, 3532-3536.
157. E. Fitzer, H. Jäger, N. Popovska and F. Von Sturm, *Journal of Applied Electrochemistry*, 1988, **18**, 178-182.
158. N. L. Weinberg and T. B. Reddy, *Journal of Applied Electrochemistry*, 1973, **3**, 73-75.
159. J. B. Donnet and P. Ehrburger, *Carbon*, 1977, **15**, 143-152.
160. S. Neffe, *Carbon*, 1987, **25**, 761-767.
161. F. Nakao, Y. Takenaka and H. Asai, 1992, **23**, 365-372.
162. S.-J. Park and M.-H. Kim, *Journal of Materials Science*, 2000, **35**, 1901-1905.
163. D.-K. Kim, K.-H. An, Y. H. Bang, L.-K. Kwac, S.-Y. Oh and B.-J. Kim, 2016, **19**.
164. S. J. Park and B. J. Park, *Journal of Materials Science Letters*, 1999, **18**, 47-49.
165. C. U. Pittman, W. Jiang, Z. R. Yue, S. Gardner, L. Wang, H. Toghiani and C. A. Leon y Leon, *Carbon*, 1999, **37**, 1797-1807.
166. M. Andideh and M. Esfandeh, *Composites Science and Technology*, 2016, **134**, 132-143.
167. Y. Q. Wang, F. Q. Zhang and P. M. A. Sherwood, *Chemistry of Materials*, 1999, **11**, 2573-2583.
168. C. L. Arnold, K. M. Beggs, D. J. Eyckens, F. Stojcevski, L. Servinis and L. C. Henderson, *Composites Science and Technology*, 2018, **159**, 135-141.
169. S. Mahouche-Chergui, S. Gam-Derouich, C. Mangeney and M. M. Chehimi, *Chemical Society Reviews*, 2011, **40**, 4143-4166.
170. M. Delamar, R. Hitmi, J. Pinson and J. M. Saveant, *Journal of the American Chemical Society*, 1992, **114**, 5883-5884.
171. P. Allongue, M. Delamar, B. Desbat, O. Fagebaume, R. Hitmi, J. Pinson and J.-M. Savéant, *Journal of the American Chemical Society*, 1997, **119**, 201-207.
172. M. Delamar, G. Désarmot, O. Fagebaume, R. Hitmi, J. Pinsonc and J. M. Savéant, *Carbon*, 1997, **35**, 801-807.
173. K. M. Beggs, J. D. Randall, L. Servinis, A. Krajewski, R. Denning and L. C. Henderson, *Reactive and Functional Polymers*, 2018, **129**, 123-128.
174. L. Servinis, K. M. Beggs, C. Scheffler, E. Wölfel, J. D. Randall, T. R. Gengenbach, B. Demir, T. R. Walsh, E. H. Doeven, P. S. Francis and L. C. Henderson, *Carbon*, 2017, **118**, 393-403.
175. F. Stojcevski, D. J. Eyckens, J. D. Randall, L. I. Marinovic, G. Méric and L. C. Henderson, *Composites Science and Technology*, 2019, **182**, 107730.
176. B. Demir, K. M. Beggs, B. L. Fox, L. Servinis, L. C. Henderson and T. R. Walsh, *Compos. Sci. Technol.*, 2018, **159**, 127-134.
177. D. J. Eyckens, B. Demir, J. D. Randall, T. R. Gengenbach, L. Servinis, T. R. Walsh and L. C. Henderson, *Composites Science and Technology*, 2020, 108225.
178. C. L. Arnold, D. J. Eyckens, L. Servinis, M. D. Nave, H. Yin, R. K. Marceau, J. Pinson, B. Demir, T. R. Walsh and L. C. Henderson, *Journal of Materials Chemistry A*, 2019, **7**, 13483-13494.
179. D. J. Eyckens, F. Stojcevski, A. Hendlmeier, C. L. Arnold, J. D. Randall, M. D. Perus, L. Servinis, T. R. Gengenbach, B. Demir, T. R. Walsh and L. C. Henderson, *Chem. Eng. J.*, 2018, **353**, 373-380.
180. L. Servinis, K. M. Beggs, T. R. Gengenbach, E. H. Doeven, P. S. Francis, B. L. Fox, J. M. Pringle, C. Pozo-Gonzalo, T. R. Walsh and L. C. Henderson, *Journal of Materials Chemistry A*, 2017, **5**, 11204-11213.
181. R. A. Evans, *Aust. J. Chem.*, 2007, **60**, 384-395.
182. T. Cañeque, S. Müller and R. Rodriguez, *Nat. Rev. Chem.*, 2018, **2**, 202-215.
183. J. D. Randall, D. J. Eyckens, L. Servinis, F. Stojcevski, L. A. O'Dell, T. R. Gengenbach, B. Demir, T. R. Walsh and L. C. Henderson, *Carbon*, 2019, **146**, 88-96.
184. D. J. Eyckens, J. D. Randall, F. Stojcevski, E. Sarlin, S. Palola, M. Kakkonen, C. Scheffler and L. C. Henderson, *Composites Part A: Applied Science and Manufacturing*, 2020, 106053.
185. J. D. Randall, D. J. Eyckens, F. Stojcevski, P. S. Francis, E. H. Doeven, A. J. Barlow, A. S. Barrow, C. L. Arnold, J. E. Moses and L. C. Henderson, *ChemPhysChem*, 2018, **19**, 3176-3181.
186. M. Ates, I. Osken and T. Ozturk, *Journal of The Electrochemical Society*, 2012, **159**, E115-E121.
187. A. S. Saraç, G. Sönmez and F. Ç. Cebeci, *Journal of Applied Electrochemistry*, 2003, **33**, 295-301.
188. M. Hejazi, W. Tong, M. R. Ibbotson, S. Prawer and D. J. Garrett, *Front. Neurosci.*, 2021, **15**.
189. A. S. Sarac, H.-D. Gilsing, A. Gencturk and B. Schulz, *Progress in Organic Coatings*, 2007, **60**, 281-286.
190. A. S. Sarac, S. E. Ozgul, A. Gencturk, B. Schulz, H.-D. Gilsing and H. Faltz, *Progress in Organic Coatings*, 2010, **69**, 527-533.
191. M. A. Miller, A. Bourke, N. Quill, J. S. Wainright, R. P. Lynch, D. N. Buckley and R. F. Savinell, *Journal of The Electrochemical Society*, 2016, **163**, A2095-A2102.
192. A. S. Sarac, M. Serantoni, S. A. M. Tofail, J. Henry, V. Cunnane and J. B. McMonagle, *Applied Surface Science*, 2005, **243**, 183-198.
193. R. B. Moghaddam and P. G. Pickup, *Electrochimica Acta*, 2011, **56**, 7666-7672.
194. D. Semitekolos, P. Kainourgios, C. Jones, A. Rana, E. P. Koumoulos and C. A. Charitidis, *Composites Part B: Engineering*, 2018, **155**, 237-243.
195. Z. Wen, X. Qian, Y. Zhang, X. Wang, W. Wang and S. Song, *Composites Part A: Applied Science and Manufacturing*, 2019, **119**, 21-29.
196. G. Deniau, L. Azoulay, L. Bougerolles and S. Palacin, *Chemistry of Materials*, 2006, **18**, 5421-5428.
197. L. Tessier, G. Deniau, B. Charleux and S. Palacin, *Chemistry of Materials*, 2009, **21**, 4261-4274.
198. J. D. Randall, M. K. Stanfield, D. J. Eyckens, J. Pinson and L. C. Henderson, *Langmuir*, 2020.
199. D. J. Eyckens, C. L. Arnold, J. D. Randall, F. Stojcevski, A. Hendlmeier, M. K. Stanfield, J. Pinson, T. R. Gengenbach, R. Alexander and L. C. Soulsby, *ACS applied materials & interfaces*, 2019, **11**, 41617-41625.
200. D. J. Eyckens, C. L. Arnold, Ž. Simon, T. R. Gengenbach, J. Pinson, Y. A. Wickramasingha and L. C. Henderson, *Composites, Part A*, 2021, **140**, 106147.
201. A. Barinov, O. B. Malcioğlu, S. Fabris, T. Sun, L. Gregoratti, M. Dalmiglio and M. Kiskinova, *J. Phys. Chem. C.*, 2009, **113**, 9009-9013.
202. R. Larciprete, S. Fabris, T. Sun, P. Lacovig, A. Baraldi and S. Lizzit, *J. Am. Chem. Soc.*, 2011, **133**, 17315-17321.
203. T. Sun and S. Fabris, *Nano Lett.*, 2012, **12**, 17-21.

204. L. N. S. Chiu, B. G. Falzon, R. Boman, B. Chen and W. Yan, *Compos. Struct.*, 2015, **131**, 215-228.
205. G. Fernlund, A. Osooly, A. Poursartip, R. Vaziri, R. Courdji, K. Nelson, P. George, L. Hendrickson and J. Griffith, *Compos. Struct.*, 2003, **62**, 223-234.
206. P. F. Liu, B. B. Liao, L. Y. Jia and X. Q. Peng, *Compos. Struct.*, 2016, **149**, 408-422.
207. S. R. Hallett, B. G. Green, W. G. Jiang and M. R. Wisnom, *Composites, Part A*, 2009, **40**, 613-624.
208. J. Gou, B. Minaie, B. Wang, Z. Liang and C. Zhang, *Comput. Mater. Sci.*, 2004, **31**, 225-236.
209. K. Guru, S. B. Mishra and K. K. Shukla, *Appl. Surf. Sci.*, 2015, **349**, 59-65.
210. K. S. Khare, F. Khabaz and R. Khare, *ACS Appl. Mater. Interfaces*, 2014, **6**, 6098-6110.
211. K. Sharma and M. Shukla, *New Carbon Mater.*, 2014, **29**, 132-142.
212. V. Varshney, A. K. Roy, T. J. Michalak, J. Lee and B. L. Farmer, *JOM*, 2013, **65**, 140-146.
213. L. Yang, L. Tong and X. He, *Comput. Mater. Sci.*, 2012, **55**, 356-364.
214. C. M. Hadden, B. D. Jensen, A. Bandyopadhyay, G. M. Odegard, A. Koo and R. Liang, *Compos. Sci. Technol.*, 2013, **76**, 92-99.
215. C. Li and A. Strachan, *J. Polym. Sci., Part B: Polym. Phys.*, 2015, **53**, 103-122.
216. C. Lechner and A. F. Sax, *J. Phys. Chem. C.*, 2014, **118**, 20970-20981.
217. B. Demir, L. C. Henderson and T. R. Walsh, *ACS Appl. Mater. Interfaces*, 2017, **9**, 11846-11857.
218. C. M. Hadden, D. R. Klimek-McDonald, E. J. Pineda, J. A. King, A. M. Reichanadter, I. Miskioglu, S. Gowtham and G. M. Odegard, *Carbon*, 2015, **95**, 100-112.
219. I. Yarovsky and E. Evans, *Polymer*, 2002, **43**, 963-969.
220. J. R. Gissinger, B. D. Jensen and K. E. Wise, *Polymer*, 2017, **128**, 211-217.
221. B. Demir and T. R. Walsh, *Soft Matter*, 2016, **12**, 2453-2464.
222. L.-h. Tam and D. Lau, *RSC Adv.*, 2014, **4**, 33074-33081.
223. C. Li and A. Strachan, *Polymer*, 2011, **52**, 2920-2928.
224. S. Nouranian, C. Jang, T. E. Lacy, S. R. Gwaltney, H. Toghiani and C. U. Pittman, *Carbon*, 2011, **49**, 3219-3232.
225. Y. Hu and J. L. Ding, *Carbon*, 2016, **107**, 510-524.
226. X. Peng and S. A. Meguid, *Comput. Mater. Sci.*, 2017, **126**, 204-216.
227. M. Li, H. Zhou, Y. Zhang, Y. Liao and H. Zhou, *RSC Adv.*, 2017, **7**, 46101-46108.
228. P. Xu, Y. Yu, Z. Guo, X. Zhang, G. Li and X. Yang, *Compos. Sci. Technol.*, 2019, **171**, 252-260.
229. M. Zhang, X. Wang, M. Zhou, Z. Zhai and B. Jiang, *Polymer*, 2020, **207**, 122915.
230. S. U. Patil, M. S. Radue, W. A. Pisani, P. Deshpande, H. Xu, H. Al Mahmud, T. Dumitrică and G. M. Odegard, *Comput. Mater. Sci.*, 2020, **185**, 109970.
231. A. N. Kolmogorov and V. H. Crespi, *Phys. Rev. B*, 2005, **71**, 235415.
232. Y. Zhang, X. Zhuang, J. Muthu, T. Mabrouki, M. Fontaine, Y. Gong and T. Rabczuk, *Composites, Part B*, 2014, **63**, 27-33.
233. Y. Li and G. D. Seidel, *Modell. Simul. Mater. Sci. Eng.*, 2014, **22**, 025023.
234. A. P. Awasthi, D. C. Lagoudas and D. C. Hammerand, *Modell. Simul. Mater. Sci. Eng.*, 2008, **17**, 015002.
235. M. Ionita, *Composites, Part B*, 2012, **43**, 3491-3496.
236. B. Yu, S. Fu, Z. Wu, H. Bai, N. Ning and Q. Fu, *Composites, Part A*, 2015, **73**, 155-165.
237. S. Saiev, L. Bonnaud, L. Dumas, T. Zhang, P. Dubois, D. Beljonne and R. Lazzaroni, *ACS Appl. Mater. Interfaces*, 2018, **10**, 26669-26677.
238. L.-h. Tam, J. Jiang, Z. Yu, J. Orr and C. Wu, *Appl. Surf. Sci.*, 2021, **537**, 148013.
239. Q. L. Xiong and S. A. Meguid, *Eur. Poly. J.*, 2015, **69**, 1-15.
240. J. Koyanagi, N. Itano, M. Yamamoto, K. Mori, Y. Ishida and T. Bazhirov, *Adv. Compos. Mater.*, 2019, **28**, 639-652.
241. T. Semoto, Y. Tsuji, H. Tanaka and K. Yoshizawa, *J. Phys. Chem. C.*, 2013, **117**, 24830-24835.
242. J. Li, J. Zhao, M. Zhang, Y. Cui and D. Kou, *Appl. Surf. Sci.*, 2021, **538**, 148049.
243. C. Jang, S. Nouranian, T. E. Lacy, S. R. Gwaltney, H. Toghiani and C. U. Pittman, *Carbon*, 2012, **50**, 748-760.
244. R. Gogoi, S. K. Sethi and G. Manik, *Appl. Surf. Sci.*, 2021, **539**, 148162.
245. T. Niuchi, J. Koyanagi, R. Inoue and Y. Kogo, *Adv. Compos. Mater.*, 2017, **26**, 569-581.
246. C. L. Arnold, D. J. Eyckens, L. Servinis, M. D. Nave, H. Yin, R. K. W. Marceau, J. Pinson, B. Demir, T. R. Walsh and L. C. Henderson, *J. Mater. Chem. A*, 2019, **7**, 13483-13494.
247. W. Jiao, T. Zheng, W. Liu, W. Jiao and R. Wang, *Appl. Surf. Sci.*, 2019, **479**, 1192-1199.
248. H. Jung, K. J. Bae, J.-u. Jin, Y. Oh, H. Hong, S. J. Youn, N.-H. You and J. Yu, *Funct. Compos. Struct.*, 2020, **2**, 025001.
249. W. Jiao, C. Hou, X. Zhang and W. Liu, *Comp. Interfaces*, 2021, **28**, 445-459.
250. M. Li, Y.-Z. Gu, Y.-X. Li, H. Liu and Z.-G. Zhang, *J. Appl. Polym. Sci.*, 2014, **131**.
251. M. Bouriga, M. M. Chehimi, C. Combellas, P. Decorse, F. Kanoufi, A. Deronzier and J. Pinson, *Chem. Mater.*, 2013, **25**, 90-97.
252. M. Laurien, B. Demir, H. Büttemeyer, A. S. Herrmann, T. R. Walsh and L. C. Ciacchi, *Macromolecules*, 2018, **51**, 3983-3993.

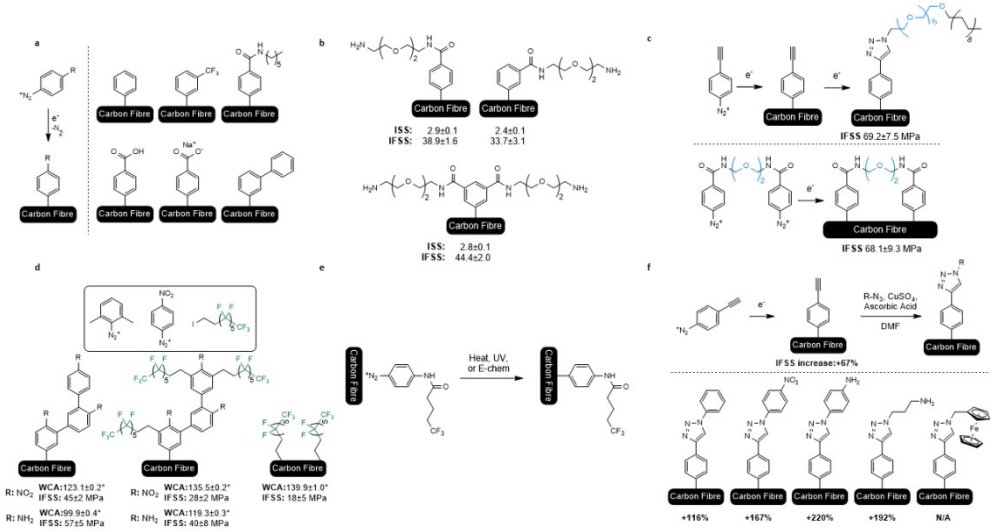

The caption for this fiigure is embedded in the text of the document.

338x190mm (96 x 96 DPI)